Funded by
the European Union

ACCREU
Assessing Climate Change Risk in EUrope

Fiscal and Financial Analysis

GA number: 101081358; Funding type: HORIZON-CL5-2022-D1-07-two-stage

Deliverable number (relative in WP)	D4.3
Deliverable name:	Fiscal and Financial Analysis
WP / WP number:	WP4
Delivery due date:	Project month 40 (July 2026)
Actual date of submission:	07 September 2026
Dissemination level:	Public
Lead beneficiary:	UNIGRAZ
Responsible scientist/administrator:	Birgit Bednar-Friedl (UNIGRAZ)
Contributor(s):	**UNIGRAZ:** Birgit Bednar-Friedl, Nina Knittel, Alexandra Lehner, Eva Preinfalk **VU**: Michiel W. Ingels, Max Tesselaar, Jan Brusselaers **UNIVE:** Stefano Battiston, Michelangelo Puliga **CMCC:** Lorenza Campagnolo
Internal reviewer:	Francesco Bosello, Enrica De Cian

Funded by the European Union. Views and opinions expressed are however those of the author(s) only and do not necessarily reflect those of the European Union. Neither the European Union nor the granting authority can be held responsible for them.

Changes with respect to the DoA

There are no major changes with respect to the description of work outlined in Task 4.3 of the ACCREU Grant Agreement.

Dissemination and uptake

- Alexandra Lehner, Presentation at the NOeG - Annual Conference of the Austrian Economic Association 2025: Session 5.5: Environmental and Ecological Economics II: Social and Fiscal Dimensions of Adapting to Environmental Stress. 24 September 2025, Krems, Austria. Presentation of the Paper "Budgets in high water? Fiscal implications of flood adaptation in the United Kingdom"
- Alexandra Lehner, Presentation at the EcoMod 2025: Session 10: General Equilibrium Modeling. 3. September 2025, Stuttgart, Germany. Presentation of the Paper "Budgets in high water? Fiscal implications of flood adaptation in the United Kingdom"
- Birgit Bednar-Friedl, Paul Watkiss, Theodoros Zachariadis, Guillaume Dolques, Clemens Haße & Eva Preinfalk, ADT stakeholder workshop "National Costing of Adaptation" (online). 26 September 2025
- Paul Watkiss & Alexandra Lehner, Presentation at European Climate and Disaster Fiscal Risks Expert Group (online). 27 March 2026. Presentation on Modeling of climate disasters and fiscal effects.
- Alexandra Lehner, Presentation at the joint Webinar by ACCREU, CROSSEU & SPARCCLE "The macroeconomics of adaptation: lessons learned from the 3 projects". 23 June 2026. Presentation of the Paper "Budgets in high water? Fiscal implications of flood adaptation in the United Kingdom"
- Nina Knittel, Presentation at the World Congress of Environmental and Resource Economists: Session Egg Timer: Net-Zero Transitions and CGE Analysis. 1 July 2026. Presentation of the Paper "Towards standardized adaptation modeling in CGE frameworks: Assessing sea level rise impacts and responses in Europe"
- Nina Knittel, Presentation at the Ecomod Conference: Session General equilibrium modeling (CGE) 4: 9 July 2026. Presentation of the Paper "Towards standardized adaptation modeling in CGE frameworks: Assessing sea level rise impacts and responses in Europe"
- Alexandra Lehner, Presentation at the World Congress of Environmental and Resource Economists: Session Climate Change Adaptation 2. 1 July 2026. Presentation of the Paper "Budgets in high water? Fiscal implications of flood adaptation in the United Kingdom"
- Alexandra Lehner, accepted presentation at the Global Conference on Environmental Taxation 2026. Presentation of the paper "Budgets in high water? Fiscal implications of flood adaptation in the United Kingdom"
- Lorenza Campagnolo, accepted presentation at IAMC 2026. Presentation of the paper "Macroeconomic Implications of Climate-Induced Heat Shocks on Effective Labour."

- Nina Knittel, accepted presentation at IAMC 2026. Presentation of the paper "Towards standardized adaptation modeling in CGE frameworks: Assessing sea level rise impacts and responses in Europe"
- Michiel Ingels, Presentation at the Dutch Environmental and Resource Economics (DEARE) symposium, "Business-level flood insurance coverage and adaptation in the Netherlands", 7 February 2026, Wageningen.
- Michiel Ingels, Presentation at the annual climate event (Klimaatmiddag) of the Dutch Association of Insurers, titled "Het modelleren van verzekeringsmarkten", 6 March 2025, the Hague.
- Michiel Ingels, Poster-presentation at the European Geosciences Union (EGU) general assembly, titled "Business-level flood insurance coverage and adaptation under climate change in the Netherlands", 1 May 2025, Vienna.
- Michiel Ingels, Presentation at the Red&Blue project symposium, titled "Modelling business-level flood insurance in the Netherlands", 10 October 2025, Rotterdam.

Short summary of results

An executive summary can be found on pages 7-8.

Evidence of accomplishment

Published Manuscripts

- Ingels, W.M., Tesselaar, M., Brusselaers, J., Aerts, J,C.J.H., & Botzen, W.J.W.B. (final round of revisions/reviews). Evaluation of flood insurance systems for businesses in a changing climate: an integrated model of flood risk and insurance markets. Under review at *Water Economics and Policy*.

Published Datasets & Code

- Model Code: The COIN-INT model documentation will be made available on ZENODO
- Dataset: The results of the COIN-INT Fiscal analysis (GDP, welfare, fiscal space, etc. by country/region x time (2050, 2070) x scenario (RCP2.6, RCP.4.5, RCP7.0) x adaptation level) will be made available on the IIASA Accelerator (Results repository)
- Model Code: The ICES_MH fiscal module documentation will be made available on ZENODO
- Dataset: The results of the ICES_MH Fiscal analysis (GDP, fiscal space, etc. by country/region x time (2050, 2070) x RCP7.0 x adaptation level) will be made available on the IIASA Accelerator (Results repository)
- Model Code: The DIFI model documentation will be made available on ZENODO

Manuscripts in Preparation

- Lehner, A., Knittel N., Preinfalk, E., Bednar-Friedl, B., Watkiss, P., Hunt, A. Budgets in high water? Fiscal implications of flood adaptation in the United Kingdom. Manuscript in preparation for submission to *Environmental & Resource Economics*

- Knittel, N., Campagnolo, L., Preinfalk, E., Bednar-Friedl, B., Lehner, A., Bacca, S., Haas, J., Hinkel, J., Lincke, D. Towards standardized adaptation modeling in CGE frameworks: Assessing sea level rise impacts and responses in Europe. Manuscript in preparation for submission to *Economic Systems Research*.

Other (web links, etc)

- ACCREU Stakeholder Workshop on Costing and Economic Analysis of National Adaptation Strategies, 26 September 2025. https://www.accreu.eu/events/accreu-workshop-on-costing-and-economic-analysis-of-national-adaptation-strategies/
- Joint Webinar by ACCREU, CROSSEU & SPARCCLE "The macroeconomics of adaptation: lessons learned from the 3 projects". 23 June 2026. https://www.accreu.eu/events/accreu-crosseu-sparccle-webinar-the-macroeconomics-of-adaptation-lessons-learned-from-the-3-projects/

Table of Contents

Executive Summary

Task 4.3 of the ACCREU project investigates the consequences of climate change impacts and adaptation for government budgets, the insurance sector and financial markets. The analyses are complementary: the macroeconomic models provide a full account of both the direct and indirect effects of impacts and adaptation for government budgets across European countries; the insurance sector and financial risk analyses provide sectoral and country deep-dives of sectoral market implications of climate change impacts and adaptation.

First, the University of Graz (UNIGRAZ) and CMCC conduct the fiscal analysis with their respective CGE models, COIN-INT and ICES-XPS (Chapter 1). The Vrije Universiteit Amsterdam (VU) reports on the impacts of flood risk on the insurance sector in the Netherlands, specifically targeting business insurance and the affordability across commercial sectors (Chapter 2). University of Venice (UNIVE) investigates the financial risks of drought and flood risk for businesses across sectors and regions in Europe (Chapter 3).

Chapter 1: Fiscal Analysis

Using the CGE model extensions that were newly developed in ACCREU (see Milestone 4.1 and Deliverable 4.1 for details), Chapter 1 explores how climate change impacts and adaptation affect government budgets. Two CGE analyses are presented: the COIN-INT model evaluates the combined effects of climate change across various RCP scenarios (2.6, 4.5, 7.0) and adaptation levels (low, medium, high) on government revenues and expenditures, assuming budget austerity where adaptation spending requires cuts elsewhere. A UK case study compares this balanced budget approach to financing adaptation through government bonds. The ICES-XPS model examines the macroeconomic and fiscal effects of specific climate impact channels, sea level rise, labor productivity, health, agriculture, wildfires, pollination loss, and flooding, disentangling impact and adaptation channels depending on the impact. Here, adaptation is assumed to be funded by expanding government debt.

The main findings from the fiscal analysis are that adaptation investment constitutes a significant burden for government budgets, even though the benefits outweigh the costs in the long run. Higher adaptation levels lead to significant reductions in residual risks, both for key macroeconomic indicators like GDP and welfare, and for fiscal space. On a macroeconomic scale, there is therefore a clear net benefit of adaptation. Yet, there are significant differences across European countries and macroregions due to risk exposure and debt dynamics. Who bears the burden of adaptation costs depends on the chosen variant of adaptation financing: the balanced budget variant leads to burdens in the short term as government spending has to be diverted from other important policy domains. In contrast, deficit expansion has less restrictive effects in the short term, but the debt burden accumulates in the longer term. Future research could place more focus on private adaptation and the interactions with public adaptation investment.

Chapter 2: Insurance Sector Analysis

Chapter 2 examines how changes in flood insurance policy can reduce the flood insurance protection gap, with a particular emphasis on business insurance, a previously underresearched topic. Using a partial equilibrium modeling framework, the chapter assesses flood damages, insurance premiums, demand for insurance, and the adoption of adaptation measures by individual homeowners. The methodology developed for business flood insurance is a key ACCREU innovation featured in this deliverable. The analysis explores both direct and indirect flood risks to businesses, under current conditions and in the context of increasing flood risk due to climate change. The Netherlands serves as the primary case study, given its extensive experience in flood risk management, though the approach can be readily adapted to other countries or flood hazards with minimal adjustments.

The study finds that government-backed reinsurance and expanded coverage to currently excluded flood-prone areas can significantly reduce the flood insurance protection gap for businesses. Public reinsurance also enables insurers to offer products in high-risk regions by lowering solvency risks. While firm-level flood adaptation is still uncommon, premium discounts and well-designed insurance schemes can encourage businesses to adopt risk-reducing measures, highlighting the potential of insurance to drive proactive adaptation.

Chapter 3: Financial Risk Analysis

Chapter 3 investigates financial risk for two climate impact drivers: drought and fluvial flooding. The first part of this chapter investigates the economic impacts of droughts on financial assets in Europe, and how these effects vary across sectors and regions. In the second part, a methodology is refined to assess asset-level financial losses from fluvial flooding.

The results show that equity holders face drought losses about 2.5–3 times greater than bond holders, due to the way corporate finance absorbs risk. This highlights the need for equity investors and regulators to treat drought as a significant risk, especially in water-dependent sectors and regions with concentrated manufacturing investment. Country-level rankings suggest adaptation policies need to be region-specific. In Central Europe, measures like floodplain restoration and groundwater licensing reform can reduce vulnerability. In Mediterranean countries, where drought impacts are much higher, water governance reforms—such as streamlined regulation, better monitoring, and incentives for conservation—are essential.

Fluvial flooding causes massive economic losses in Europe, but current flood risk data lack uncertainty estimates and direct links to asset-level financial losses. This study fills these gaps by recalculating risk metrics, validating flood data, and applying land-cover-based loss estimates. The results are integrated into a credit-risk model to assess bond and equity losses for EU financial portfolios.

1 Fiscal Analysis

1.1 Introduction

As reconfirmed by the 2024 United Nations Adaptation Gap Report, the global gap between adaptation needs and available financing is increasing (UNEP, 2024). One reason for this gap is the substantial lack of coordinated and long-term adaptation financing strategies by public actors, which so far come primarily from public sources (UNEP, 2024). However, adaptation is an important pillar to mediate the increasing damages from climate change (Ara Begum et al., 2022).

Planned adaptation is often seen as a responsibility of the state (Catalano et al., 2020; Woodruff et al., 2020), which raises questions about fiscal sustainability, namely the balance between revenues and expenditures, the cost of debt, and the sustainability of public service delivery and financial commitments (Ekins & Speck, 2014). Planned adaptation involves upfront investments that primarily deliver benefits in the future. While early adaptation measures might strengthen the fiscal resilience of public actors in the longer run (Catalano et al., 2020; Gilmore et al., 2022), the costs of doing so either burdens present or future generations. Present generations are burdened when governments opt for a budget neutral approach because then either expenditures need to be cut in other valuable policy areas or taxes need to be raised. Financing adaptation by diverting other government expenditures or by raising taxes can lead to efficiency losses due to volatility in taxes and public good provision (Azzimonti et al., 2016). If on the contrary, governments allow for expansive adaptation policies, government debt is increased, thereby burdening future generations. Even if debt financing of early adaptation measures can be effective in the long run, it may be necessary to pursue public debt reduction to have funds to deal with future residual damages (Catalano et al., 2020).

In addition to direct climate damages to capital and other assets, indirect economic damage costs arise from system responses and complex interconnections in the economic system, leading to price changes, income effects and GDP losses (Van Der Wijst et al., 2023). These damages are of relevance to the governments and public finances, as tax revenues rely on economic activity (Catalano et al., 2020; Jones et al., 2013). Moreover, climate-related extreme events necessitate public support for households and corporations through relief payments, and unemployment transfers, reconstruction of destroyed state-owned assets, bail-outs of failing financial institutions, spending on public emergency measures and increased healthcare costs (Agarwala et al., 2021; Barrage, 2023). These public spending requirements in combination with decreased tax revenues can put pressure on governmental budgets (Bachner et al., 2019).

In general terms, the public sector, which usually has to come up with most of the funding for adaptation measures, can finance public adaptation through shifts in expenditure allocations (e.g. from other spending areas to adaptation), increased taxes and/or through debt financing. Financing adaptation measures involves trade-offs and challenges, as different instruments, like shifts within existing budgets, increased taxes and/or through debt financing (Gilmore 2022, Woodruff 2020), can have adverse effects. Public investment decision making thus requires information both on adaptation effectiveness and consequences from different financing decisions, which is a largely under-investigated research field. The complexity of these decisions is increased by the phasing of adaptation costs and benefits, as well as the high uncertainty regarding future climate change. The assessment of adaptation efficiency and effectiveness, while taking indirect effects from financing decisions into account, is thus central to public investment decision making (Watkiss, 2015), while it is a largely under-investigated research field.

Using the CGE model extensions that were newly developed in ACCREU,, Chapter 1 investigates the implications of climate change impacts and adaptation for government budgets. In Section 1.2, we summarize the main model characteristics in relation to climate change impact and adaptation modeling, as well as on modeling of the government budget. For further details, we refer to Milestone 4.1 and Deliverable 4.1. Section 1.3 presents and discusses the results, again with a focus on direct and indirect effects of climate change impacts and adaptation on government budgets. Section 1.4 summarizes the main findings and draws conclusions.

1.2 Methods

Each of the two CGE analyses described in this chapter have a unique focus: the COIN-INT model is used to assess the combined effects of all climate change impact channels and different adaptation levels (low, medium, high) on both the revenue and expenditure side of government budgets. This analysis is done under the assumption of budget neutrality. Complementary to the COIN-INT model simulations, the ICES-XPS model is used to detail the budgetary consequences of the different climate impact channels (labor, agriculture, health etc.) which helps to better understand which impact channels and adaptation types/levels affect which country/region most strongly.

1.2.1 COIN-INT

COIN-INT implemented the available new data on impacts and adaptation costs/effectiveness along the ACCREU scenarios as explained in detail in section 7.1 in Deliverable 4.1 (except for forest fires, as data is only available for Spain). Table 1 provides information on the underlying assumptions regarding the three adaptation levels for each of the impacts considered.

In the following, we assess how climate change and adaptation affects GDP, mortality-adjusted welfare and the fiscal space across Europe. We consider three levels of adaptation - low, medium and high. In alignment with the scenario protocol, all model runs are SSP2 with different RCPs. We model impacts and adaptation policies on a country scale, except for two regions: Region BLU aggregates Belgium and Luxembourg, and BAL aggregates Estonia, Latvia, and Lithuania. For matters of clarity we display some results on European macro regions (European Environment Agency., 2024) in section 1.3.1. Impacts are available for EU countries as well as the United Kingdom, Switzerland and Norway, except for agricultural impacts from GLOBIOM, which are only available for the EU. Note that we exclude the EU member states Malta and Cyprus from the assessment due to the used model resolution, where the according model region “Rest of Europe” also includes non-member states Albania and Serbia.

Table 1. *Inclusion of impact dimensions and adaptation levels in the COIN-INT model.*

Impact category	WP2 data source (model)	General configuration	Explanation of adaptation levels		
			low	**medium/ reference**	**high**
Sea level rise	DIVA	GCM uncertainty: 50th quantile, including migration	Constant dike heights	Constant flood protection standards	Quadrupling flood protection standards
Flooding	GLOFRIS	GCM IPSL-CMSA-LR, no zoning	Constant dike heights	Constant flood protection standards	Optimal flood protection standards
Agricultural impacts	GLOBIOM	GCM IPSL, including RCP mitigation effects	Limited expansion of irrigation to already equipped areas	Sustainable irrigation expansion in equipped areas	Sustainable expansion of irrigation in equipped areas and conversion of rainfed areas
	Biodiversity loss	CLIM_RCP configuration, no SSP	No adaptation considered (not available from sectoral modeling)		
Labour productivity and supply, and energy-related adaptation	*Impact*: Labour productivity (CMCC) *Adaptation*: Sectoral energy demand estimated for agricultural, industrial and commercial sectors (CMCC)	GCM uncertainty: 50th quantile, including heating and cooling	No additional technological adoption, frozen technology at historical climate. Variation in the intensive use of existing stock due to climate change (costs included).	Variation in energy-intensive capital stock due to future climate (costs not available) . Intensive use changes due to the underlying variation in energy-intensive capital stock under future climate (costs included).	Variation in energy-intensive capital stock due to a variation in per capita income, on top of future climate (costs not available). Intensive use changes due to the variation in per capita income, affecting energy-intensive capital stock on top of future climate (costs included).
	Labour supply (CMCC)	GCM uncertainty: 50th quantile	No adaptation considered (not available from sectoral modeling)		
Health (mortality and morbidity) and energy-related adaptation	*Impact*: Health (BC3) *Adaptation*: Residential energy demand and AC investment costs	GCM uncertainty: 50th quantile; mortality measured as value of a statistical life (VSL) added ex-post to welfare	No additional technological adoption, frozen technology at historical climate.	Variation in energy-intensive capital stock due to future climate (costs included) . Intensive use	Variation in energy-intensive capital stock due to a variation in per capita income, on top of

	(CMCC)		Variation in the intensive use of existing stock due to climate change (costs included).	changes due to the underlying variation in energy-intensive capital stock under future climate (costs included).	future climate (costs included). Intensive use changes due to the variation in per capita income, affecting energy-intensive capital stock on top of future climate (costs included).

We consider a budget-neutral financing scheme, where public and private households finance adaptation expenditures from their running budgets by shifting other expenditures. This means that in this case, households do not restrict their savings or take up deficits.

However, to account for potential variation originating from alternative financing choices, we consider a case study for public flood adaptation in the UK. Considered flood costs are based on projections from the latest national risk assessment for damages to private capital and public infrastructure, combined with estimates of flood-induced health impacts. Analysed financing mechanisms for flood adaptation include shifts in public expenditures maintaining budget neutrality in line with the European assessment, and deficit financing via domestic green bonds and deficit financing via international bonds. Debt financing is modelled through the issuance of public bonds in the height of required financing needs. Private households in the UK (for domestic) or in the EU (for international bonds) take parts out of their savings to buy these bonds. In return, they receive interest payments determined by an exogenously given interest rate (calculated as a 20-year mean of conventional gilts interest rates). This results in payment flows between households - bond payments from private households to the public household, and interest payments from the public to the private household. For this analysis, we perform a static comparative analysis for the years 2030 and 2050 under two warming scenarios.

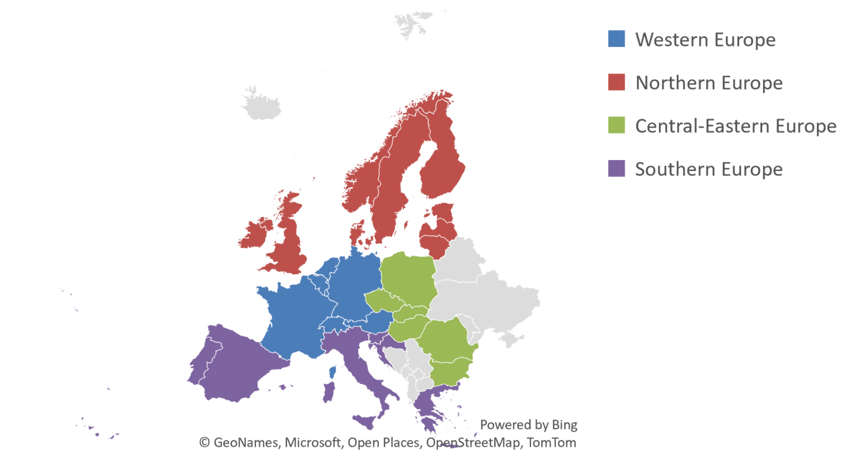

Figure 1. *Allocation of European country regions into model region aggregates, adapted from* EUCRA, 2024

1.2.2 ICES-XPS

The ICES-eXtended Public Sector model (ICES-XPS) provides a comprehensive and internally consistent framework for tracking the full chain of macroeconomic and fiscal implications of climate change impacts and adaptation measures, from aggregate output losses down to debt sustainability (Parrado et al., 2020). Building on the standard ICES recursive-dynamic CGE structure, the extended public sector version introduces a fundamental architectural change by separating government and private households into two distinct agents, each subject to its own budget constraint and income-expenditure identity. This separation, absent from the core model, adds to the analysis a systematic scrutiny of the fiscal channels through which climate shocks and adaptation responses propagate across the economy.

On the output side, the model tracks climate change impacts and adaptation expenditure effects on each of the key components of GDP: private consumption, investment, government expenditure and net exports. This decomposition is particularly valuable for understanding the structural transmission of climate shocks. Impacts primarily compress factor incomes and reduce household consumption and investment demand through their effect on the returns to capital and labor. Adaptation measures, by contrast, generate additional public expenditure and investment that may partially offset these losses or introduce new distortions through reallocation effects across sectors and demand components. The model's multi-sector, multi-country structure further allows these effects to spill over through trade linkages, affecting net exports and the external balance in ways that vary across countries depending on their degree of openness and sectoral composition.

On the fiscal side, the explicit modelling of government income, comprising tax revenues, factor income remuneration, international aid inflows, interest receipts, and other income sources, allows to trace precisely how climate damages erode the public revenue base over time. As economic activity contracts and taxable incomes fall, government revenues decline relative to baseline, progressively reducing the fiscal space available for discretionary expenditure. The tax revenue channel is particularly important: the broad-based nature of climate related losses means that virtually every component of the tax base is simultaneously compressed, leaving governments with limited ability to substitute across revenue sources. At the same time, adaptation measures increase the pressure on the government budget through higher public investment and expenditure, creating a simultaneous squeeze on both the revenue and expenditure sides of the government budget. Differently from the COIN-INT model, we do not constrain government budgets and savings, which respond to climate change shocks and adaptation choices.

The resulting gap between government income and expenditure determines government savings, which together with household savings feeds into the aggregate investment-savings balance of the economy. When government savings are insufficient to finance the required level of public investment, as is increasingly likely under high damage, high adaptation cost scenarios, the model endogenously generates government borrowing sourced from both domestic and foreign investors according to base-year financing shares. This borrowing is not an accounting residual but a behaviorally grounded outcome of the fiscal dynamics, reflecting the actual financing choices that governments face when confronted with simultaneous revenue shortfalls and expenditure pressures. The sign and magnitude of net lending and borrowing thus provide a direct indicator of the fiscal sustainability implications of each climate and adaptation scenario, capturing both the crowding-out effects on private investment and the external financing requirements that arise when domestic savings are insufficient.

The introduction of explicit interest payments on accumulated public debt further enriches the fiscal dynamics by creating a feedback loop between current borrowing and future fiscal capacity. As governments borrow more to finance adaptation and offset revenue shortfalls, the interest burden on outstanding debt increases, further reducing the net resources available for productive public expenditure in subsequent periods. This debt-service channel can generate self-reinforcing fiscal deterioration in countries where the initial debt stock is already large or where the pace of borrowing is rapid, creating potential debt sustainability concerns even under moderate climate damage scenarios. The model captures this dynamic through an interest rate applied to the debt stock, ensuring that the interest burden evolves endogenously in response to the accumulation of public liabilities over the simulation horizon.

Finally, the dynamic debt accumulation equation compounds these annual borrowing flows into changes in the public debt stock over the full simulation horizon to 2070, allowing the analysis to assess whether climate-induced fiscal pressures are transitory or persistent and whether they generate trajectories of debt accumulation that may threaten long-run fiscal sustainability. Countries that enter the simulation with high existing debt levels, limited fiscal space, or structural exposure to climate damages face compounding pressures from both sides, lower revenues and higher expenditure needs, that the model tracks in full dynamic detail. By capturing all these dimensions within a single internally consistent general equilibrium framework, ICES-XPS provides a uniquely powerful tool for quantifying not only the macroeconomic costs of climate change but also the fiscal space constraints and debt sustainability risks that will shape governments' capacity to finance adaptation, maintain public services, and meet their long-run debt obligations over the coming decades.

The results section (section 1.3.2) analyses the implications of climate change impacts and adaptation across the full set of modelled channels, i.e. sea level rise, labor productivity, heat-related morbidity, agriculture, wildfire, biodiversity-related pollination loss and flooding, focusing on the SSP2 RCP7.0 pathway, which represents the highest emission scenario considered and generates the largest impacts and adaptation needs. Table 2 details the data sources and characterizes the adaptation scenarios for each channel.

Table 2. *Inclusion of impact dimensions and adaptation levels in the ICES model.*

Impact category	WP2 data source (model)	General configuration	Meaning Translation of adaptation levels		
			Low	**Reference**	**High**
Sea level rise	DIVA	GCM uncertainty: 50th quantile, including migration	Constant dike heights	Constant flood protection standards	Quadrupling flood protection standards
Flooding	GLOFRIS	GCM IPSL-CMSA-LR, no zoning	Constant dike heights	Constant flood protection standards	Optimal flood protection standards
Agricultural impacts	GLOBIOM	GCM IPSL, including RCP mitigation effects	Limited expansion of irrigation to already equipped areas	Sustainable irrigation expansion in equipped areas	Sustainable expansion of irrigation in equipped areas and conversion of rainfed areas
Labour	*Impact*: Labour productivity (CMCC) *Adaptation*: Sectoral energy demand estimated for agricultural, industrial and commercial sectors (CMCC)	GCM uncertainty: 50th quantile	Shift in sectoral energy demand under current income and no climate change (intensive margin)	Shift in sectoral energy demand to adapt to climate change under current income (intensive and extensive margin)	Shift in sectoral energy demand under climate change and income growth (intensive and extensive margin)
	Labour supply (CMCC)	GCM uncertainty: 50th quantile	No adaptation considered (not available from sectoral modeling)		
Health	*Impact*: Health (mortality and morbidity) *Adaptation*: Private household energy demand	GCM uncertainty: 50th quantile	Shift in household energy demand under current income and no climate change (intensive margin)	Shift in household energy demand to adapt to climate change under current income (intensive and extensive margin)	Shift in household energy demand under climate change and income growth (intensive and extensive margin)

Biodiversity loss	Yield shock due to pollination-related biodiversity loss (CMCC)	CLIM_RCP configuration: 50th quantile	No adaptation considered
Wilfire	Land loss due to wildfire	GCM uncertainty: 50th quantile	No adaptation considered

For each channel, the analysis disentangles the macroeconomic and fiscal consequences of climate damage from those of adaptation measures by separately examining the impact-only and adaptation-only scenarios, after presenting the combined total effect. This decomposition allows for a clearer understanding of the distinct roles played by climate damages, which erode output, incomes and fiscal revenues, and adaptation policies, which generate additional expenditure pressures while partially offsetting damages, in shaping the overall economic trajectory. Results are further disaggregated across three adaptation levels, low, reference and high, to assess how the scale of adaptation ambition modulates both the macroeconomic outcomes and the fiscal implications, and to identify the marginal returns to increasing adaptation effort across countries and impact channels.

Finally, a synthesis of the aggregate GDP loss and debt increase is provided, highlighting the contribution of each impact and explaining how much of this contribution is due to damage versus adaptation cost, thereby highlighting the different mechanisms at play in the case of GDP loss and debt accumulation. The results are presented for EU27+UK and EU macroregional aggregates.

1.3 Results

1.3.1 COIN-INT

This section gives an overview of the results obtained with the COIN-INT CGE model. In this subsection, we describe first the results for the combined impact channels across all European regions. Afterwards, the European scale analysis is completed by a case study analysis for the UK comparing different financing variants for public adaptation investment.

All results are expressed relative to a baseline without climate change until 2070, accounting for recursive dynamics. According to the ACCREU scenario protocol, all simulations are based on the SSP2 baseline scenario development, and considered for different warming levels (RCP2p6, RCP4p5 and RCP7p0). Results are shown for EU countries (excluding Malta and Cyprus due to restrictions in the model aggregation) and the United Kingdom (UKD), Switzerland (CHE) and Norway (NOR).

Macroeconomic effects: GDP and welfare effects

Macroeconomic effects are expressed in terms of effects on gross domestic production (GDP) across scenarios, impact channels and regions accumulating between 2020 and 2070. Figure 2 shows EU-wide estimates of GDP effects across warming scenarios for low, medium and high levels of adaptation until 2070. We find negative impacts on GDP evolve until 2070 and are highest for high warming scenarios under the assumption of low adaptation levels. In this scenario, GDP losses are estimated to accrue to up to 7% of annual GDP, compared to the no climate change baseline.

High levels of adaptation can reduce this effect by up to 3 percentage points, suggesting that adaptation is effective in mitigating the macroeconomic disruptions caused by the climate impacts considered. In addition to the adaptation level, we find that the warming scenario has a significant effect on estimated GDP effects. While In the medium run (2050), the choice of the adaptation scenario creates significant levels of variation, by 2070, the difference among warming levels becomes more distinct.

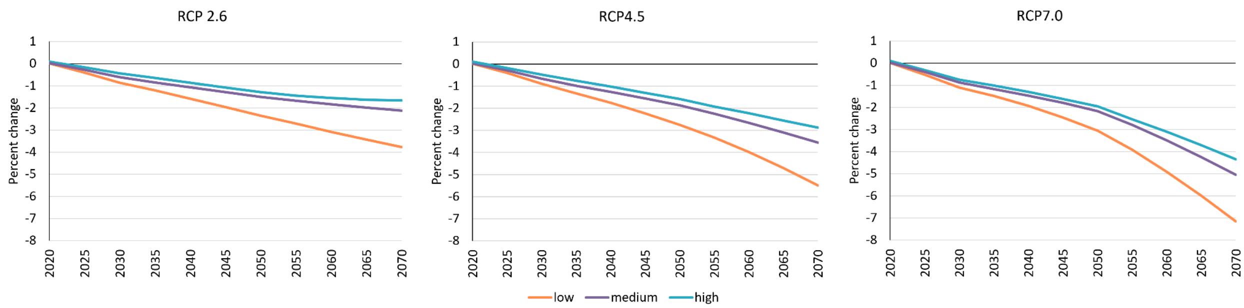

Figure 2. *GDP effects for the European Union (including the UK, Switzerland and Norway), for the model run with all impact channels, across RCP scenarios and for low, medium and high adaptation levels, percentage change relative to SSP baseline without climate change*

The results suggest that climate change reduces European real GDP. Generally, trends show that losses grow over time and vary between RCPs, as evident in Figure 2, where results are expressed relative to a baseline without climate change. The presented trajectories show that the level of adaptation is a relevant factor for residual impacts, as low levels of adaptation lead to especially severe GDP (and welfare) losses under all global warming scenarios. The observed pattern reveals that the disparity between low-adaptation levels and medium adaptation scenarios is consistently larger than that between the medium and high-adaptation scenarios.

Figure 3 pictures all separate impact channels by impact type and connects these model runs to joint model results. Due to the optimizing nature of CGE models, the sum of separate model runs will not line up with the joint run, but this quasi-decomposition helps to contextualise magnitudes of different impact drivers. This comparison shows that losses stemming from temperature-induced labour losses, moderated by energy usage for heating and cooling, are the most prominent driver. This is due to the fact that a disruption of the production factor labor affects all sectors within the economy, creating significant effects already in the first round which then further perpetuate across sectors and consumers. For the low adaptation scenario, sea level rise, floods and agricultural losses can be identified as significant drivers as well. Losses can be significantly moderated by higher adaptation levels. Temperature-induced labour losses exhibit the highest residual impacts, while GDP losses from sea level rise, agricultural impacts and to some degree flooding can be reduced considerably.

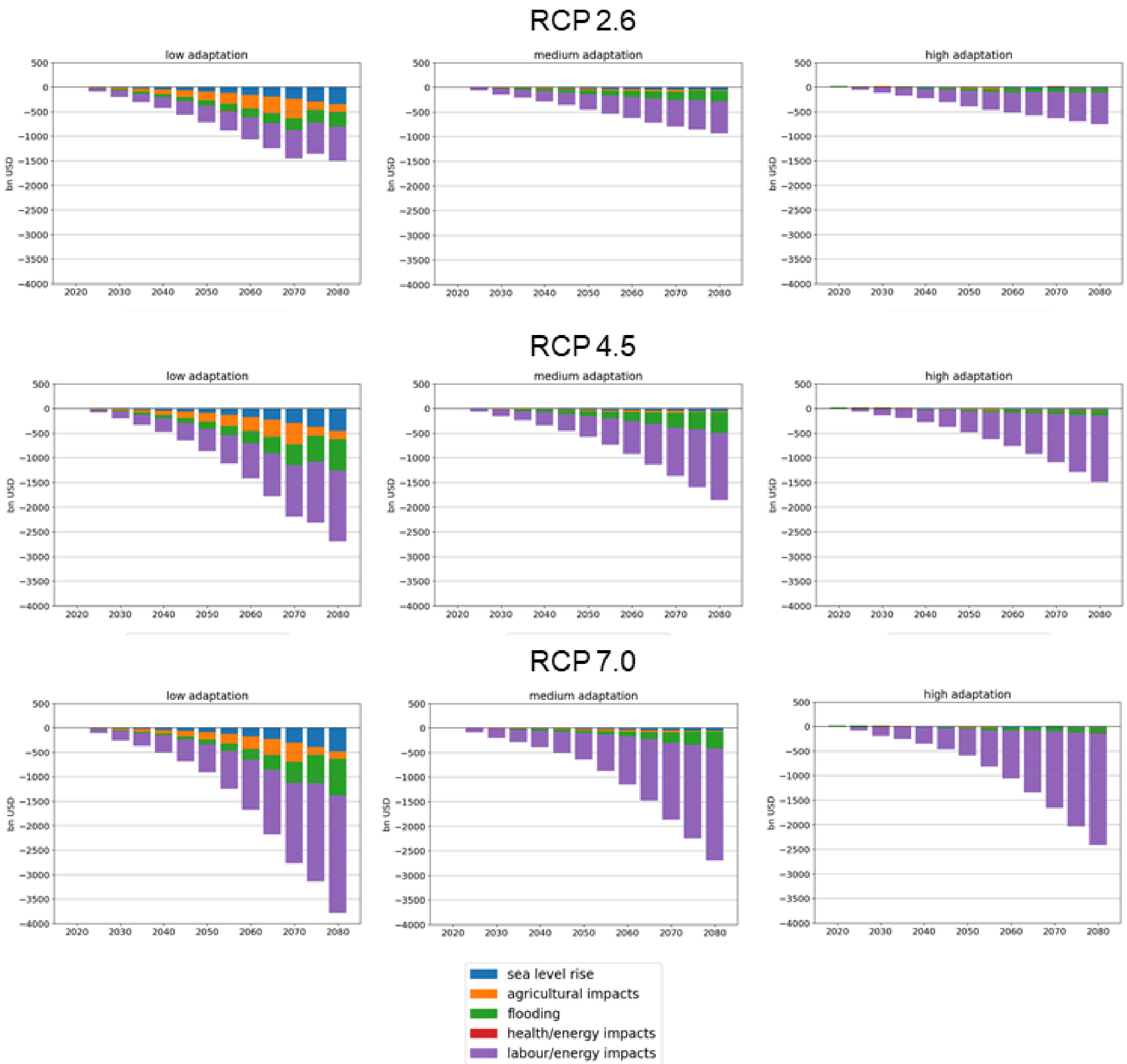

Figure 3. *Decomposition of GDP effects across impact categories and RCPs and with low, medium and high adaptation as an aggregation of separate model runs for sea level rise (DIVA), agricultural impacts (GLOBIOM and biodiversity loss), flooding (GLOFRIS), health/energy impacts (CMCC, BC3) and labour/energy impacts (CMCC).*

Figure 4 shows the main macroeconomic channels, through which aggregate real GDP effects relative to the reference adaptation scenario ("medium adaptation") can be analysed. The decomposition into expenditure categories demonstrates that under a low adaptation scenario, most additional GDP losses in Europe accrue due to reduced private consumption and private investments, and to some degree public consumption. In all higher adaptation scenarios for all RCPs, increased public adaptation investments can not only revert negative GDP losses, but lead to positive public consumption effects until 2070 for RCP2p6 and RCP4p5 compared to the reference adaptation scenario. Positive effects from increased public adaptation investments extend to private consumption and aggregate GDP, showing the potential of high adaptation levels. These effects are more pronounced towards 2070 by a factor of 2 compared to 2050, and much stronger discrepancies between warming scenarios. However, timely implemented adaptation yields significant benefits in terms of reduced losses for all, but particularly for private actors in the economy. This highlights the risk of climate change for a vast part of the macroeconomy and the importance of timely adaptation action that yields benefits especially in the future.

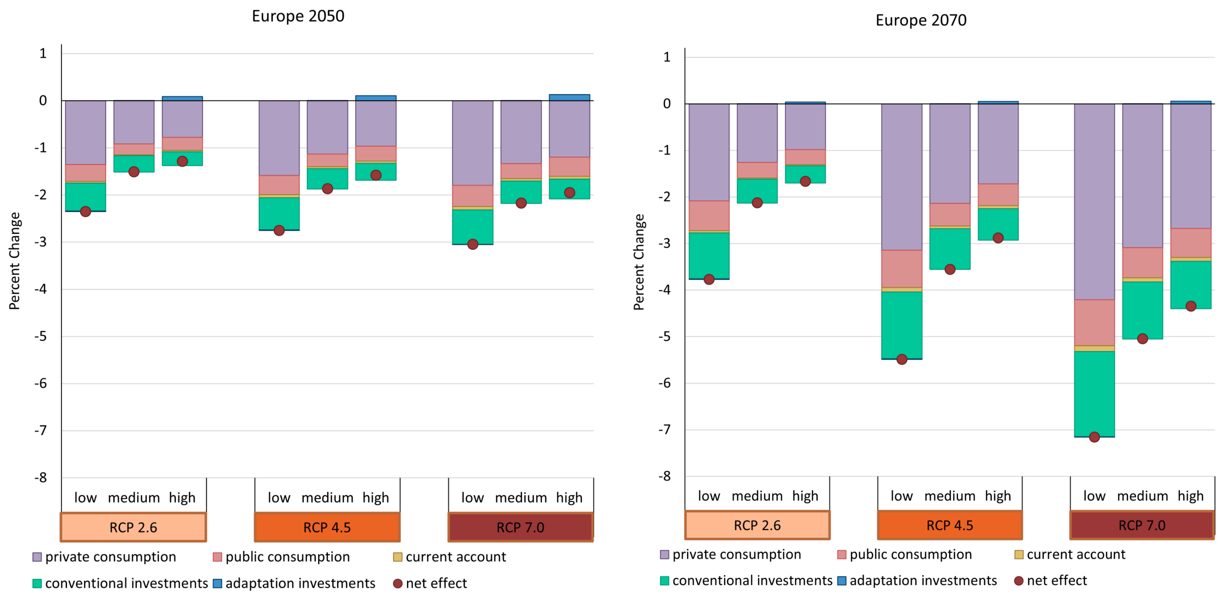

Figure 4. *Decomposition of GDP effects for European regions on the expenditure side relative to the baseline for different RCP scenarios and adaptation levels (low, medium, high); top panel: 2050; bottom panel: 2070. Adaptation investments in the panel refer to incremental public adaptation investments and conventional investments to investments made by private households.*

Effects by country and region

The country-specific results show that GDP effects are regionally heterogenous. On the country level, all countries experience net gains in terms of GDP from pursuing high levels of adaptation. As shown in Figure 5, GDP losses are significantly higher in panel a) reflecting low levels of adaptation compared to medium or high levels of adaptation illustrated in panels b) and c) respectively.

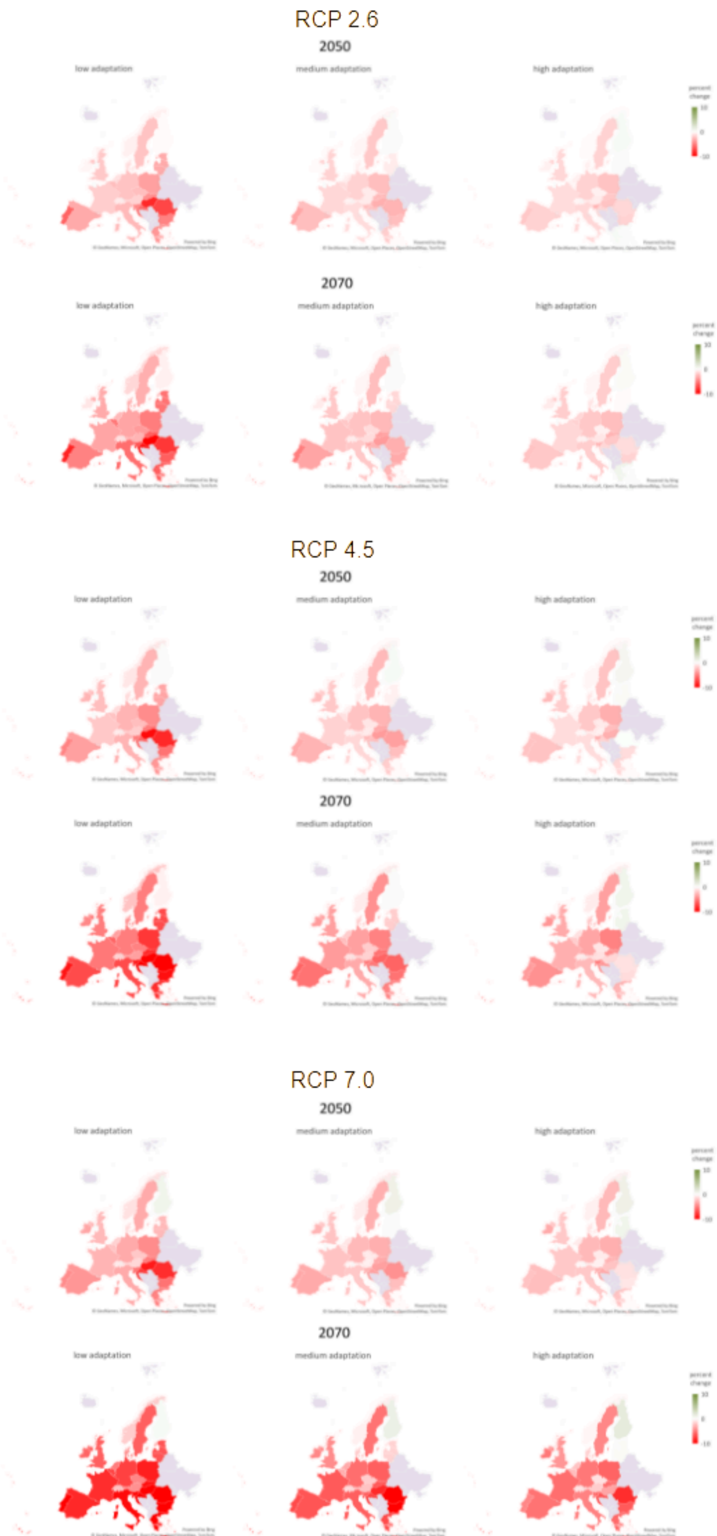

Figure 5. *Decomposition of GDP effects across countries for all RCPs compared to the baseline; top panel per RCP: period 2050; bottom panel: period 2070; left: low adaptation; middle: medium adaptation; right: high adaptation*

For an enhanced understanding of broader regional effects, we subsume countries into four wider European regions based on the regional aggregation from EUCRA, 2024.

As can be seen in Figure 6, Southern Europe and Central-Eastern Europe are especially at risk under all warming scenarios. In a medium warming scenario (RCP4.5) GDP losses for Central-Eastern Europe range from -3% to up to -9% until 2070 for high and low adaptation levels, respectively. While GDP effects are negative also for the regional aggregates of Western and Northern Europe, losses are significantly smaller (in the range of 2.6-4.7% of GDP by 2070). Also, while high levels of adaptation are consistently better in terms of GDP effects across scenarios, we see that differences between adaptation levels are less distinct compared to large differences across Southern and Central-Eastern Europe.

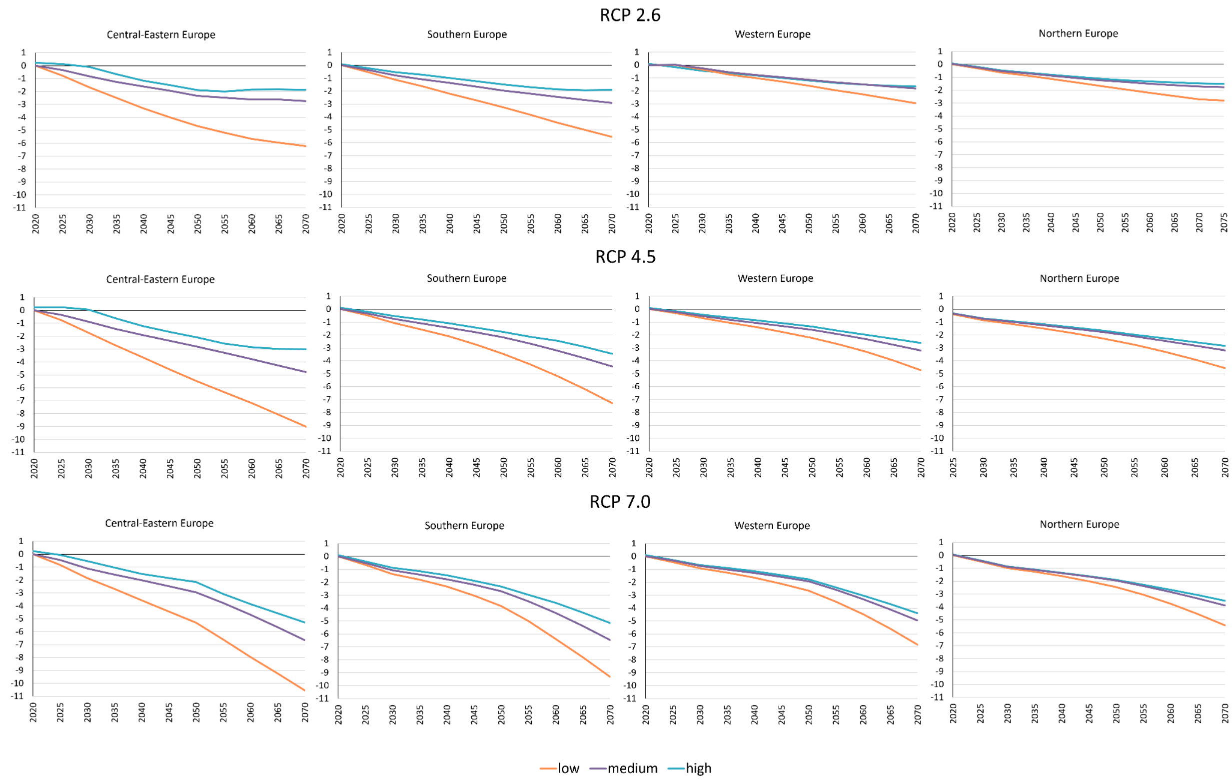

Figure 6. *GDP effects across European macroregions compared to the baseline, scenarios and with different adaptation levels; top: RCP 2.6, middle: RCP 4.5, bottom: RCP7.0*

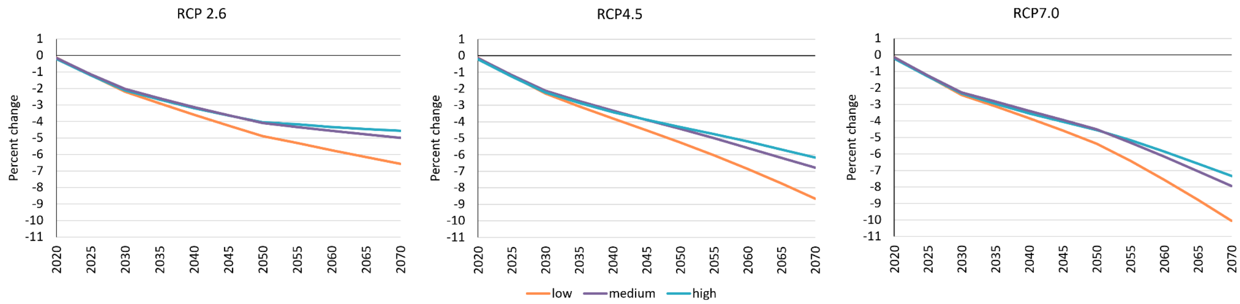

Figure 7. *Aggregated welfare effects for Europe across RCP scenarios and for low, medium and high adaptation levels, percentage change relative to the baseline*

Welfare effects (expressing changes in terms of private and public consumption levels and mortality) are reflective of overall GDP effects. Figure 7 shows how climate change affects welfare under different adaptation scenarios. Welfare is represented in terms of the Hicksian equivalent of welfare-enhancing private and public consumption and welfare losses from health-induced increased mortality. Consumption is considered welfare-enhancing when it does not represent incremental reconstruction costs that occur in order to restore the status-quo before disasters occured. Higher levels of adaptation reduce residual impacts on welfare for all warming scenarios.

Central-Eastern Europe and Southern Europe are most at risk from climate change impacts, as shown in Figure 8. Higher levels of adaptation translate to less severe welfare losses for all regions, under all RCPs.

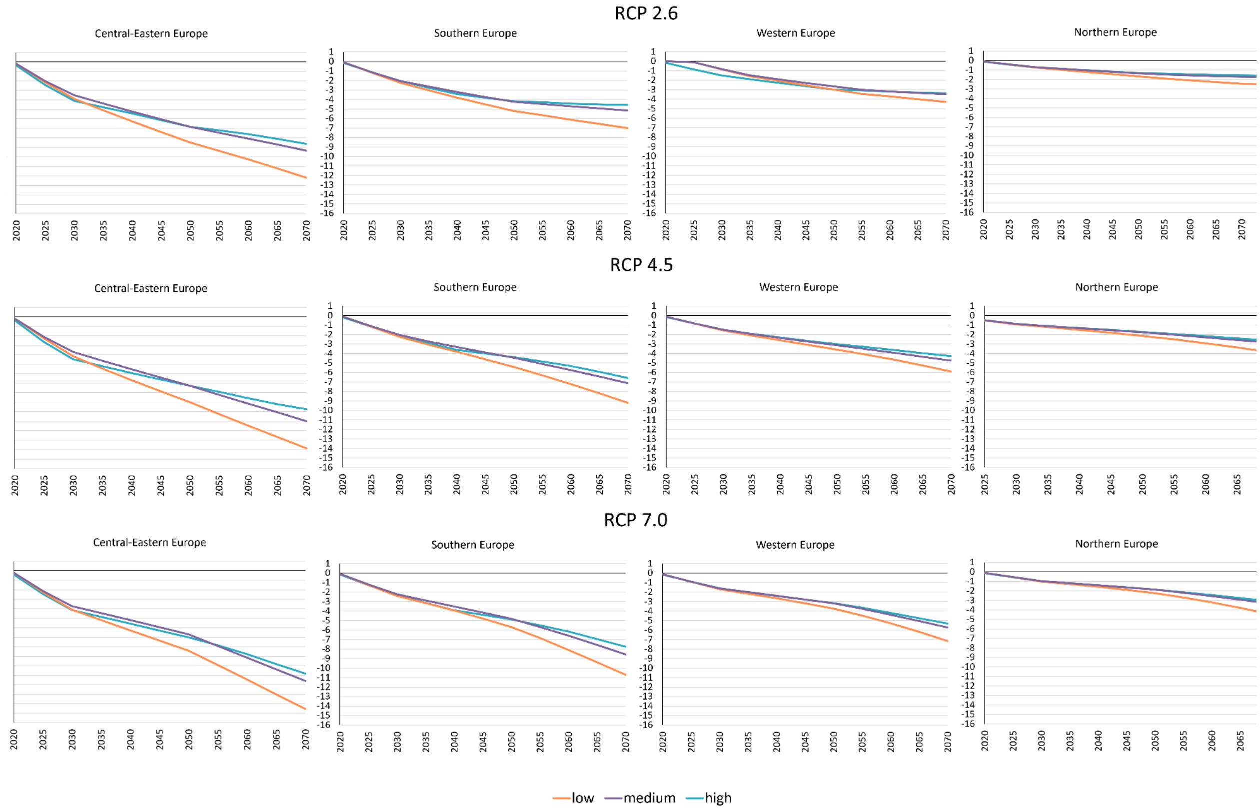

Figure 8. *Welfare effects across European macroregions compared to the baseline, for different warming scenarios and for low, medium and high adaptation levels; top: RCP 2.6, middle: RCP 4.5, bottom: RCP7.0*

Fiscal Effects

Figure 9 shows fiscal effects for all three RCPs under low, medium and high adaptation under budget-neutral financing in absolute terms aggregated for all European regions considered. Climate change impacts put pressure on public budgets through several channels. Damages to capital, labour stoppages, health impacts and other productivity losses in the economy erode the tax base, reducing public revenues, while at the same time they raise expenditure needs for certain public services. On the other hand, while adaptation can alleviate losses from climate change impacts, the implementation of adaptation requires funding, limiting other spending options. Based on the considered adaptation implementation pathways, upfront adaptation costs in the high adaptation scenario are generally higher in 2050 than in 2070, reflecting investment costs of flood protection infrastructure. Conversely, benefits of high adaptation levels compared to medium or low adaptation for the public finances are more distinct towards 2070, especially under high warming levels, where adaptation effectively reduces macroeconomic disruptions from climate impacts. In the results it becomes evident that higher adaptation spending can expand the fiscal space in all RCPs and over time alleviates the pressure exerted on public budgets. The cost of inaction within the low adaptation scenario is demonstrated by strong negative net effects on the fiscal space both in 2050 but especially in 2070 for all RCPs, limiting the government’s ability to deliver public services and transfers. In particular, significant additional losses on the revenue side, especially in the long run, are evident. In the high adaptation scenario, although additional adaptation investments limit spending on public consumption initially, the effect on public consumption is positive when compared to the low adaptation case, and net positive for RCP2p6 and RCP4p5 when compared to the reference adaptation.

Figure 10 relates annualised additional public investment needs to public revenue gains from adaptation as a difference between high and low adaptation level scenarios for the year 2050. This shows that all European countries in Europe gain fiscal space in 2050 through adaptation. The fiscal burden to finance adaptation however does result in differing benefits for the public budgets. Countries towards the upper left corner of the figure can benefit from higher returns on investment, while for countries towards the bottom right corner, like Bulgaria, costly investment in adaptation results in smaller fiscal gains. However, adaptation is always beneficial for the fiscal space, and revenue gains from timely adaptation can facilitate budget consolidation. This is of interest for high-debt countries with high potential for strengthening the fiscal space through adaptation, as evident in Figure 11. This figure relates the current debt-to-GDP ratio (EUROSTAT, 2025) to fiscal benefits from adaptation in 2050. It becomes evident that several countries with higher initial indebtedness, in particular Greece and Italy, can significantly gain fiscal space from adaptation, strengthening their budget consolidation strategy.

Figure 9. *Fiscal effects for Europe on revenue and expenditure side in nominal terms, for different RCP scenarios and with different adaptation levels; top: 2050; bottom: 2070*

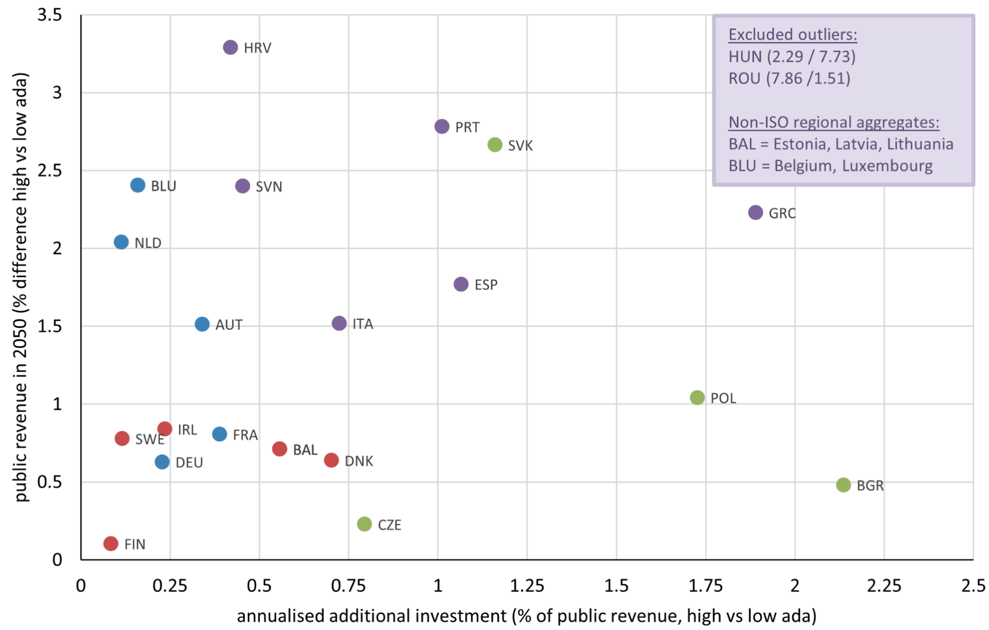

Figure 10. *Net gains from adaptation for government revenues in 2050 (vertical axis) in comparison to annualised adaptation finance needs until 2050 (measured by adaptation investment cost relative to government revenue; horizontal axis) for ISO-alpha3 regions in Europe; RCP 4.5, 2050*

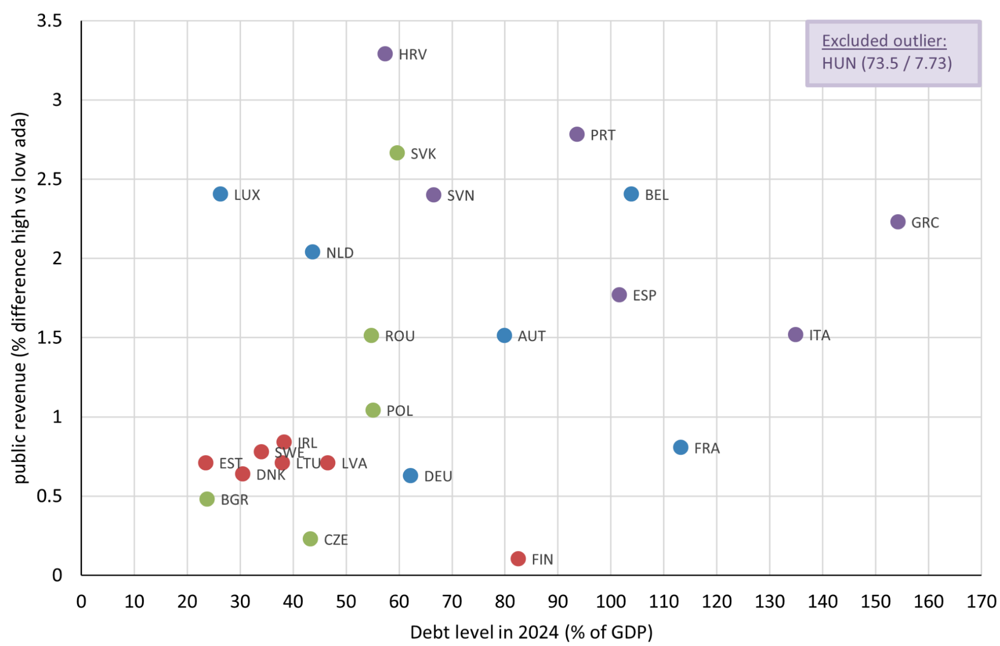

Figure 11. *Net gains from adaptation for government revenues (vertical axis) in comparison to government indebtedness (debt to GDP ratio, according to EUROSTAT, 2025) (horizontal axis); for ISO-alpha3 regions in Europe, RCP 4.5, 2050*

Case study: Fiscal effects under different financing mechanisms for flood adaptation in the UK

Employing a case study for public flood adaptation in the UK, we aim to explore the influence of the financing decision on the macroeconomic and fiscal outcome. We find that adaptation moderates both GDP and welfare losses from flooding, and increases the fiscal space under all financing mechanisms. However, the choice of financing mechanism and time horizon matter. Budget-neutral financing requires cuts in public consumption, which can be averted by deficit financing. However, domestic bond financing comes at the cost of suppressing private investment, which is not the case for international bond financing. Deficit financing allows for more spending opportunities and thus increased public consumption. Nevertheless, in the long run, this effect is counteracted by interest payments on accumulating public debt.

This effect is subject to uncertainty considering future lending conditions for green bonds. Therefore we analyse three different interest rate scenarios. We show that GDP effects as well as welfare effects considerably vary under three different interest rate environments and financing schemes. In particular, when higher interest rates put further pressure on the budget under debt financing, this aggravates the public household's ability to provide public services. Moreover, in the long run, higher interest rates lead to considerable payment flows abroad under international bond financing. However, under domestic bond financing, financial flows are bound within the economy and increase private households' disposable income, leading to less severe GDP and welfare effects. Still, all financing schemes lead to improvements compared to the case without adaptation.

The results demonstrate that fiscal outcomes depend on the financing decision, interest rate environments and the time perspective, while long-term welfare and wider macroeconomic effects benefit from timely implemented adaptation irrespectively.

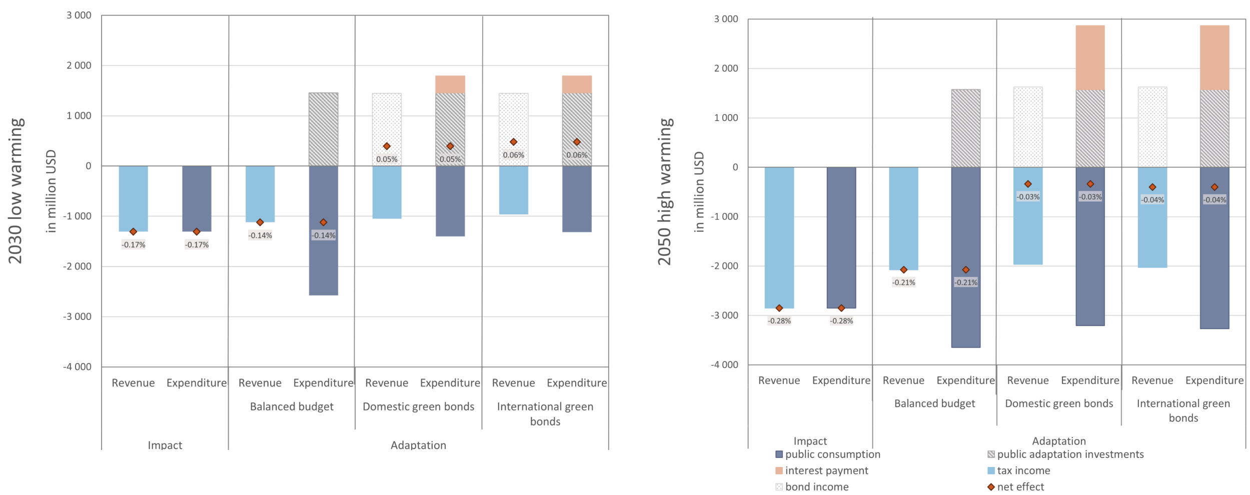

Figure 12. *Comparison of different government funding options in terms of fiscal effects for flood adaptation in the UK: budget neutral, domestic green bonds, international green bonds (for a medium interest rate environment); left: 2030; right: 2050*

1.3.2 ICES-XPS

This subsection presents the macroeconomic, fiscal, and debt sustainability implications of climate change across seven impact channels, i.e. sea level rise, labor productivity, heat-related morbidity, agriculture, wildfire, biodiversity-related pollination loss and flooding for EU27 and UK regions. The analysis is organized around three interconnected dimensions. First, the GDP and growth effects, which capture how climate damage and adaptation responses alter the trajectory of economic output relative to the baseline. Second, the budgetary implications, which quantify how climate change impacts and adaptation expenditure, through both government consumption and capital investment, affect the country's fiscal position. Third, the debt sustainability assessment, which examines how the interaction between lower growth and higher fiscal pressure shapes public debt trajectories across regions and scenarios.

Results are shown for low, reference, and high adaptation scenarios under the SSP2-RCP7 (high global warming) median scenario, allowing for a comparison of both the direct costs of inaction and the marginal returns and costs associated with different levels of adaptation ambition (Table 2 in Section 1.1.2 characterises the adaptation scenarios by channel). To allow for a consistent comparison, the three adaptation scenarios are expressed as percentage changes relative to the baseline scenario, which assumes no climate change impacts and no adaptation costs. The analysis covers the period 2020–2070, with particular attention to the acceleration of impacts in the second half of the century under higher emission pathways. All variables are deflated and expressed in real terms. The section examines each impact channel individually before concluding with an overall synthesis. The results are presented for EU27+UK and EU macroregional aggregates, disentangling the impact and adaptation channels.

Labor impact channel

The labor impact channel models the effect of heat stress on workers through two pathways: changes in labor supply (employment) and in labor productivity (differentiating between exposed and non-exposed sectors). The adaptation channel captures the changes in energy demand for cooling and for heating in indoor (industry and service) sectors; they are implemented as shifts of opposite signs in the efficiency of electricity and fossil fuel use for heating and cooling. For the labour impact channel, we consider only a private adaptation strategy.

Figure 12 shows the real GDP percentage change relative to the baseline for EU27 and UK countries under the labor impact channel, disaggregated by low, reference, and high adaptation scenarios over 2020-2070. The results present the total effect combining both climate impacts and adaptation responses. The "EU27+UK" aggregate, providing the overall impact for the region, experiences a GDP loss between 9.5% (high adaptation) and 10.8% (low adaptation). Almost all countries show monotonically increasing GDP losses over time, remaining limited before 2030 and accelerating markedly from 2035-2040 onward. The scenario ordering is consistent across virtually all countries and years, high adaptation (blue) shows the smallest losses, followed by reference (purple) and low (orange), confirming that higher adaptation ambition generates positive economic returns relative to inaction. However, the differences between scenarios remain modest relative to the total losses, suggesting that the adaptation measures modeled, primarily energy efficiency improvements for cooling, provide limited but consistent offsetting capacity and that more comprehensive strategies would be needed to meaningfully counteract the macroeconomic consequences of heat stress on labor productivity. A clear geographical gradient emerges, with Southern and Central-Eastern European countries experiencing the largest losses under low adaptation, at -12.4% and -12.3%, respectively. Cyprus, Romania, and Bulgaria reach losses exceeding 14% below baseline by 2070, reflecting their higher exposure to heat stress. While the lowest impact (less than 5%) is observed under reference and high adaptation (Estonia and Finland). Denmark, Finland, Estonia, and Lithuania show slightly positive values in early periods before turning negative, possibly reflecting positive effects of climate change in the short-term and positive effects of adaptation investment before climate damage dominates.

The results reveal a non-linear relationship between adaptation ambition and GDP losses, with the gap between low and reference adaptation being notably wider than between reference and high in several southern and eastern European countries, particularly Estonia, Greece, Finland, and Latvia, suggesting that the marginal returns to adaptation are highest at lower levels of ambition and that ensuring at least a moderate level of adaptation is critical to avoiding disproportionate economic losses in the most exposed regions.

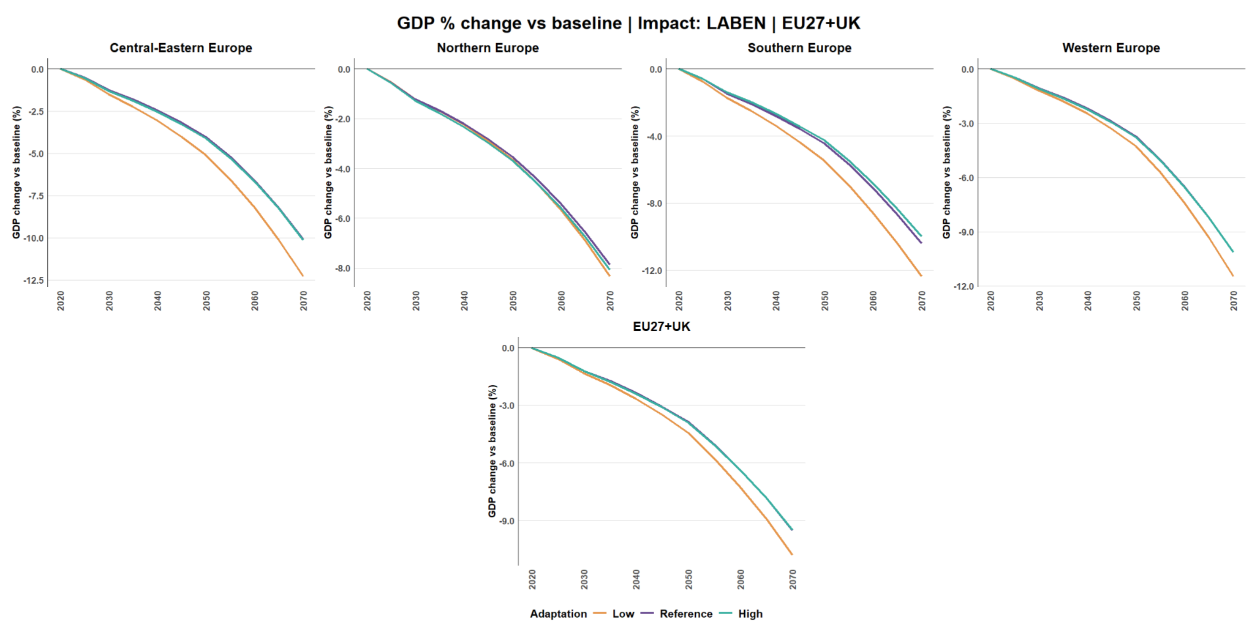

Figure 12. *Real GDP loss due to the labor impact channel across different adaption levels (with respect to the baseline scenario)*

Figure 13 shows the percentage change in real GDP and its main components relative to the baseline in 2070 across EU27 and UK countries under the labor impact channel. Solid bars represent the climate impact effect and transparent bars the adaptation cost effect, for low, reference, and high adaptation scenarios, the red mark indicates the composite effect. The component bars reveal how this aggregate loss is distributed across GDP components.

For the “EU27+UK” aggregate, the impact channel results are almost overlapping with the impact + adaptation scenario. All countries show negative GDP deviations consistent with the previous analysis, but the decomposition into impact and adaptation components highlights that climate damage is the dominant driver of GDP losses, with the adaptation measures modeled playing a limited role. Only in Central-Eastern Europe, adaptation bars show a slightly more pronounced effect on GDP and across components.

Investment is the largest contributor to GDP losses, at around 25% relative to the baseline for EU27+UK, reaching 28% in Southern, Central-Eastern, and Western Europe under the low adaptation scenario. This is a direct result of the contraction in private and public income reducing savings and resulting in lower investment. Countries such as Cyprus, and Romania show investment losses above 30% below baseline by 2070 due to the sole impact channel.

Private consumption shows the second largest drop up to 6.1% in a low adaptation scenario consistent with the income effect of reduced labor productivity on household spending. The influence of the adaptation channel on this result is negative although marginal in Central-Eastern Europe and Western Europe (in general higher demand for cooling and lower demand for heating by sectors has a small inflationary effect on energy prices and determines a small contraction of consumption). In the case of Greece, Bulgaria and Cyprus, the adaptation measures, particularly under reference and high adaptation scenarios, trigger a positive shift in investment and private consumption that marginally counteracts the impact results. In Estonia and Finland, the adaptation measures have a negative impact on investment, private and public expenditure.

Net exports show mixed patterns, some countries experience deterioration while others show slight improvement, reflecting differences in trade openness and the relative competitiveness effects of the shock across trading partners. Government expenditure changes are very small and close to zero across all countries, as expected since the scenario does not directly affect the fiscal stance.

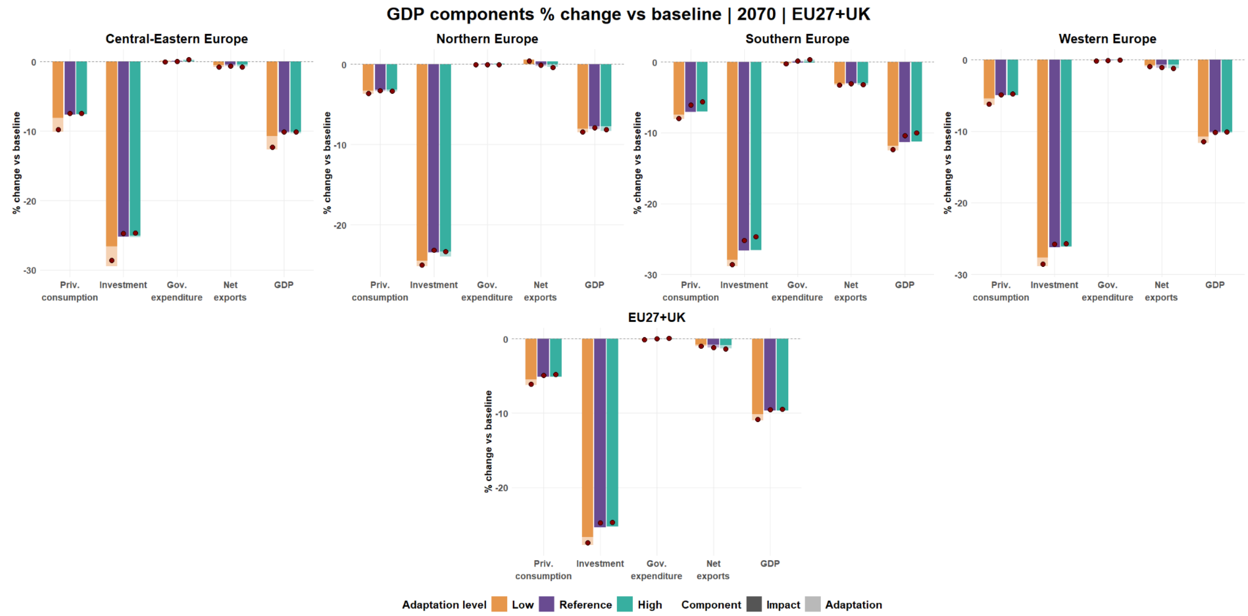

Figure 13. *GDP components change due to the labor channel across different adaption levels (with respect to the baseline scenario)*

Figure 14 shows the percentage change in four key fiscal variables, government income, government investment, net lending/borrowing, and public debt, relative to the baseline in 2070 across EU27 and UK countries under the labor impact channel, decomposed into impact (solid) and adaptation (transparent) effects for low, reference, and high adaptation scenarios. The most pronounced fiscal effect operates through the government income channel; climate damages compress factor incomes across the economy, directly eroding the tax base and reducing government revenues relative to the baseline. The tax revenues contraction is higher than 3% for all EU countries and Cyprus and Romania experience the strongest cut, respectively 17.3% and 13.8% with respect to the baseline results. For the EU27+UK, the government income loss ranges between 20.8% under low adaptation and 19.5% under reference adaptation. The contraction in government income is widespread across all EU countries, but Southern and Western Europe show the strongest changes respectively -24.4% and 21.5%.

This revenue narrowing propagates through the fiscal accounts, squeezing government savings and, despite a contraction in public investment, all countries increase their reliance on net borrowing, ultimately driving public debt above baseline levels. At the EU27+UK aggregate level, public debt expands by between 15.4% under the reference adaptation scenario and 16% under the high adaptation scenario relative to the baseline. Notably, the small reduction in debt attributable to lower climate damages under higher adaptation is completely offset by the shifts related to the sectoral adaptation choices, resulting in a net debt level that is marginally higher under high than under reference adaptation; the reference adaptation scenario is the one guaranteeing a marginally lower pressure on debt accumulation. Public debt rises above baseline in all countries by more than 5%, but the Western Europe reaches the high debt levels independently on the adaptation scenarios. Countries such as Luxembourg, Germany and Sweden show particularly large debt deviations, suggesting potential debt sustainability concerns under high climate damage scenarios.

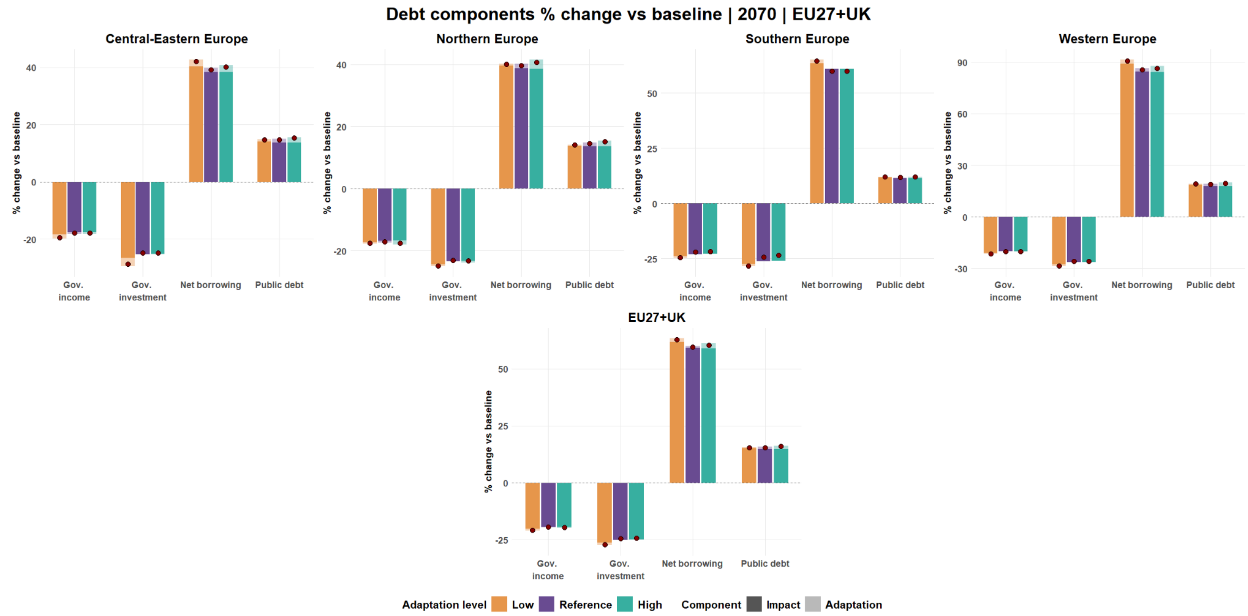

Figure 14. *Changes in public debt components due to the labor channel across different adaptation levels (with respect to the baseline scenario)*

SLR impact channel

Sea level rise (SLR) impacts are transmitted into the ICES-MH model through two channels, impact and adaptation, each derived from DIVA variables and applied to distinct production factors. On the impact side, Expected Annual Damages are combined with annual asset values to generate a shock on capital stock, while Expected People Flooded are combined with the year's population to estimate the affected share, which is then converted into a labor productivity shock assuming an average flood recovery time of two weeks (Parrado et al. 2020; Bachner et al. 2022). Land loss is applied directly as a shock to the land stock, limited in ICES-XPS to agricultural land. Displaced Population generates two simultaneous effects: a labor productivity shock, using a longer recovery time of 13 to 52 weeks to reflect the more disruptive nature of permanent displacement (Athey et al. 2023), and a capital stock shock capturing migration-related asset losses, again computed by combining the displaced population with annual asset values. On the adaptation side, the costs of coastal protection measures (sea dikes) are translated into fiscal shocks: the investment cost of building dikes is applied as a shock to government investment, while their maintenance cost is applied as a shock to government expenditure in the construction and public service sectors, which also feeds through to a coherent shock on total government expenditure. A further methodological adjustment was applied to the adaptation investment shocks. Since government investment as reported in the CGE model captures only the real component of public capital formation, the adaptation investment shocks were rescaled, reflecting the assumption that 60% of total adaptation costs translate into real government investment, with the remaining associated with financial and transaction costs that do not directly enter the real economy as productive capital formation. Together, these mechanisms mean that impact shocks degrade the economy's productive factors, capital, labor, and land, through damage and displacement pathways with differentiated recovery assumptions, while adaptation shocks represent the fiscal burden of protective infrastructure, entering the model through government investment and spending rather than directly affecting productive capacity.

Figure 15 presents the real GDP percentage change relative to the baseline for EU27 and UK countries under the sea level rise (SLR) impact channel, showing the combined effect of climate impacts and adaptation responses across low, reference and high adaptation scenarios over the 2020-2070 horizon. The “EU27+UK” aggregate experiences a GDP loss between 2.8% (high adaptation) and 4.2% (low adaptation). The low adaptation scenario (orange) consistently shows the largest GDP losses, while the reference (purple) and high (blue) adaptation scenarios produce almost overlapping results, indicating that the marginal benefit of moving from reference to high adaptation is limited. This pattern suggests a significant value added in scaling up adaptation from low to reference level, while the additional gains from further increasing ambition to the high scenario are comparatively modest, pointing to diminishing returns to adaptation investment beyond a moderate level of effort. The GDP losses are very similar across regions, slightly more pronounced in Central-Eastern (-4.4%) and Western Europe (-4.3%). Furthermore Central-Estern Europe shows the lowest gap between low and reference/high adaptation likely related to low effectiveness of adaptation measures or high adaptation costs. Belgium, Ireland, Denmark, and Latvia are the most impacted countries, with Belgium reaching the largest loss at approximately -8%. Switching from low to reference adaptation almost halves the GDP losses in Belgium, Denmark, UK and Croatia, further confirming the significant returns to moving from minimal to moderate adaptation effort identified across impact channels.

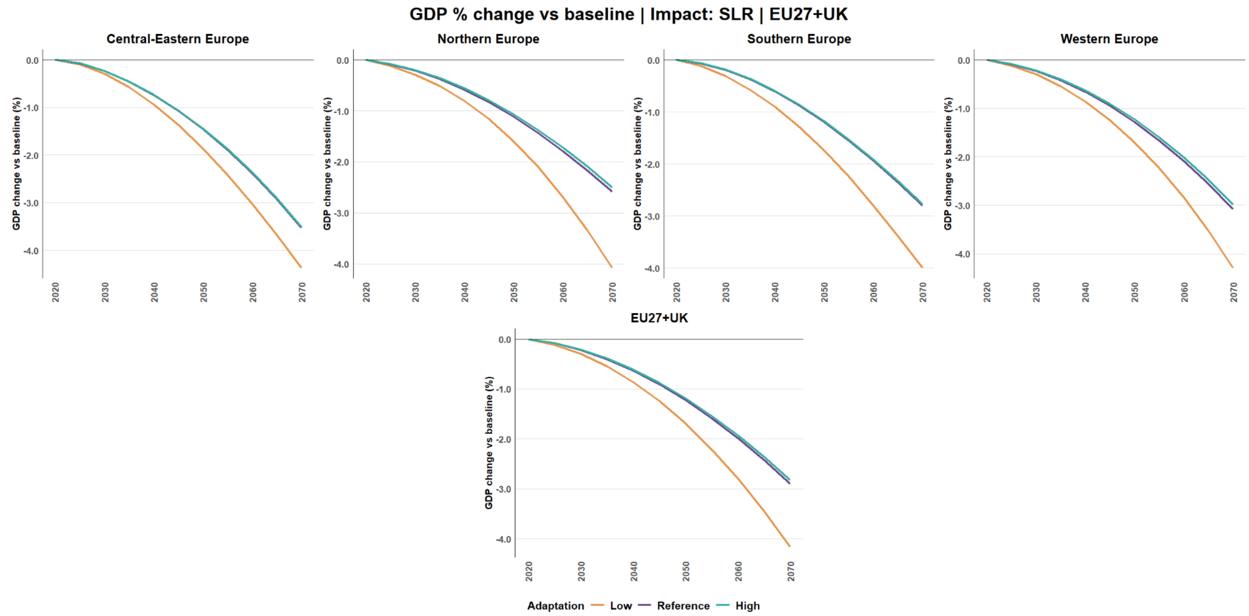

Figure 15. *Real GDP loss due to the SLR impact channel across different adaptation levels (with respect to the baseline scenario)*

Figure 16 shows the percentage change in GDP and its main components relative to the baseline in 2070 across EU27 and UK countries under the SLR impact channel. For each adaptation level, the results separate the climate impact effect (solid bars) from the adaptation effect (transparent bars); the red marker indicates the combined outcome of both shocks together. At the EU27+UK aggregate level, the adaptation and impact channels are of comparable magnitude under the low adaptation scenario, with adaptation costs generating GDP losses broadly similar to those attributable to climate damage (-2.2% versus -1.9%). Although low adaptation implies only additional government expenditure to cover maintenance costs, with no government investment, the similar magnitude of the GDP losses between the adaptation and impact channels may partly reflect the fact that each scenario is deflated by its own price index. Since prices rise under the adaptation scenario and fall under the impact scenario, this amplifies the real GDP loss in the adaptation scenario and dampens it in the impact scenario, making the two appear more similar than the underlying nominal effects actually are. Under reference and high adaptation scenarios, however, the adaptation channel dominates, i.e. the macroeconomic costs of adaptation measures exceed those of the climate impacts themselves, reflecting the substantial public investment and expenditure required to implement higher levels of coastal protection and the associated crowding-out effects on private demand components. The other side of this trade-off, however, is that reference and high adaptation levels almost entirely cancel out the SLR-related climate damage, suggesting that while adaptation is costly in macroeconomic terms, it is highly effective at neutralizing the direct economic losses from sea level rise.

Investment is the strongest channel of GDP reduction in the region: it contracts by approximately 9% under the adaptation channel alone, both in the reference and high adaptation scenarios, compared to a contraction of less than 1% under the impact channel alone. This gap reflects the crowding-out of private investment by the large increase in public investment required to finance coastal protection, which competes with private capital for available savings and depresses private investment disproportionately. Under the low adaptation scenario, both channels contribute to the investment contraction, with the impact channel generating a 3.6% decline and the adaptation channel a 7.6% decline, suggesting that even at lower levels of adaptation ambition, the fiscal pressure of adaptation measures already dominates the direct damage effect on investment. Central-Eastern and WesternEurope appear to show the steepest investment contractions under high adaptation via the adaptation channel (in the range of -9.5%). At the country level, Ireland shows the largest investment drop, at around 11%, driven by the adaptation channel alone (high adaptation scenario).

Government expenditure rises by approximately 3% at the EU27+UK level, this outcome is entirely driven by the maintenance costs associated with coastal protection infrastructure. This component is more pronounced in Northern (6.2%) and Western Europe (3.3%). Net exports and private consumption show modest declines across all scenarios. In summary, the GDP loss observed in the region is primarily driven by the crowding-out of private investment by public investment requirements, and this negative effect is not sufficiently counterbalanced by the increase in government expenditure, resulting in a net contraction of aggregate demand and output relative to the baseline.

Figure 16. *GDP components change due to the SLR channel across different adaptation levels (with respect to the baseline scenario)*

Figure 17 shows the percentage change in four key fiscal variables, government income, government investment, net lending/borrowing, and public debt, relative to the baseline in 2070 across EU27 and UK countries under the SLR impact channel, decomposed into impact (solid) and adaptation (transparent) effects for all adaption level scenarios with the red marker indicating the combined outcome. At the EU27+UK aggregate level, we observe a small contraction in government income ranging from 0.5% (impact channel under high and reference adaptation) to around 5% (adaptation channel under high and reference adaptation). In the low adaptation scenario, the main driver is the reduction in tax revenues caused by climate damage, whereas in the reference and high adaptation scenarios it is the contraction of total and private investment, driven by public investment crowding out private investment for available capital. Southern Europe is the most exposed to the government income contraction under low adaptation (-7.7%), followed by Central-Eastern Europe. At the country level, Belgium and Ireland show the strongest government income contractions in the low adaptation scenario, reaching approximately 10%, reflecting their high coastal exposure and relatively large government adaptation expenditure relative to the size of their economies.

In the region, government investment rises the most under the high adaptation scenario (6.7%), whereas it contracts under the low adaptation scenario. This trend is more pronounced in Northern Europe, although Belgium shows the strongest variation.

To finance the additional public investment and the contraction of government income, governments increase their reliance on borrowing, with net lending rising in the EU27+UK aggregate by approximately 32% above baseline in the adaptation-only scenarios. This increased borrowing translates into a moderate but persistent expansion of public debt, which rises by slightly less than 10% above baseline in the reference and high adaptation scenario, highlighting the long-run fiscal implications of sustained adaptation investment even in the absence of direct climate damage. The strongest debt surge is observed in Northern Europe (+13%). At the country level, Denmark, the Netherlands, and Latvia show the largest increases, driven by the high adaptation costs associated with coastal protection under the reference and high adaptation scenarios. These countries, characterized by extensive low-lying coastlines and high asset exposure, face particularly large adaptation investment requirements that generate substantial borrowing needs and persistent upward pressure on public debt.

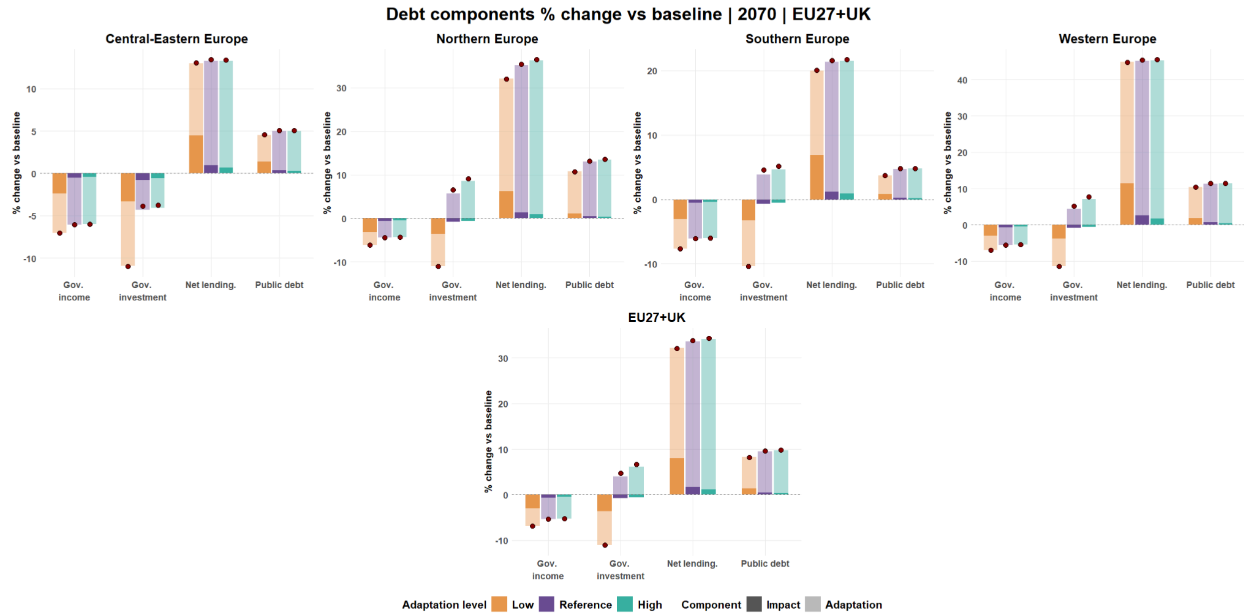

Figure 17*. Changes in public debt components due to the SLR channel across different adaptation levels (with respect to the baseline scenario)*

Health impact channel

The health impact channel models the effects of climate change on human health through two pathways. The impact component captures mortality effects through a shock on population growth, not altering the labor force, and morbidity costs through a shock on government expenditure in the health sector, with a coherent adjustment to total government expenditure reflecting the additional public resources required to treat climate-related illness. Unlike the COIN-INT model, we do not consider the value of a statistical life (VSL) loss under climate change impacts as a proxy for mortality. The adaptation component captures the behavioral response to rising temperatures through shifts in residential electricity and fossil fuel demand for cooling and heating, reflecting changes in household energy consumption patterns as populations adapt to warmer conditions.

Figure 18 presents the real GDP percentage change relative to the baseline for EU27 and UK countries under the health impact channel, combining climate impacts and adaptation responses across low, reference, and high adaptation scenarios over 2020–2070. It is worth noting first the very narrow scale of impacts. At the EU27+UK aggregate level, GDP remains slightly below the baseline in 2070 across all scenarios, at -0.02% under low adaptation, -0.15% under reference adaptation, and -0.14% under high adaptation. Despite the narrow magnitude of impacts, GDP losses peak around 2050 before declining. Health-related impacts also generally imply only a small GDP loss across all macro-regions, with two exceptions: Central-Eastern Europe under the low adaptation scenario, and Southern Europe under the high adaptation scenario.

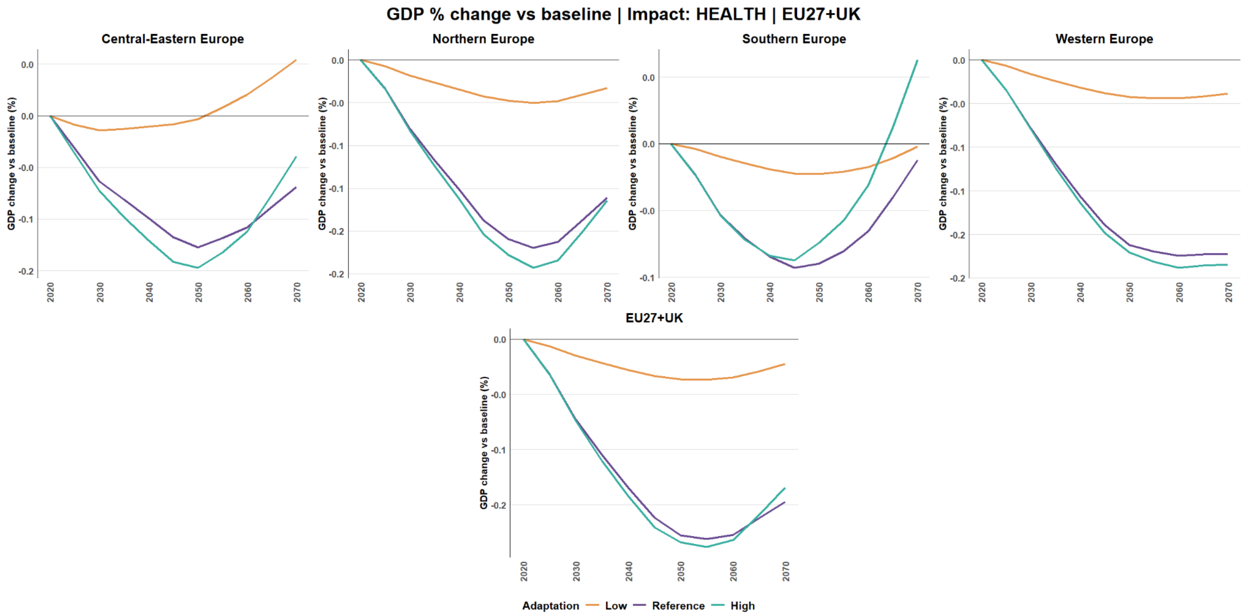

Figure 18. *Real GDP loss due to the health impact channel across different adaptation levels (with respect to the baseline scenario)*

Figure 19 shows the percentage change in GDP and its main components relative to the baseline in 2070 across EU27 and UK countries under the health impact channel. For each adaptation level, results are decomposed into the climate impact effect (solid bars) and the adaptation effect (transparent bars), and overall effect (red marker). At the EU27+UK aggregate level, the GDP loss related to health dimension in 2070 is driven almost entirely by the adaptation channel rather than by residual climate impacts, excluding the low adaptation scenario.

Decomposing the adaptation channel by GDP component, we see that the variation is narrow across the board, ranging between -1% and 1%. Government expenditure rises in response to the climate-driven increase in morbidity, while net exports drop slightly, as resources are drawn toward health services (a non-tradable sector) at the expense of tradables. Analysing the adaptation channel, we observe a rise in real private expenditure on energy, driven by the shift in household energy demand. This increase in private consumption crowds out real investment, as resources are diverted away from savings-financed capital formation. Government expenditure rises slightly, and net exports decline further, likely reflecting increased energy imports to meet the higher domestic demand. Part of this apparent magnitude, however, may reflect the fact that each scenario is deflated by its own price index and the adaptation scenarios are characterised by higher prices compared to the impact scenarios. Overall, these results indicate that under climate-related health impacts, implementing adaptation measures has a small negative effect on GDP.

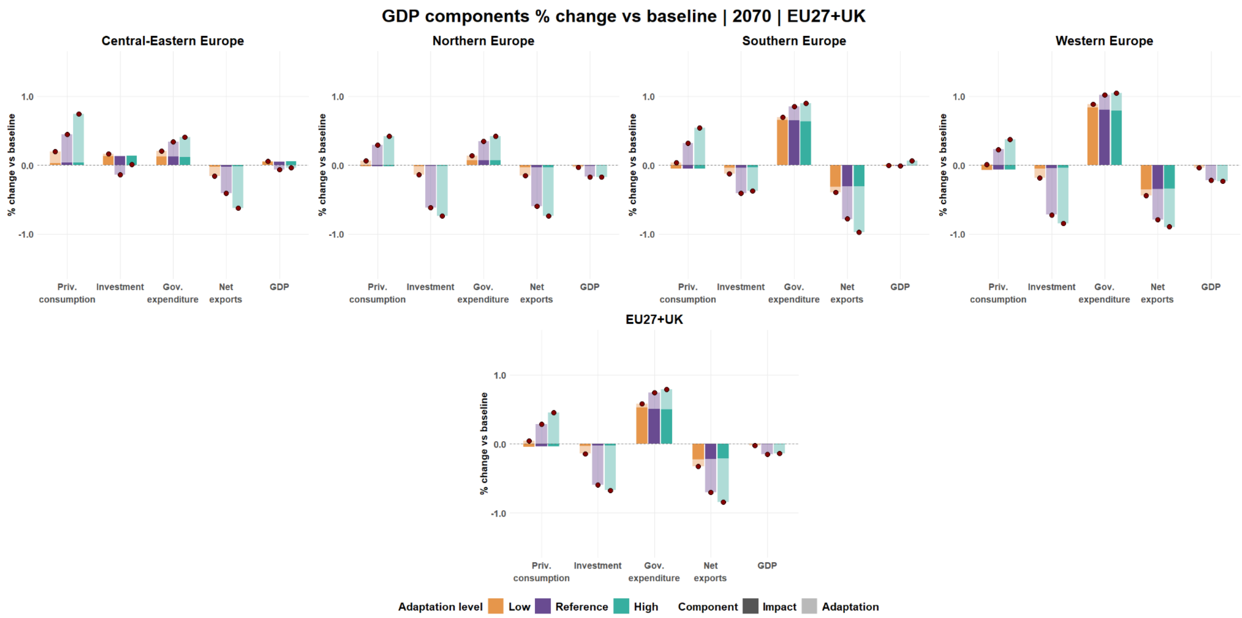

Figure 19. *GDP components change due to the health channel across different adaptation levels (with respect to the baseline scenario)*

This pattern is mirrored, and amplified, in the fiscal variables (Figure 20). Government income deteriorates as adaptation ambition rises, ranging from -0.2% under low adaptation to -1.5% under reference adaptation and -1.9% under high adaptation via the adaptation channel. This effect becomes more evident at the increase of adaptation which implies lower investment (crowding out with private expenditure), slowed down capital formation and reduced capital revenues. The reduction of public savings translates into a rise in net borrowing, which increases from 1.2% under low adaptation to 5.8% under reference adaptation and 7.5% under high adaptation via the adaptation channel, dwarfing the impact channel's contribution of around +1.7% to +1.8%. As a result, public debt rises correspondingly, from 0.9% (low) to 2.3% (reference) and 2.7% (high). Central-Eastern Europe reaches a 4.3% debt increase under a high adaptation scenario. Overall, these results indicate that climate-related health impacts imply modest GDP loss and public debt rise, with the cost of implementing adaptation measures playing a major role in driving these outcomes. It is worth noting that the impact and adaptation scenarios follow different price paths: the impact scenario shows a negative aggregate price effect, as population loss reduces overall demand more than the targeted rise in morbidity-related spending can offset, while the adaptation channel raises the overall price.

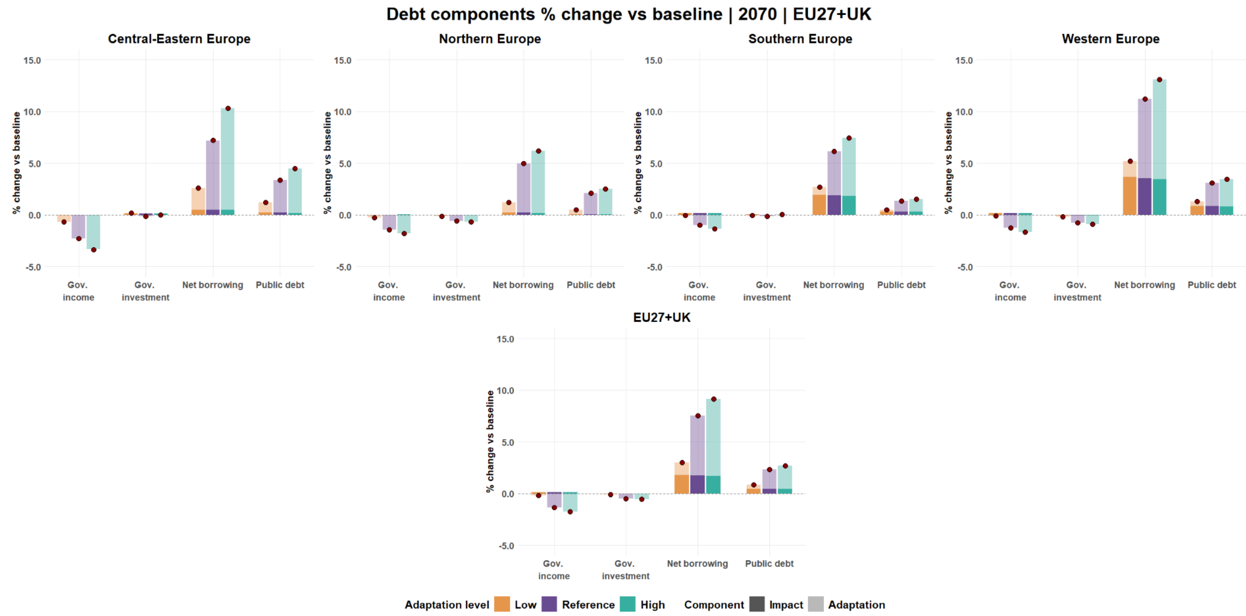

Figure 20. *GDP components change due to the health channel across different adaptation levels (with respect to the baseline scenario)*

Flood impact channel

The flood impact channel models the macroeconomic consequences of river and coastal flooding through two distinct impact pathways. The first operates through physical capital damage: Expected Annual Damages (EAD) from GLOFRIS model are combined with sectoral capital asset values from the ICES model to compute annual shocks on sectoral capital stocks, capturing the destruction of productive capacity across agriculture, industry and services. The second operates through labor productivity: the Expected Affected Population (EAP) is combined with the total population of the year to compute the annual share of the workforce affected by flooding events, which is then converted into a labor productivity shock under the assumption that recovery takes on average two weeks, following Parrado et al. (2020) and Bachner et al. (2022). The adaptation component captures the costs of flood protection infrastructure through two channels. Dike investment costs are modelled as a shock on government investment, computed by adding the adaptation investment costs to baseline public investment, reflecting the capital expenditure required to build or raise flood protection structures. Dike maintenance costs are modelled as a shock on government expenditure in the construction sector, computed by adding the annual maintenance costs to baseline public expenditure in construction, with a coherent adjustment applied to total government expenditure to ensure macroeconomic consistency. A further methodological adjustment was applied to the adaptation investment shocks. Since government investment as reported in the CGE model captures only the real component of public capital formation, the adaptation investment shocks were rescaled by a factor of 0.6, reflecting the assumption that 60% of total adaptation costs translate into real government investment, with the remaining associated with financial and transaction costs that do not directly enter the real economy as productive capital formation.

Figure 21 shows the real GDP percentage change relative to the baseline for EU27 and UK countries under the flood impact channel, disaggregated by low, reference, and high adaptation scenarios over 2020-2070. The results present the total effect combining both climate impacts and adaptation responses.

The “EU27+UK” aggregate shows a GDP loss between 2.8% (low adaptation) and 2.1% (high adaptation). At the regional level, some heterogeneity emerges both in the magnitude of impacts (strongest in Central-Eastern under low adaptation,at -3.8%, and lowest in Northern, at -1.8%). In Northern, Southern, and Western Europe, high adaptation levels imply almost the same GDP losses as reference adaptation. At the country level, significant heterogeneity emerges both in the magnitude of losses and in the scenario ordering. Hungary shows the largest losses, reaching -5.7% below baseline by 2070 in the low adaptation scenario, followed by Slovakia and Romania.

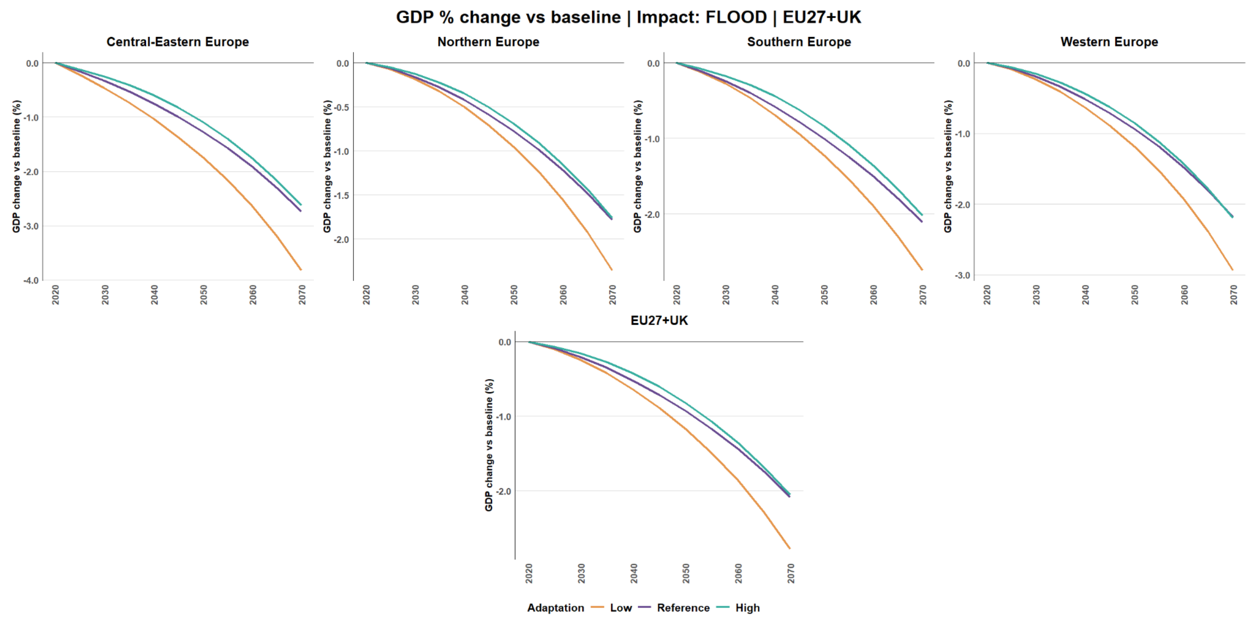

Figure 21. *Real GDP loss due to the flood impact channel across different adaptation levels (with respect to the baseline scenario)*

Figure 22 shows the percentage change in GDP and its main components relative to the baseline in 2070 across EU27 and UK countries under the flood impact channel. For each adaptation level, results are decomposed into the climate impact effect (solid bars) and the adaptation effect (transparent bars), and combined effect (red marker).

From a quick look, it is evident that the adaptation channel is not relevant in defining the overall result for the low and reference adaptation levels. The impacts are driving GDP loss compared to the baseline, excluding in the high adaptation scenario .

Among the GDP components, investment proves to be the most sensitive, contracting sharply under the sole-impact scenario because of the broader economic contraction. As expected, the investment contraction is more pronounced under low-adaptation assumptions and diminishes as the level of adaptation protection increases, but under reference and high (optimal) adaptation, the crowding-out effect of public investment also progressively reduces investment. However, the impact-related investment reduction always plays a major role in EU27+UK. Private consumption and net exports slightly reduce and government expenditure increases due to the maintenance adaptation costs.

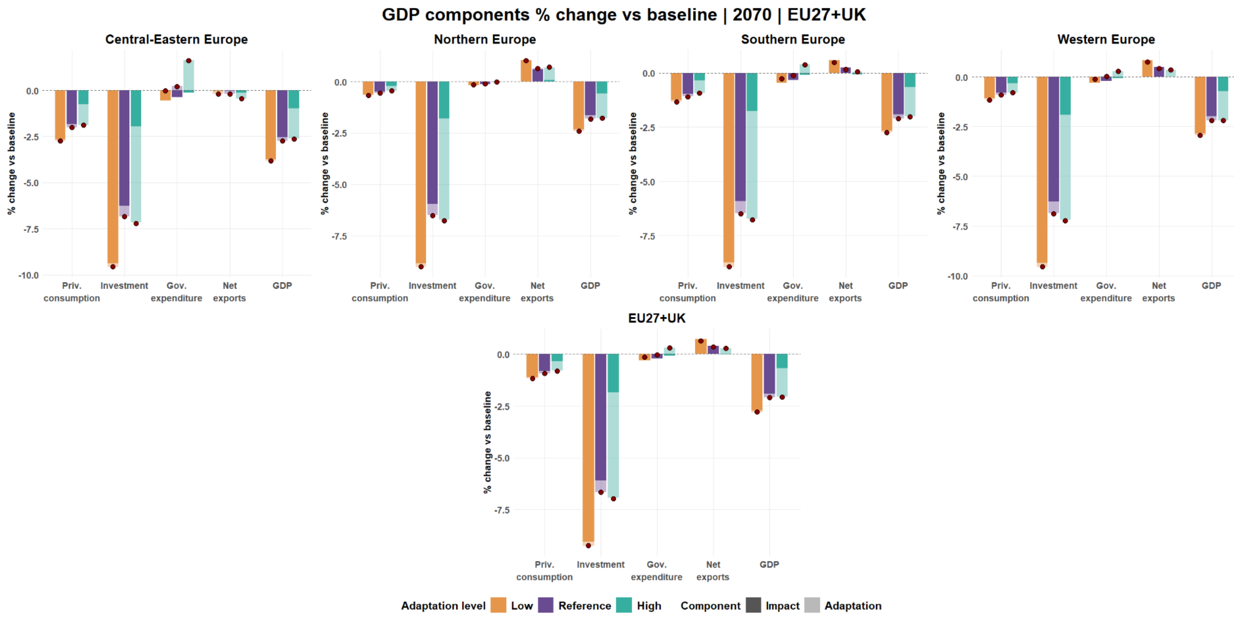

Figure 22. *GDP components change due to the flood channel across different adaptation levels (with respect to the baseline scenario)*

Figure 23 focuses on the percentage change in four key fiscal variables, government income, government investment, net lending/borrowing, and public debt, relative to the baseline in 2070 across EU27 and UK countries under the flood impact channel, decomposed into impact (solid) and adaptation (transparent) effects for all adaption level scenarios. The figure shows that when considering debt sustainability, the level of adaptation also plays a relevant role.

At the EU27+UK aggregate level, we observe a change in government income ranging from -5.2% (low adaptation) to -3.7% (reference adaptation). Government income shrinks following the contraction of tax revenues related to flood damage (impact channel) and is more pronounced in Southern and Western Europe. At the country level, Cyprus, and Hungary show the strongest government income contraction, around -7.9%.

This effect cumulates with a reduction in government investment due to the impact channel under the low adaptation scenario, which is counterbalanced by a rise in government investment for adaptation, reaching up to 12% under the reference adaptation scenario. This rise in government investment under reference adaptation is particularly evident in Western Europe.

Reliance on net borrowing is therefore increasing under the low adaptation scenario, due to the government income contraction related to the impact channel, whereas under the reference and high adaptation scenarios, the rise in government investment and the reduction of government income related to the adaptation channel adds to this effect. This rise in reliance on net borrowing pushes debt accumulation. This reinforcing effect is particularly evident in the high (optimal) adaptation scenario, where the 0.8% rise of debt related to the impact channel is combined with 3.7% increase related to the adaptation channel. In the reference scenario, the two channels are more balanced with a 2.1% increase in debt due to the impact channel and only 2% due to the adaptation channel. The most exposed region is again Central-Eastern Europe, with an 8.6% rise in public debt in the high adaptation scenario. Debt sustainability is strongly affected by flood impacts in Slovenia and Bulgaria.

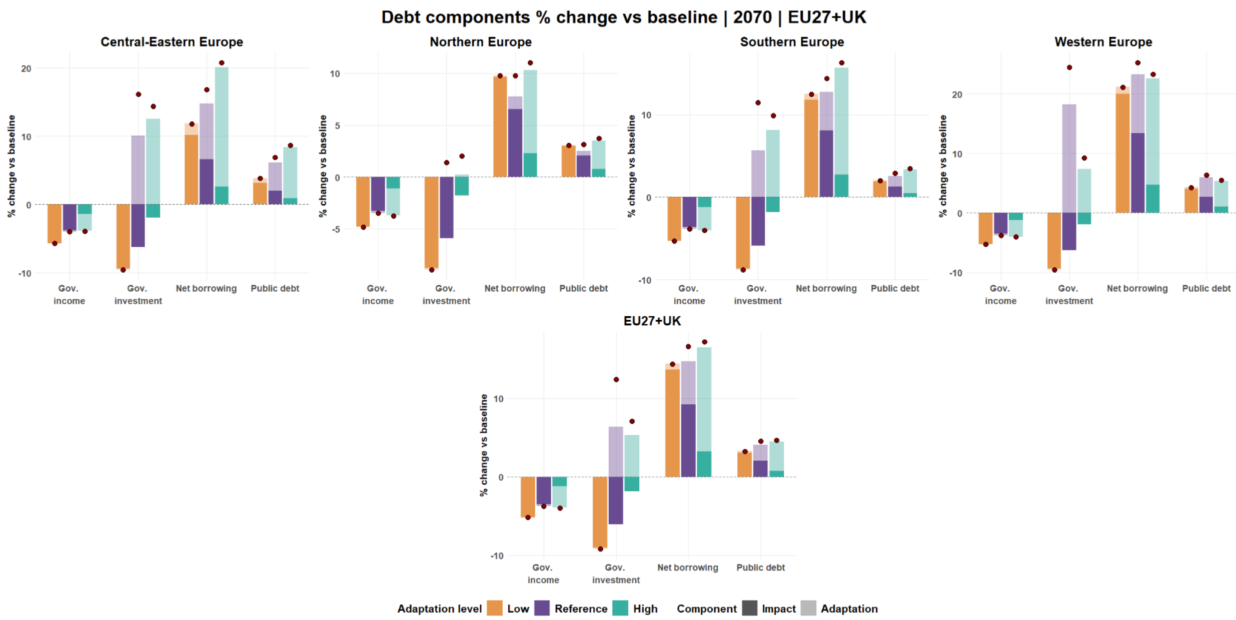

__Figure 23.__ Changes in public debt components due to the flood channel across different adaptation levels (with respect to the baseline scenario)

Agriculture impact channel

The agricultural impact channel captures climate-related effects on crop-specific yields, livestock production and pastureland, and forest production of roundwood, translating these into the ICES-XPS model as percentage changes in land productivity for crops and livestock, and in natural resource productivity for the timber sector. On the adaptation side, two mechanisms are implemented: public investment costs, comprising expansion costs, investment costs, and efficiency improvement costs, are modeled as a shock on government investment, while water withdrawal for irrigation, differentiated by crop, is captured through an efficiency shift in agricultural water use, translated into a shock on water demand by the agriculture sector.

Figure 24 shows the real GDP percentage change relative to the baseline for EU27 and UK countries under the agriculture impact channel, disaggregated by low, reference, and high adaptation scenarios over 2020–2070. The results present the total effect, combining both climate impacts and adaptation responses. This figure and those that follow exclude the results for Bulgaria, Romania, Spain, Greece, Hungary and Poland, which are characterized by extreme swings in government investment and debt that would compromise the readability of the graphs.

At the EU27+UK aggregate level, GDP change relative to baseline in 2070 under RCP7 is negligible -0.05% under low adaptation, -0.02% under reference adaptation, and -0.07% under high adaptation. Here the reference adaptation scenario shows the smallest GDP loss, although the range is very small. This pattern is not common across EU regions: in Central-Eastern Europe, all adaptation scenarios result in a small GDP gain, strongest under reference and low adaptation. In Southern and Western Europe, reference adaptation gives the best outcome, but the worst outcome occurs under high adaptation in Southern Europe and under low adaptation in Western Europe.

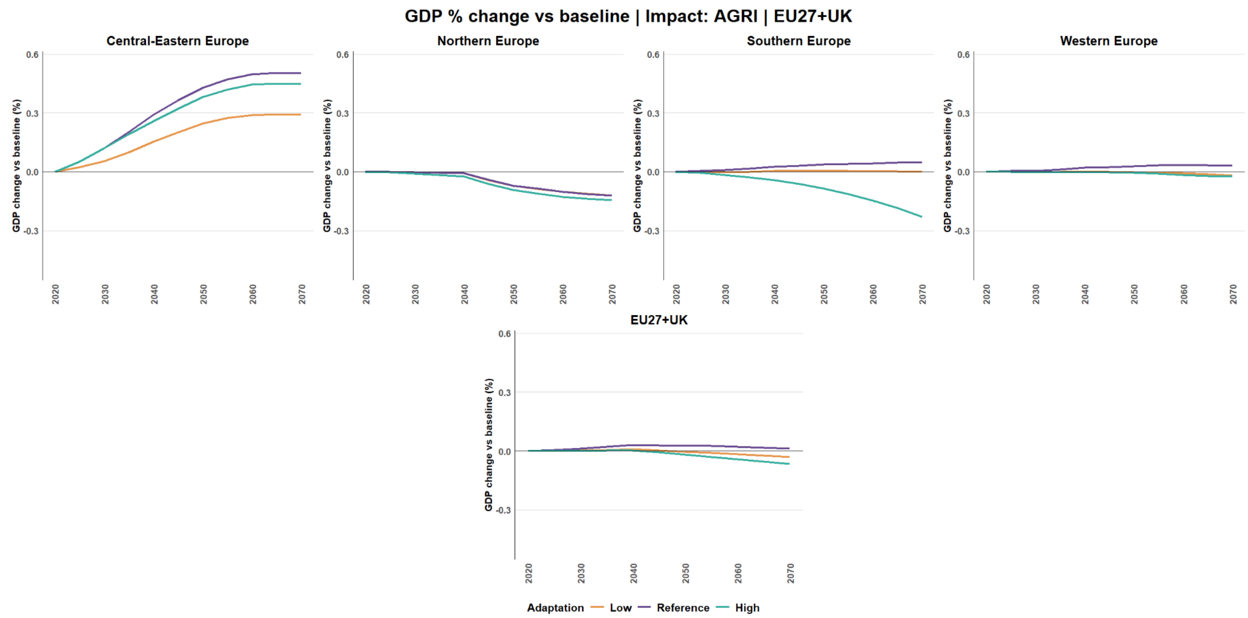

__Figure 24.__ Real GDP change due to the agriculture impact channel across different adaptation levels (with respect to the baseline scenario)

Figure 25 shows the percentage change in GDP and its main components relative to the baseline in 2070 across EU27 and UK countries under the agriculture impact channel. For each adaptation level, results are decomposed into the climate impact effect (solid bars), the adaptation effect (transparent bars), and the combined effect (red marker).

At the EU27+UK aggregate level, decomposing the GDP change by channel reveals that the two components contribute very differently depending on the adaptation scenario. Under low adaptation, the total GDP loss is driven almost entirely by the impact channel; the pattern is similar under reference adaptation. Under high adaptation the adaptation channel contributes more to the overall result. In Central-Eastern and Northern Europe, the impact channel is the main driver of GDP change, whereas in Southern and Western Europe, the adaptation channel determines the result under the high adaptation scenario. Among the GDP components, private consumption is the most consistently negative and largest-magnitude driver of the overall result at the EU27+UK level, ranging from -0.13% (low adaptation) to -0.16% (reference) and -0.18% (high adaptation), meaning private consumption losses worsen as adaptation ambition increases. Government expenditure and net exports are both positive but modest, ranging from +0.03% to +0.07% and

+0.02% to +0.07% respectively across the three scenarios, acting as small offsetting forces rather than major drivers. At the country level, Greece is the most extreme case, where private consumption collapses by -2.6% and investment by -2.5% under high adaptation, far exceeding any other country and confirming that Greece's overall GDP loss is concentrated in these two components.

Figure 25. *GDP components change due to the agriculture channel across different adaptation levels (with respect to the baseline scenario)*

Figure 26 focuses on the percentage change in four key fiscal variables, government income, government investment, net lending/borrowing, and public debt, relative to the baseline in 2070 across EU27 and UK countries under the agriculture impact channel, decomposed into impact (solid) and adaptation (transparent) effects for all adaption level scenarios. The figure shows that when considering debt sustainability, the level of adaptation plays a major role. Despite excluding a set of countries with a more than doubling debt , government investment and net borrowing remain out of range in Southern and Western Europe, as well as for the EU27+UK aggregate.

At the EU27+UK aggregate level, government income is driven almost entirely by the impact channel, which contributes a modest positive effect that actually grows with adaptation ambition (+0.2% under low, +0.3% under reference, +0.3% under high), while the adaptation channel's contribution stays negligible throughout and turns slightly negative under high adaptation, suggesting the impact channel (via changes to the tax base) matters far more for revenue than the adaptation channel itself.

Government investment shows the opposite pattern: the impact channel contributes only a small, fairly flat effect, while the adaptation channel contribution is disproportionately large and escalates sharply with adaptation ambition, from nearly 0 under low adaptation to +10% under reference adaptation and an extreme +276% under high adaptation, a figure clearly distorted by a small government investment baseline in some countries and by steep adaptation costs under the high adaptation scenario. The same pattern carries through to net borrowing and debt: the impact channel consistently reduces reliance on borrowing and debt, while the adaptation channel is the main driver pushing both measures upward, especially under high adaptation (+92%). The implications for public debt are quite strong, with a +20% increase in the EU27+UK, with Southern Europe experiencing the steepest rise, at +70%, under high adaptation. The takeaway is that, in aggregate, it is specifically the cost of adaptation investment that drives up government investment, net borrowing, and debt, an effect that intensifies sharply as adaptation ambition rises, and which is likely exaggerated at the EU aggregate level by one or two countries with unusually small investment/debt baselines.

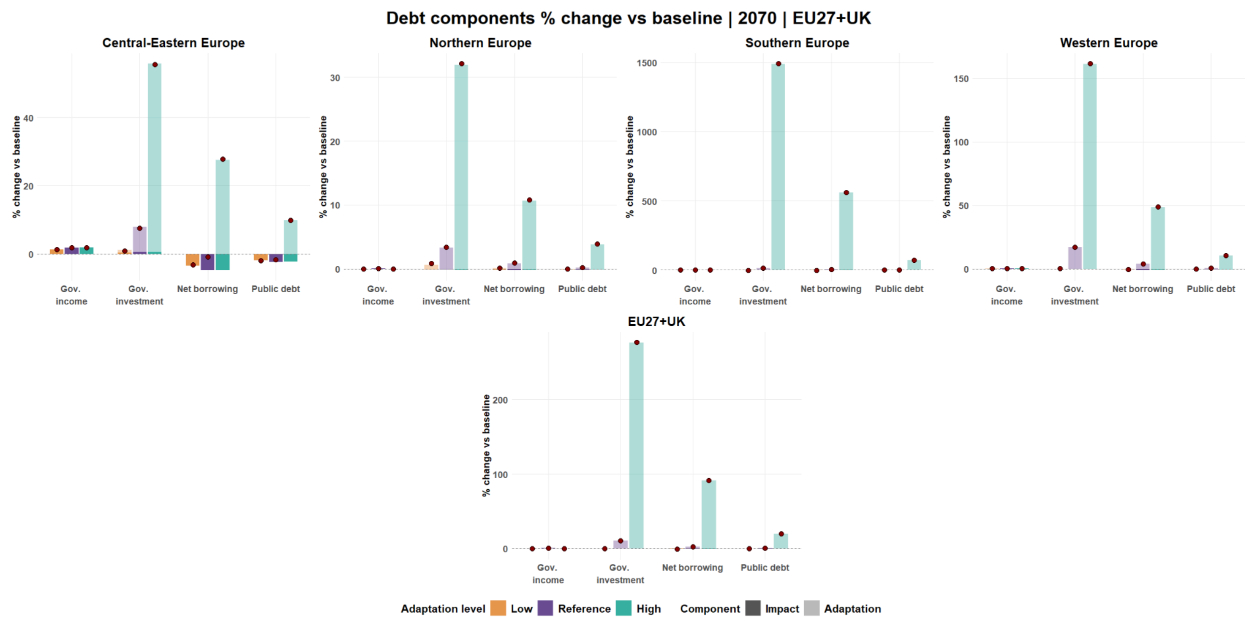

Figure 26. *Changes in public debt components due to the agriculture channel across different adaptation levels (with respect to the baseline scenario)*

Fire and biodiversity loss impact channel

This section briefly describes GDP loss and debt accumulation when accounting for wildfire (FIRE) impacts and biodiversity loss impacts on pollination and agricultural yield (POLL). Wildfire impacts are computed as the share of sector-specific burned area, covering crops, livestock, and forestry, relative to the corresponding sectoral land availability over each five-year simulation step. For crops and livestock, these impacts are implemented as land-productivity shocks, reflecting the assumption that land becomes fully available again in subsequent periods and that no permanent land loss occurs; the same assumption applies to forestry, where wildfire impacts are instead modelled as shocks to forest resource productivity rather than as permanent reductions in land endowments. Biodiversity loss impacts, by contrast, are based on pollination loss: reduced pollinator availability lowers crop yields, and this effect is captured in ICES-XPS through a land-productivity shock in the corresponding agricultural sectors. No adaptation actions are foreseen for these impacts.

Figure 27 highlights changes in GDP and public debt components due to the wildfire and biodiversity loss channel. The overall impact on EU27+UK is very small for both GDP and debt, with wildfire slightly stronger than pollination-driven biodiversity loss. GDP falls under both impacts in every region except Northern Europe, where the effect is negligible. Southern Europe shows by far the largest GDP loss under FIRE and a comparable, only slightly smaller loss under POLL. Central-Eastern Europe is the second most affected region, with GDP falling under both impacts, POLL producing a marginally larger decline than FIRE there. Public debt rises under both impacts in every region. Southern Europe again shows the largest increase, but here FIRE dominates clearly. Central-Eastern Europe shows the next-largest debt increase, with FIRE and POLL producing similar magnitudes.

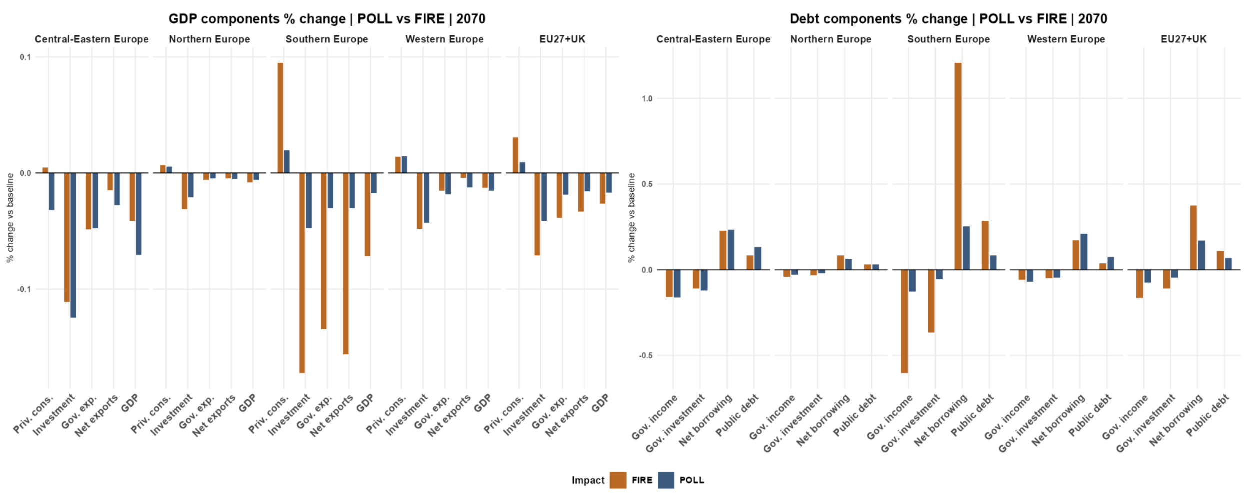

Figure 27. *Changes in GDP and public debt components due to the wildfire and biodiversity loss channel (with respect to the baseline scenario)*

All impact channel recap

This subsection aims to summarize the channel-by-channel analysis, quantifying the contribution of each impact channel to GDP and government debt change, and how much of these changes are due to climate change related damage versus adaptation measures. Figure 28 decomposes the 2070 GDP change relative to baseline by impact channel and by impact-versus-adaptation contribution across EU macro-regions. Total climate-related GDP loss ranges between 15% (high and reference adaptation) and 18% (low adaptation). Labor impacts with energy for adaptation (LAB) dominate the aggregate GDP loss in the region , with GDP loss between 9.5% (high adaptation) and 10.8% (low adaptation). Sea-level rise and flooding contribution is smaller but still meaningful, and health and agricultural impacts remain marginal by comparison, with agriculture even showing a small positive contribution in several regions. Central-Eastern and Southern

Europe experience the largest total GDP losses, reaching roughly -15% to -18%, while Northern Europe shows a comparatively smaller loss of around -13%.

When decomposed into impact versus adaptation channels, the impact channel accounts for the large majority of the total effect in every region, typically 72 and -83% of the total magnitude, while the adaptation channel contributes a smaller residual share. Central-Eastern Europe stands out with the highest adaptation-channel share, around 33%, indicating that adaptation costs play a comparatively larger role there relative to direct climate impacts, whereas Southern Europe shows the lowest adaptation-channel share, around 10-16%, meaning its losses are almost entirely attributable to climate impacts themselves rather than the cost of responding to them.

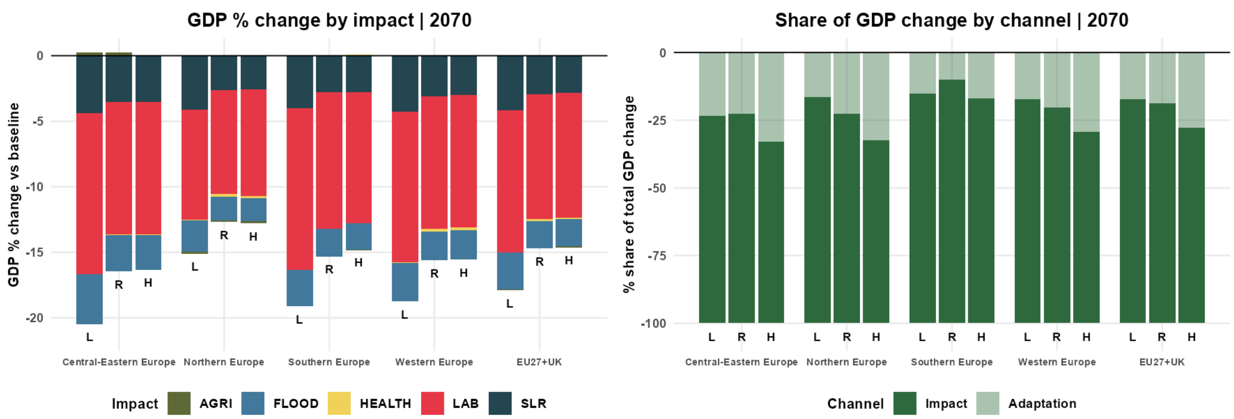

Figure 28. *Changes in GDP across all channels (relative to the baseline scenario), and share of GDP losses attributable to adaptation and impact components.*

Figure 29 provides the same decomposition for the change in government debt with respect to the baseline. Debt increase ranges between 28% and 53%. Labor and sea-level rise contribute with stable shares across all regions and adaptation levels to the debt rise, around 15% for the former and 9 % for the latter. Agriculture (AGRI) emerges as a dominant driver of debt for the region (around 20%); this is the result of still present outlier in Southern Europe where debt climbs from17% under low adaptation to 92% under high adaptation; given that AGRI's government investment and debt figures were previously shown to be distorted by near-zero baselines in some countries and very high adaption costs, these magnitudes should be interpreted with caution. When decomposed by channel, the pattern reverses relative to GDP: the impact channel accounts for the majority of debt increase under low adaptation in most regions, but its share shrinks as adaptation ambition rises, passing from 72% to 30% of the total debt, while the adaptation channel's share grows correspondingly.This is most visibly in Southern Europe, where the adaptation-channel share rises from about 19% (low adaptation) to over 87% (high adaptation), and in Central-Eastern Europe, from around 29% (low adaptation) to over 75% (high adaptation). This suggests that, as adaptation ambition increases, a growing proportion of the debt burden stems directly from the cost of adaptation measures; this a much higher share than is observed for

GDP loss, highlighting how government investment and expenditure drive higher net borrowing and debt accumulation.

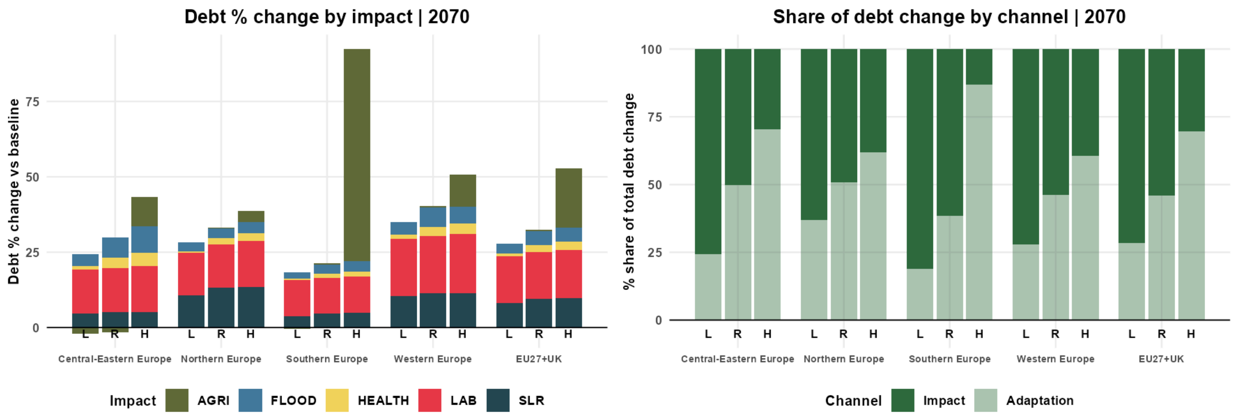

Figure 29. *Changes in government debt across all channels (relative to the baseline scenario), and share of debt change attributable to adaptation and impact components.*

1.4 Conclusion/Key takeaways

In this chapter, we used two CGE models to assess the fiscal implications of climate change impacts and adaptation. While the same data on impact and adaptation costs was assessed in both models, the simulation exercises differ in two distinct dimensions: (1) government budget closure and (2) capital (im)mobility. In the COIN-INT model, a balanced government budget is required in the sense that public adaptation investment needs to be met by reduced government expenditures (consumption). But since adaptation reduces some climate impacts, additional revenues are generated that then again increase the fiscal space. As a second option in the COIN-INT model, adaptation investment is financed via the issuance of government bonds. In the ICES-XPS model, adaptation investment is financed via increasing government debt, so governments borrow from other countries to finance adaptation. Regarding capital, the COIN-INT model assumes that capital is mobile across sectors but not across countries, while the ICES-XPS model assumes capital mobility across countries, which amplifies climate impact transmission across borders but also dampens the costs of impacts and adaptation.

We find in the COIN-INT model that adaptation consistently moderates GDP and welfare losses across all climate scenarios, with the most substantial gains achieved when moving from low to medium adaptation levels; further increases to high adaptation yield diminishing additional benefits. Among the various impact modules, labor and energy—specifically, labor productivity losses due to temperature extremes, partially offset by heating and cooling adaptation—emerge as the strongest drivers of GDP decline. While adaptation measures can significantly reduce losses from sea level rise, agriculture and flooding, residual losses remain high for labor/energy even after adaptation is implemented. Though adaptation brings improvements across all regions, Central-Eastern and Southern Europe experience the highest relative GDP and welfare losses in

2050, with Romania and Hungary among the most impacted. By 2070, losses intensify across most European regions, making medium and high adaptation particularly cost-effective for all countries, especially under RCP4.5. The majority of adaptation benefits arise from both public and private adaptation efforts, underscoring the importance of comprehensive adaptation strategies.

These results are qualitatively confirmed in the analysis with the ICES-XPS, but effects on GDP tend to be stronger in magnitude. By 2070, total climate-related GDP losses range from 15% under high and reference adaptation to 18% under low adaptation, with Central-Eastern and Southern Europe experiencing the most severe declines. Across the EU27+UK, the effects of labor and energy impacts account for the majority of the aggregate decline, while sea-level rise and flooding contribute smaller but still notable shares, and health and agriculture impacts remain marginal. Notably, the vast majority of GDP losses in all regions are attributable to direct climate impacts rather than adaptation costs, with adaptation accounting for a larger share only in Central-Eastern Europe, where it reaches about one-third of the total effect.

From a fiscal perspective, low adaptation scenarios are characterized by tax revenue losses that constrain fiscal space in the COIN-INT model, whereas higher adaptation levels enhance government spending capacity across all climate scenarios. Although adaptation investments require reductions in public consumption by design in the budget-neutral financing scenario, medium and high adaptation scenarios still allow for increased public consumption compared to low adaptation, both in 2050 and 2070—demonstrating the clear fiscal payoff of adaptation. In the UK case study on public flood adaptation, the choice of financing mechanism plays a critical role: budget-neutral approaches necessitate cuts in public consumption, while bond financing supports higher public consumption in the short term but is offset by rising interest payments over time. Moreover, domestic bond financing suppresses private investment—a crowding-out effect which is absent for international bond financing. These findings highlight that while adaptation improves long-term welfare and fiscal resilience, the ultimate fiscal outcomes are highly sensitive to the chosen financing strategy, emphasizing the need for adaptation policies that explicitly account for their fiscal implications.

According to the findings of the ICES-XPS model, the drivers of government debt accumulation shift as adaptation ambition rises. While the impact channel is the primary source of debt accumulation under low adaptation, its share diminishes with higher adaptation levels, as the fiscal burden of adaptation investment grows. By 2070, government debt increases range from 28% to 53% above baseline, with labor, sea-level rise, and agriculture as the main contributors. The adaptation channel's share of debt growth becomes especially pronounced in Southern and Central-Eastern Europe, where it rises to 87% and 75% respectively under high adaptation. This underscores that, although adaptation is essential for moderating GDP losses, its fiscal costs can become a strong driver of public debt, particularly in regions with a huge adaptation need. The analysis underscores the need for carefully targeted adaptation strategies and prudent fiscal planning, as the costs and benefits of adaptation are highly uneven across regions and over time.

2 Insurance sector analysis

2.1 Introduction

Floods are one of the most impactful natural disasters, causing both direct and indirect impacts (Dottori et al., 2018; Kreibich et al., 2014). The July 2021 floods in Europe, for example, caused approximately €46 billion in damages (Munich Re, 2022). Climate change is expected to substantially increase flood risk in many areas globally (Alfieri et al., 2018; Vousdoukas et al., 2018). For firms, floods may have dual impacts, initially causing direct damage to their properties, but afterwards also causing lost income due to business interruptions (Kreibich et al., 2014). Through both types of risks, floods may jeopardize the survival of small and medium-sized enterprises (SMEs) (Fatica et al., 2024). On a macroeconomic level, business interruption impacts can cause far-reaching and long-lasting economic losses (Gertz et al., 2019; Koks et al., 2019; Taguchi et al., 2022).

Flood adaptation is crucial to limit the societal adverse impacts of climate change. A wide range of adaptation measures are available, including large-scale engineered flood risk reduction measures, property-level measures, but also insurance coverage, which is an economic mechanism to spread risk, making the impacts of floods more bearable for those affected. Moreover, insurance arrangements may be designed in such a way that it incentivizes building-level adaptation measures, such as constructing flood barriers or applying flood resistant building materials. It may do so by providing premium discounts for policyholders that apply such measures (Kunreuther, 1996; Hudson et al., 2016). Despite the clear benefits of flood insurance coverage, the availability and uptake of flood insurance products is limited (Munich Re, 2024; Bellia et al., 2025), causing substantial flood insurance protection gaps in many countries.

To increase flood insurance uptake and stimulate adaptation investments by businesses, flood insurance policy may need to be revised. In some countries, such as the Netherlands, flood insurance is provided by private insurance companies. Through such arrangements flood insurance coverage is likely actuarially expensive through considerable premium markups, particularly by reinsurance providers (Froot, 2001), who generally cover the risk of the most catastrophic events. Moreover, private insurers may refrain from providing coverage in areas where risk is too large or too uncertain, as this becomes commercially unattractive. For these reasons, countries where flood insurance is organized on the private market may benefit from certain policy changes. A policy change that is gaining popularity is to introduce a public reinsurer, who is able to bear the risk of the most catastrophic events at an actuarily fair rate (Hudson et al., 2019), making coverage in these areas commercially attractive, and cheaper for (potential) policyholders.

Although there are some studies that address the benefits of flood insurance policy changes on the flood insurance protection gap (Tesselaar et al., 2020a; 2022), there is no study that addresses this topic for business insurance. This research gap is addressed in this study, which applies a partial equilibrium modeling framework to assess flood damages, insurance premiums, insurance demand, uptake of adaptation measures, and the flood insurance protection gap for direct and indirect flood risk to businesses, under current conditions and considering increasing flood risk under climate change. This study applies the Netherlands as a case study, which is a country notorious in terms of managing flood risk. However, with relatively little effort can the approach developed here be applied elsewhere, or for different flood hazards.

The remainder of this section is organized as follows: Subsection 2.2 describes the applied methodology, Subsection 2.3 presents and discusses results, and Subsection 2.4 provides policy recommendations and concludes.

2.2 Method

This research applies the Dynamic Integrated Flood Insurance (DIFI) model (Hudson et al., 2019) and further extends it by integrating flood insurance for businesses. The simulation is calibrated using collected survey data on insurance uptake in the Netherlands. Throughout this study, outcomes are presented and compared between four scenarios, with two different insurance market structures (private versus public-private insurance), and two coverage limits (partial versus full coverage of flood risk). For each of these scenarios, premiums, insurance uptake, and uptake of risk reduction measures by exposed firms are assessed.

2.2.1 Case study

The Netherlands has a long tradition of flood adaptation, with particular expertise in engineered flood risk reduction, such as building dykes and levees. Flood insurance, on the other hand, is poorly developed, particularly since after the large North-Sea floods Dutch insurers announced that flooding of primary waterways and seas is no longer insurable. Such floods instead need to be covered by the public disaster compensation act ("Wet Tegemoetkoming Schade bij Rampen", WTS). However, recently there is renewed interest in the advantages that formal flood insurance gives over the informal WTS structure, including more certainty of compensation after floods and better incentives for risk reduction by policyholders through risk-based insurance pricing. This renewed interest also counts for the insurance of small and medium-sized enterprises (SMEs), a market that has been virtually nonexistent (Verbond van Verzekeraars, 2018). In light of the escalating flood risks linked to climate change (IPCC, 2023) and the widespread perception that a substantial portion of flood risk in the Netherlands is uninsurable, there is a pressing need to explore alternative insurance market structures. Such structures could improve insurance uptake while also incentivizing adaptation measures. As flood risk continues to rise worldwide, the Dutch case offers valuable insights into the shortcomings of conventional insurance markets, as well as the potential of innovative insurance mechanisms. Consequently, lessons drawn from the Dutch experience may prove relevant for other countries aiming to expand insurance coverage and encourage effective flood adaptation strategies.

Flood insurance for SMEs in the Netherlands is currently available, but only for specific types of flood risk. In particular, coverage for types C (failure of secondary flood defenses) and D (floodings from regional water bodies) floods, which are generally smaller river systems, is available (MoneyView, 2023; Findinet, 2023), but to a limited extent (Ooms et al., 2024). Coverage of type A and B flooding is currently not available in the Netherlands (Verbond van Verzekeraars, 2025), mainly because of the decision made after the 1953 North Sea floods. In this study we assess the potential of two different flood insurance market structures, as well as expanding the coverage of flood insurance to include type A (floods in unembanked areas) and B (failure of primary flood defenses) flood risk. Type A, B, C, and D flood risk together we refer to in this report as “extended flood risk”.

2.2.2 Flood risk

Flood risk is defined as the product of hazard, exposure, and vulnerability. Hazard refers to the frequency and intensity of flooding events, exposure denotes the presence and value of assets located in flood-prone areas, and vulnerability represents the susceptibility of these exposed assets to damage (Botzen, 2021).

For this study we apply flood risk estimates from the ‘Slachtoffer en Schade Module (SSM) (Slager and Wagenaar, 2017), which is a publicly owned and available flood risk model for the Netherlands, which is also used in several peer-reviewed Dutch case studies (Kok et al., 2023; Caloia et al., 2023). SSM distinguishes flood risk for seven economic sectors and considers direct damages and indirect impacts due to business interruption.

To simulate flood hazard in SSM we apply flood inundation maps from Landelijk Informatiesysteem Water en Overstromingen (LIWO) (LIWO, 2024). The LIWO maps estimate flood inundation for various flood return periods on a 25x25 meter resolution and for each of the flood types (A, B, C, and D) separately. For present results in this study, we aggregate the outcomes to NUTS3 level.

The simulation of flood exposure and vulnerability in this study is taken from Bruijn et al. (2015), who apply exposure estimated from the Basisregistratie Adressen en Gebouwen (BAG) (PDOK, 2024), which distinguishes several building occupancy types. To simulate flood vulnerability we apply depth-damage curves for several building-types. The seven economic sectors are merged into three vulnerability curves: one for healthcare, office, and education; one for hospitality and retail; and one for industry and sports (Slager and Wagenaar, 2017). For business interruption losses, a single vulnerability function is applied across all sectors (Slager and Wagenaar, 2017). Based on this approach, we estimate direct and indirect flood damages for each flood type, return period, economic sector and NUTS3-region in the Netherlands.

To estimate flood insurance premiums, we need information on flood EAD as well as the volatility associated with these figures. EAD is estimated using a flood probability-impact curve that can be established from the steps described above. Volatility of damages is estimated based on the standard deviation of flood losses.

The SSM approach only allows the estimation of current flood risk. For future projections we apply simulations from the GLOFRIS model (Ward et al., 2017; Winsemius et al., 2016), which allows the use of RCP and SSP information to simulate flood risk until 2080. For this study we apply the “middle-of-the-road” pathway of RCP4.5 and SSP2 (Riahi et al., 2017). We apply these future projections by rescaling the obtained SSM results accordingly for the years 2050 and 2080.

2.2.3 Insurance module

The insurance module of the DIFI model translates the EAD and its associated standard deviation, as estimated in the risk module, into insurance premiums for both direct and indirect damages. Premiums for these two products are calculated separately for the current baseline insurance market structure and for three stylized alternative market scenarios. These alternative scenarios vary along two key dimensions: the extent of flood risk coverage—either partial coverage (including only Types C and D) or full coverage (including Types A through D)—and the nature of the reinsurance arrangement, distinguishing between private reinsurance and a public reinsurance arrangement.

The simulation of insurance premiums follows the risk-layering approach identified by Paudel et al. (2015), in which part of the EAD remains uncovered in the form of a deductible, and another part of the EAD is transferred from the insurer to a reinsurer. Accordingly, the transferred flood risk is divided into three components: A deductible, insurance coverage, and reinsurance coverage.

We estimate premiums for two stylized types of insurance arrangements, which mainly differ in the reinsurance market arrangement. In the fully private system, reinsurance coverage is provided by private reinsurers, who charge actuarially high fees for such coverage. This is due to relatively low competition and high market power of reinsurance companies, allowing them to charge high (profit) markups. In the alternative insurance market arrangement reinsurance coverage is provided by the government, who charges actuarially fair fees for such coverage. The main difference between the two insurance market types is therefore the estimated premium, which is the result of the difference in premium markups between public and private reinsurance arrangements. For a more formal description of the applied premium-setting rules in DIFI we refer to Hudson et al. (2019).

2.2.4 Insurance uptake

To simulate insurance uptake and adaptation behavior at the firm level, each company evaluates four possible strategies: purchasing insurance, investing in flood risk reduction measures, combining both actions, or taking no action. These decisions are informed by building-specific EAD, insurance premiums, and investment costs. Due to bounded rationality, decisions by individuals or SMEs are likely biased based on subjective risk perceptions. The applied framework considers this bounded rationality by transforming flood risk into perceived flood risk, which is done by multiplying this estimate for each simulated SME by a flood risk misperception parameter. This parameter is drawn randomly from a gamma distribution, which is calibrated using survey data from businesses located in regions of the Netherlands affected by the 2021 floods (Endendijk et al., 2024; Ooms et al., 2024).

Financial constraints are incorporated at the firm level by assessing companies' financial health alongside their premium-to-asset and investment-to-asset ratios. A firm's financial health is evaluated using threshold values for three key financial indicators derived from balance sheet data and recognized as benchmark standards by the Dutch Chamber of Commerce (KVK, 2024).

First, the current ratio (current assets divided by current liabilities) is considered, with values below 1 indicating limited liquidity. Second, working capital (current assets minus current liabilities) is assessed, where negative values likewise signal low liquidity. Third, the solvency ratio ((total assets minus total liabilities) divided by total assets) is evaluated, with values below 0.25 indicating low solvency. Firms for which all three indicators fall below their respective thresholds are classified as financially constrained and are assumed not to undertake new investments

(Fleckenstein and Longstaff, 2018; Saltari and Travaglini, 2001). In contrast, if at least one indicator exceeds its threshold, the firm is considered sufficiently liquid to invest or sufficiently solvent to borrow for investment.

After assessing whether insurance and/or risk-reduction measures are affordable for a firm, the decision framework has three stages. The first stage simulates whether a firm invests in adaptation given the price and perceived benefits of adaptation. A firm undertakes an adaptation measure when the perceived benefits exceed the associated costs. The cost of adaptation is assumed to be €37 per square meter, which is derived from cost figures reported by Aerts et al. (2013) and Kreibich et al. (2015), combined with building size data from FEMA (2022). Specifically, the costs of dry-proofing, wet-proofing, and their combination are averaged to obtain a single representative adaptation cost per square meter. Moreover, the adaptation measure is assumed to have a lifetime of 30 years (Aerts, 2018). Therefore, the costs and benefits of adaptation measures are discounted over this period. The discount rate is set at 3% based on (Aerts et al., 2024). Based on Aerts et al. (2013) and Kreibich et al. (2015), the adaptation effectiveness is set at 0.65, meaning that the adaptation measure reduces the EAD by 35%.

The second stage simulates whether a firm purchases flood insurance coverage. If a firm did not invest in adaptation in stage 1, this decision is based on whether the subjective benefits of insurance coverage outweigh the premium. If a firm did invest in adaptation in step 1, this decision is similar except that flood risk and, therefore, the insurance premium is lower if risk reduction measures were applied. If the subjective benefit minus the premium cost is greater than zero, the company chooses to purchase an insurance policy. Insurance is assumed to be a yearly decision; hence, stage two is evaluated over a single time period.

If no adaptation is chosen in stage 1 and insurance coverage is purchased in stage 2, stage 3 simulates whether a premium reduction would incentivize a firm to invest in adaptation. The reduction in insurance premiums equals the effectiveness of adaptation at reducing flood risk.

Firm simulation

To simulate insurance uptake and the adoption of adaptation measures, company-level data are used to construct representative firm populations for each NUTS3 region. Each simulated firm is assigned a balance sheet, as well as values for EAD, insurance premiums, and adaptation investment costs, all scaled according to firm size. The simulation also accounts for the sectoral composition of each NUTS3 region.

Data on current assets (CA), noncurrent assets (NCA), current liabilities (CL), and noncurrent liabilities (NCL) are obtained from the Dutch Chamber of Commerce. A dataset containing financial statements from fiscal year 2022 is classified to match the 7 SSM sectors, yielding a total of 491,742 financial statements. Based on this data, we construct a multivariate normal distribution for each of these variables for both assets and liabilities and across all seven sectors. This allows us to generate sector-specific synthetic balance sheets.

For each NUTS3 region, we run the simulation 10.000 times, which are later adjusted to the actual regional sector composition based on the BAG registry. This approach allows us to generate a representative sample per region without having access to actual location-specific balance sheets of firms. The resulting samples contain the essential information on firm balance sheets that are needed for the insurance and adaptation uptake simulation.

2.2.5 Insurance coverage gap

The coverage gap is defined as the share of flood risk that remains uninsured and must therefore be absorbed by either the government or affected firms. It is quantified by modeling insurance uptake, baseline adaptation efforts, and additional adaptation incentivized by insurance. For firms that implement adaptation measures, flood risk is assumed to decrease by 35%, reflecting the effectiveness of such measures. Subtracting this reduction from the initial EAD yields the residual, unmitigated EAD. The insured portion is then calculated based on this residual damage, taking into account a 15% deductible.

The proportion of unmitigated damage considered insurable differs between the baseline and extended coverage scenarios. This distinction also extends to the insurance incentive mechanism, where under the baseline scenario fewer firms qualify for incentives than under extended coverage. To prevent overstating adaptation effects in the baseline case, the resulting increase in adaptation uptake is adjusted accordingly through weighting.

2.3 Results & Discussion

This section presents and discusses outcomes of flood insurance premiums, coverage, and incentivized flood risk reduction concerning flood insurance for businesses in the Netherlands. We consistently present outcomes for four policy scenarios: (1) the baseline insurance system; (2) expanded coverage to areas where insurance is currently unavailable; (3) a transition from current private towards public reinsurance; and (4) a combination of scenarios (2) and (3).

2.3.1 Flood risk

Table 3 shows total EAD for the Netherlands under the baseline and extended flood coverage scenarios across the seven economic sectors considered from the SSM model. Industry accounts for the largest share of EAD in the Netherlands for both direct and indirect damages, followed by offices. It can also be seen in Table 3 that indirect EAD exceeds direct EAD for most sectors, except the retail and hospitality sectors. Moreover, EAD in the extended coverage scenario is approximately four times higher than under the baseline scenario. This means that although the number of exposed firms is higher under the extended coverage scenario, average EAD per company is also higher. This finding is not surprising, as the inclusion of types A and B flooding in the extended coverage scenario means that this scenario considers the flooding of large waterways.

Table 3 also shows that the increase in EAD between baseline and extended coverage scenarios varies across sectors. For the education sector, for example, business interruption impacts rise by nearly 400%, whereas this rise is only 50% for the hospitality sector. Such disproportional changes in EAD are, therefore, largely driven by sector-specific exposure growth. Figure 30 shows how flood impacts for firms are dispersed regionally.

Table 3. *Average Insurable direct EAD per company per sector across NUTS3 region in 2011 euros.*

	Baseline	**Extended Coverage**	**Baseline Avg EAD per company**	**Extended Avg EAD per company**
Direct EAD per sector (2025)				
Industry	16,778,500	74,828,336	307	913
Hospitality	553,952	2,200,075	24	43
Office	5,510,809	21,526,261	543	1,159
Retail	3,262,686	14,692,950	417	851
Healthcare	1,967,497	7,090,073	352	1,135
Education	1,515,168	5,299,463	561	2,056
Sport	56,284	207,414	27	83
Business interruption EAD per sector (2025)				
Industry	22,140,411	84,266,505	412	1,037
Hospitality	495,274	1,854,775	21	36
Office	11,693,739	37,890,079	1,109	2,052
Retail	1,484,910	5,980,246	196	379
Healthcare	2,452,522	8,263,839	416	1,174
Education	727,900	2,587,267	274	1,025
Sport	123,400	367,818	67	158
Total direct EAD totals per time period				
Current	29,644,896	125,844,571	268	727
2050	59,586,240	252,947,600	539	1,462
2080	101,978,400	432,905,300	923	2,502
Total business interruption EAD totals per time period				
Current	39,118,158	141,210,528	349	806
2050	78,627,500	283,833,200	701	1,620
2080	134,566,500	485,764,200	1,200	2,772

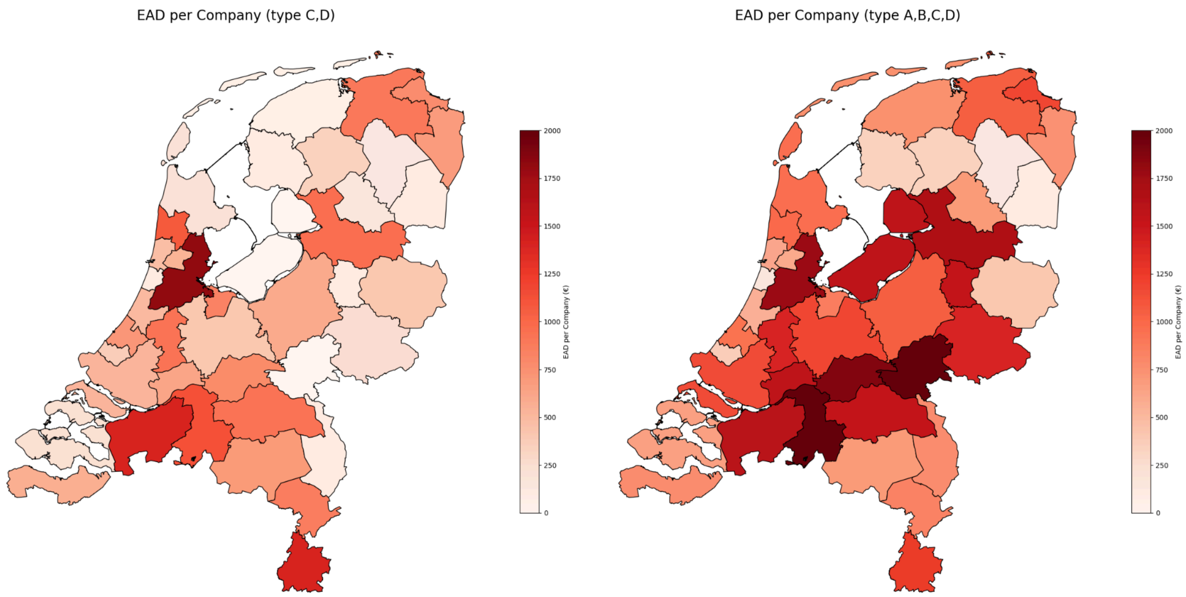

Figure 30. *Average EAD per company in the 1/1000 flood zone at the NUTS3 level. The left panel (baseline flood risk) shows risk from Flooding types C and D. The right panel (extended flood risk) shows risk from Flooding types A, B, C, and D.*

2.3.2 Premiums

Figure 31 shows the simulated firm-level flood insurance premiums for direct and indirect damages on NUTS3-level under the four assessed insurance policy scenarios. Since premiums are for the most part based on EAD, the variation in premiums across sectors follows similar trends as shown in the previous section. Premiums for business interruption coverage are higher than for direct damages for most of the seven sectors, except for the education and retail sectors.

Comparing premiums across the insurance policy scenarios, we can observe that public reinsurance results in notably lower premiums than an insurance system with private reinsurance. This result is due to the generally lower markups charged by a public reinsurer compared to markups charged on the private reinsurance market (Froot., 2001). The difference in premiums between private and public reinsurance is most pronounced concerning the variation of premiums. As the dispersion is much lower for public reinsurance arrangements, this means that such a system is particularly effective at reducing premiums for firms that face high flood risk.

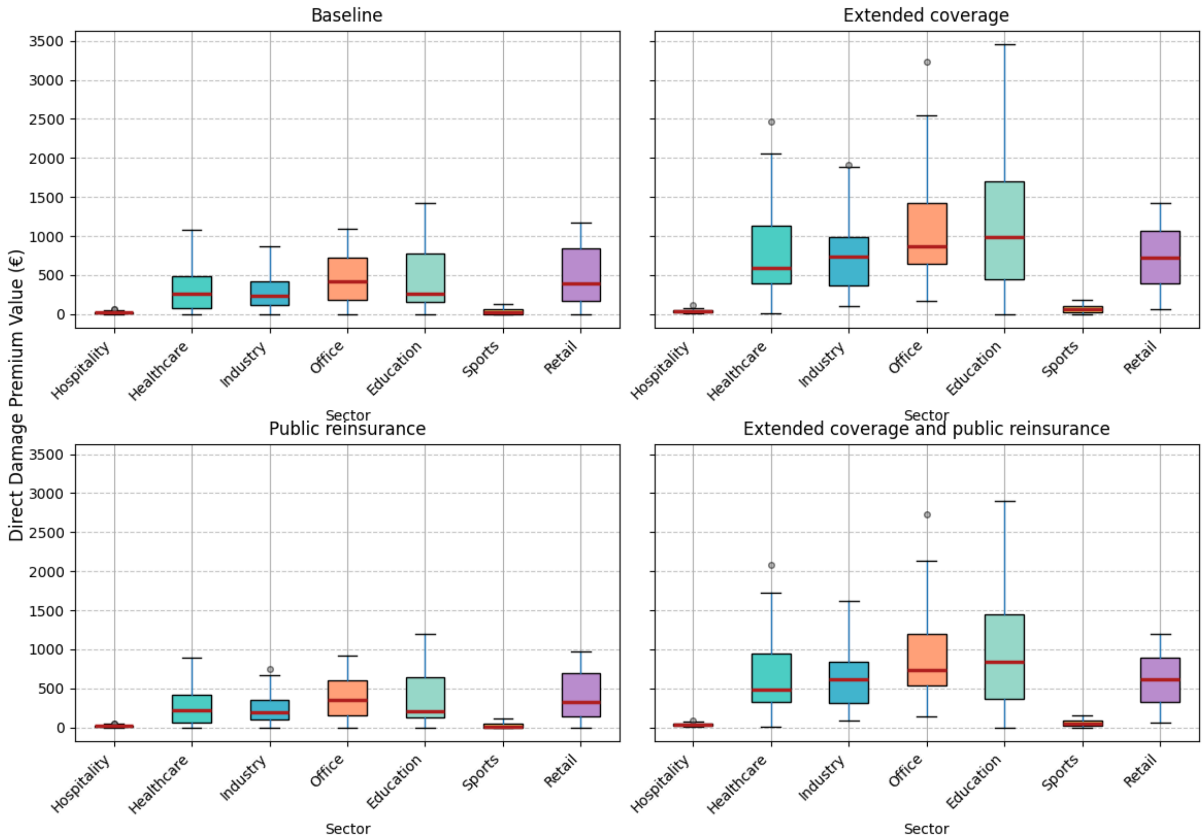

Figure 31. *Insurance premium distribution by sector and insurance system across NUTS3 region in the Netherlands (direct damage).*[1]

2.3.3 Insurance uptake

Figure 32 presents demand for flood insurance in the Netherlands for coverage of both direct damages and business interruption impacts. The figure shows that for each consecutive policy change leads to higher insurance coverage, with the largest increase occurring by both extending coverage and introducing a public reinsurer for flood coverage. This increase can be attributed to two important effects, which are that by expanding coverage more firms become eligible for insurance uptake, and that public reinsurance lowers premiums, meaning coverage becomes more affordable and attractive.

An analysis of sectoral variation in flood insurance uptake reveals that differences between sectors are quite aligned with sectoral differences concerning EAD and premiums found in earlier sections

[1] To enhance visualization clarity, outliers that exceed 1.5 times the interquartile range have been removed from the display. They were predominantly observed in the education and healthcare sectors, where the relatively low number of businesses results in a high risk concentration per individual business entity, consequently generating a disproportionately high insurance premium per business.

of this report. Overall, the assessed sectors seem to take insurance for the type of risk they are more exposed to, given that they can afford the premiums.

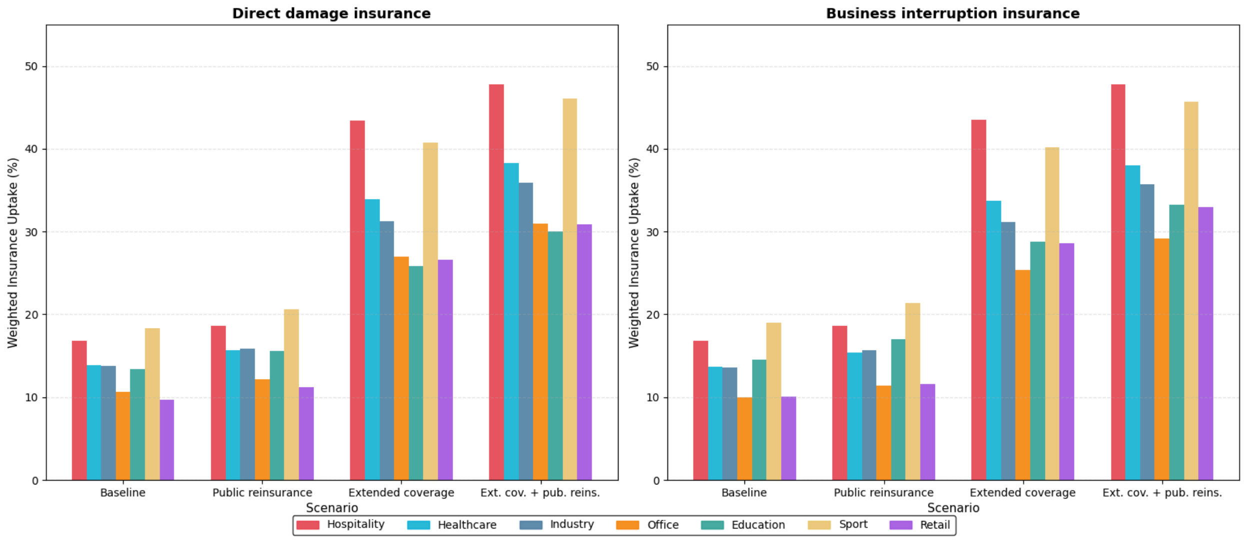

Figure 32. *Average insurance demand across policy scenarios (standardized percentages)*

Across all sectors, Figure 33 reports the mean proportion of firms that cannot secure insurance coverage as a result of financial limitations. These limitations are categorized into two distinct types. The first relates to balance sheet conditions, where simulated firms fall short of the required minimum thresholds for key liquidity and solvency indicators. The second concerns the affordability of insurance, capturing situations in which the premium, relative to total assets, surpasses a predetermined cutoff value.

A noteworthy observation is that financial constraints in the hospitality sector are almost fully driven by balance sheet constraints instead of the height of insurance premiums. Moreover, the most financially constrained economic sector is the education sector, where approximately 30% of firms within 1/1000 year floodzones are unable to purchase coverage for direct flood damages under the extended coverage scenario. However, as the education sector is largely publicly owned in the Netherlands, it may be fair to assume that the government finances flood damages when a flood occurs. However, this may be a suboptimal outcome, particularly concerning budgetary resilience of governments after large floods (Unterberger et al., 2019). Finally, we find that financial constraints to insurance uptake may be somewhat reduced by introducing a public reinsurer.

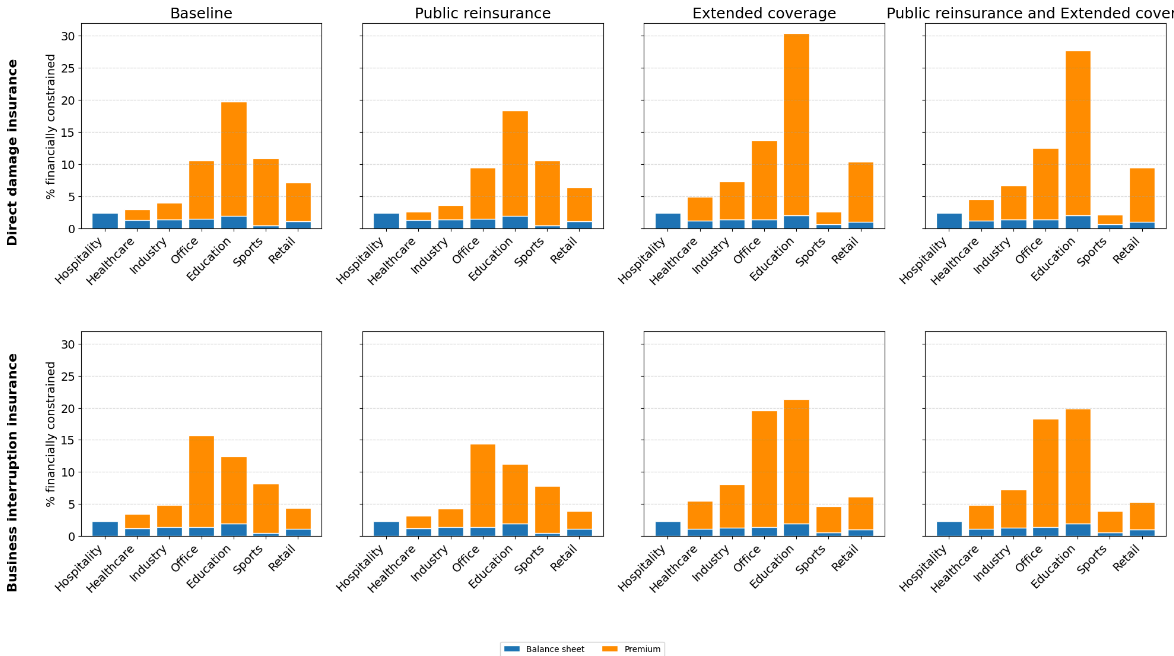

Figure 33. *Percentage of companies facing financial constraints to insurance coverage*

2.3.4 Adaptation and insurance incentive

Next, we assess the extent to which insurance can incentivize risk reduction effort by insured firms through a premium discount. In our simulation this discount is 35% of the initial premium, which equals the effectiveness of our assessed adaptation measure, which is a combination of dry- and wet flood-proofing measures. Figure 34 shows that increasing insurance availability in the extended coverage scenarios is effective at stimulating risk reduction by businesses exposed to floods. For example, from the figure it can be seen that EAD can be reduced by €7 million for the industry sector, by €2.5 million for the office sector, and by approximately €1 million for the retail and healthcare sectors. For the hospitality and sports sectors the effectiveness is negligible. The variation across sectors can largely be explained by differences in flood exposure, which affect the financial benefits of investing in flood adaptation.

Comparing the insurance scenarios it is clear that extending coverage to include areas at risk of large-scale floods is most effective at stimulating risk reduction measures. This policy measure substantially increases the amount of firms exposed to floods to the insurance incentive. Introducing a public reinsurer but not expanding flood coverage has the opposite effect; it reduces incentivized risk reduction by exposed firms. This finding is largely due to lower premiums and, therefore, lower premium discounts under this insurance scenario.

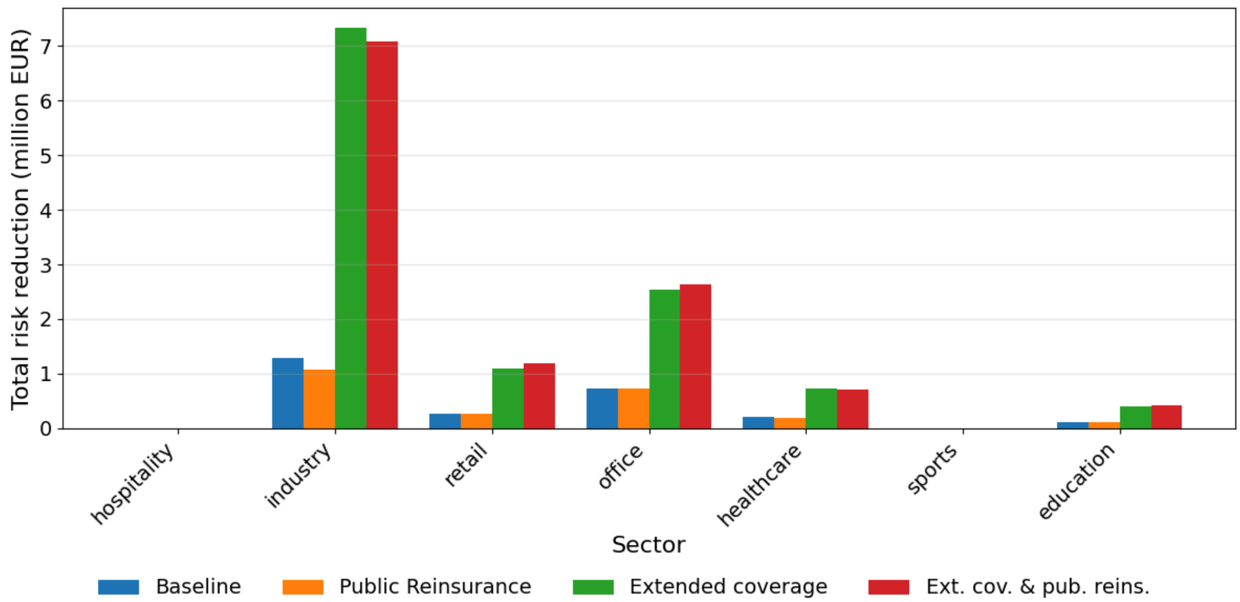

Figure 34. *Total risk reduction due to insurance incentive by sector and scenario*

2.3.5 Insurance coverage gap and risk reduction

Finally, based on the simulation of EAD, insurance coverage, and adaptation uptake, we can estimate the flood insurance protection gap. Figure 35 presents the annual flood insurance protection gap for the base year (2025), 2050, and 2080. We can see that the insurance protection gap increases steadily over time, from €207 million in 2025 to €668 million in 2080. However, the figure also shows that insurance reforms, by increasing coverage and incentivizing risk reduction by policyholders, can limit the increase in the insurance protection gap. Introducing a public reinsurer is only modestly effective at limiting the rise in the protection gap, saving €0.6 million in 2025 and €5 million in 2080. On the other hand, extending coverage reduces the insurance protection gap by €34 million in 2025 and €100 million in 2080. Combining both a public reinsurer and extending coverage is most effective, with reductions in EAD of €38 million in 2025 and €123 million in 2080.

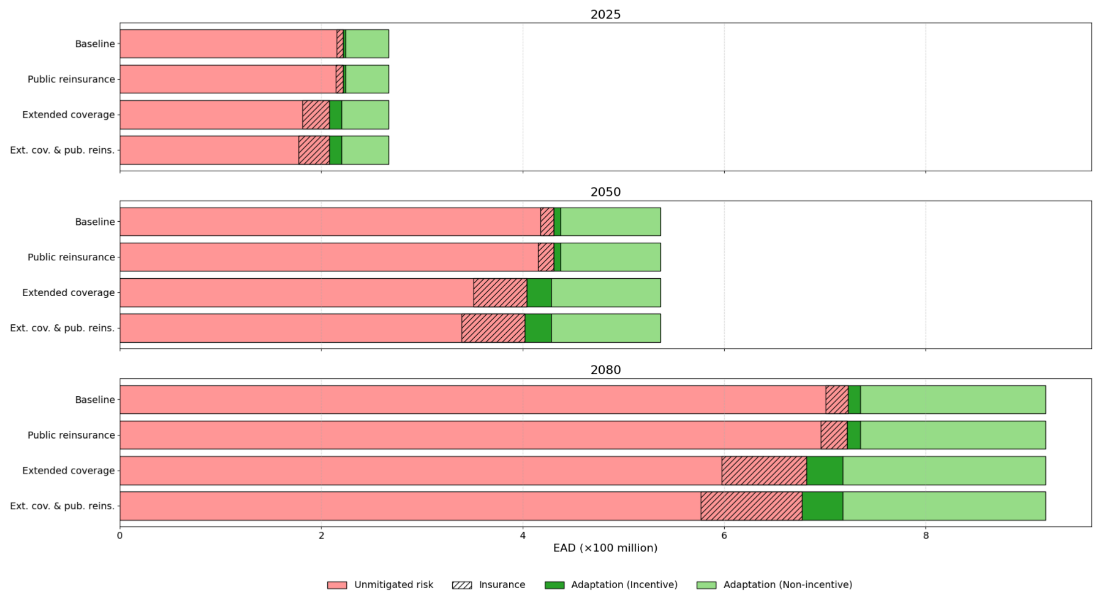

Figure 35. *Annual insurance coverage gap development over time (direct damage + business interruption), including adaptation incentive*

2.4 Conclusion/Key takeaways

This study presents a novel, model-based assessment of alternative flood insurance systems for businesses using a partial equilibrium climate risk framework. The model integrates an object-based flood risk module that captures both direct and indirect losses, while accounting for sectoral heterogeneity. Firm-level financial constraints are explicitly represented using detailed balance sheet data, and insurance demand is calibrated with local survey data.

Although applied to the Netherlands, the policy challenges examined are representative of those faced in many countries. The modeling approach is transferable to other contexts and climate hazards. Overall, the study provides the first comparative evaluation of business-level flood insurance systems, offering insights into improving financial resilience under rising climate risk.

Climate change is increasing flood risk in many areas globally. Firms face dual challenges because of this, as they may face increasing direct damages to their property, but also face the risk of business interruption, which negatively impacts their income. Despite increasing risks, there remains a considerable flood insurance protection gap for businesses, which is the share of flood risk not covered by insurance. In this study we show various policy options that governments may undertake to reduce this protection gap. Firstly, governments can reduce premiums by providing reinsurance coverage to private insurers that offer flood insurance. We show that reducing premiums this way makes insurance more attractive and affordable for firms, reducing the flood insurance protection gap. A more effective policy change is to expand insurance coverage to areas where currently no flood insurance is available in the Netherlands, which are areas that are unprotected by dykes or are located in floodplains of so-called primary waterways (coastal areas or large river deltas). By increasing coverage to include these areas, more firms may purchase insurance coverage and more firms are exposed to the risk-reduction incentive in the form of a premium discount. This scenario is particularly impactful in limiting the flood insurance protection gap. Governments can facilitate the development of flood insurance products to cover flood risk in currently uninsurable regions by providing public reinsurance coverage. By providing more affordable coverage of damages caused by the most extreme events, insurers considerably lower the risk of solvency issues after such events occur, making the development of flood insurance products in these areas commercially attractive.

While existing empirical research indicates that structural flood adaptation remains uncommon among firms, the results of this study suggest that the design of insurance mechanisms can improve this. In particular, offering premium reductions appears to encourage businesses to undertake adaptation measures. This finding is important considering the scarce empirical evidence on firms' responsiveness to such incentives. More broadly, the results highlight the potential of insurance schemes to drive proactive risk reduction at the firm level and offer relevant insights for the redesign of flood insurance systems.

Finally, this report presents a flexible novel method for modeling object-based climate risk and insurance markets for businesses, which future research may apply to other countries and climate hazards. Since there exists a wide variety of flood insurance mechanisms between EU-countries, an interesting analysis is to compare how each mechanism is able to deal with the challenges posed by climate change. Such an analysis would allow researchers to observe which existing mechanisms are more robust to climate change impacts.

3 Financial Risk Analysis

3.1 Assessment of Financial Risks Related to Drought

3.1.1 State of the Art and Issues Addressed

Drought is increasingly recognised as a material financial risk for European investors, banks and insurers, yet the literature translating physical drought hazard into euro-denominated losses remains comparatively underdeveloped relative to sudden-onset hazards such as floods and windstorms (Blauhut et al., 2016; JRC PESETA IV, 2020). The urgency of closing this gap has been underscored by the summer of 2026, one of the most severe drought and heat episodes recorded in Europe in decades. In August 2026, Triodos Bank's “Hot Summer Economics” analysis — a piece of grey literature aimed squarely at investors — estimated that extreme heat and drought conditions could shave close to 1% off EU GDP in 2026 alone, on the order of EUR 180 billion — the entirety of the EU's expected growth for the year. The largest channel is lost labour productivity (roughly 0.40 percentage points of GDP), with further drags from agriculture and food (≈0.15 pp), energy production (0.12–0.15 pp) and transport and logistics (≈0.15 pp); France and the Netherlands were estimated to lose 1.4 and 0.8 percentage points of GDP growth respectively (Stegeman et al., 2026).

This single-year estimate illustrates a feature of drought risk that is central to how financial institutions must think about it: individual extreme years can generate losses an order of magnitude above the long-run average, so average-damage figures alone understate the tail risk that matters for capital adequacy and portfolio management. The JRC's PESETA IV assessment puts current annual average drought damages for the EU and UK at approximately EUR 9.0 billion per year (90% confidence interval: EUR 7.4–14.2 billion), equivalent to roughly 0.07% of GDP, with Spain (EUR 1.5 billion/year), Italy (EUR 1.4 billion/year) and France (EUR 1.2 billion/year) the most exposed countries. Under a static 2015 economy, average losses are projected to reach EUR 17.3 billion/year at 3°C of warming — a 90% increase on the historical baseline — and EUR 45.4 billion/year once future economic growth is taken into account (JRC PESETA IV, 2020). Even against these elevated long-run averages, the Triodos estimate for 2026 alone is roughly four times the current annual-average damage figure, and the gap is wider still against reported insured losses: Munich Re's NatCatSERVICE records only around EUR 1.3 billion per year in drought losses over 35 years — less than one-sixth of the JRC's independently modelled estimate (JRC PESETA IV, 2020). This gap between average and individual-year losses, and between modelled and recorded losses, is exactly the distinction that financial risk assessment needs to resolve, and that this section addresses.

Three gaps limit the ability of financial institutions to price and manage drought risk today. First, there is a persistent lack of granular data on the economic impacts of drought: recorded loss databases such as Munich Re's NatCatSERVICE undercount drought relative to model-based estimates by a factor of six or more, in part because slow-onset, diffuse hazards such as drought are harder to attribute and record than discrete events such as floods (JRC PESETA IV, 2020). Second, existing damage functions are rarely harmonised across countries and economic sectors: most climate–economic damage functions relate an aggregate hazard indicator to aggregate output (Burke et al., 2015) rather than differentiating impacts by sector and climate regime, even though drought vulnerability is known to vary sharply — by a factor of around four between Mediterranean and Atlantic climate zones, for instance (JRC PESETA IV, 2020; Cammalleri et al., 2020). Third, and most acutely for financial-sector applications, there are very few estimates of how drought-driven physical damages translate into losses on the specific bonds and equities held by financial institutions, as opposed to losses on aggregate GDP or capital stock. This last gap is becoming urgent in light of recent EU regulatory developments: the ECB's 2025 EU-wide climate stress test began, for the first time, incorporating physical-risk transmission channels into bank capital assessments — initially via flood events only, with the ECB itself noting that extending the analysis to hazards such as drought and wildfire "would provide a more comprehensive view" (ECB, 2025) — and EIOPA's 2026 statement on the climate insurance protection gap warns that only around a quarter of EU natural-catastrophe losses are currently insured, with that gap projected to widen further as extreme events increase (EIOPA, 2026). Supervisors are moving toward requiring banks, insurers and asset managers to demonstrate they can quantify drought-related losses at instrument level — a capability the current literature, including the current generation of stress tests, does not yet support.

Our work addresses these three gaps in two complementary ways. First, we develop a new approach to estimating a drought damage function that captures heterogeneity of impacts across economic sectors and countries. We use the well-established Köppen–Geiger climate classification to represent regional heterogeneity, and construct a drought intensity metric from the SPEI index, defined as the fraction of the year in which a location is in extreme drought (SPEI < −2). We draw on the European Drought Impact Database (EDID), whose 209,103 records describe drought impacts in free text and mostly qualitative terms; we address the unstructured and qualitative nature of this dataset by developing a keyword-based classification and severity-scoring scheme, then cross-match the resulting classified EDID events with the SPEI-derived intensity metric, grouped by economic sector and Köppen zone. This produces, for the first time, sector- and zone-specific empirical samples of drought intensity and impact, from which we estimate calibrated damage functions.

Second, we use these damage functions as an input to the CLIMACRED-PHYS structural credit-risk model (Mandel et al., 2025), already used in NGFS short-term climate scenarios, to estimate financial losses on a portfolio representative of EU financial institutions' holdings — 3,848 EU-domiciled firms with 8,745 geolocated production facilities. Facility-level impacts are aggregated to firm-level losses on fixed capital and output, and from there losses on bonds and equity are computed with the CLIMACRED-PHYS model.

As summarised in the Results section below, we find substantial heterogeneity in the fit and magnitude of sector-specific damage functions (e.g. Agriculture: $R^2 = 0.996$; Energy: $R^2 = 0.684$), and mean equity losses of around 11.7% against mean bond losses of around 4.5% under a central RCP 4.5 scenario — an equity/bond amplification of roughly 2.6× that is itself informative for how drought risk should be treated in portfolio construction and prudential capital requirements.

3.1.2 Data

This subsection briefly describes the datasets underpinning the analysis and their key descriptive statistics; full construction and quality-control details are provided in the underlying technical paper (Battiston & Puliga, 2026, Appendices A and D).

The European Drought Impact Database (EDID; Stahl et al., 2026) contains 209,103 news-based drought impact records spanning 1970–2023 across 33 European countries, each classified by sector (NACE codes) and geographic location (NUTS2/NUTS3). After correction for sector misclassification (24.3% of records reassigned), impact underestimation (64.9% recomputed), and historical event references (18.1% flagged), the database sector distribution is reported in Table 4.

Table 4. *Distribution of EDID records across macro-sectors after quality correction.*

Sector	Records	% of total
Agriculture	134,983	64.6%
Riverine transportation	19,702	9.4%
Water supply	12,564	6.0%
Energy	9,767	4.7%
Tourism	9,023	4.3%
Other	23,064	11.0%

Of these, 6,812 records are quantifiable and intersect with SPEI observations from the European Drought Observatory (EDO), which provides SPEI at 10 km resolution for six distinct accumulation periods — 3, 6, 9, 12, 24 and 48 months — chosen to capture drought signals ranging from short meteorological deficits to multi-year hydrological drought. Tourism (75 intersecting records) was ultimately excluded from damage-function calibration for lack of sufficient temporal precision, leaving five sectors — Agriculture, Water supply, Riverine transportation and Energy — in the calibration set.

Climate zone classification follows the Köppen–Geiger system (Beck et al., 2023), simplified to 15 zones for Europe at 1 km resolution. Mediterranean zones (Csa, Csb) exhibit impacts up to 4× those of Atlantic zones (Cfb), consistent with JRC PESETA IV (2020) and Cammalleri et al. (2020).

The financial portfolio merges plant-level asset inventories from Global Energy Monitor (GEM) and Climate Trace (CT) with firm-level revenue-segment data from Trading View (TV), comprising 20,649 unique ISINs and 54,584 plant–firm assignment records globally. Filtered to the European domain (34.5–72°N, −25–45°E), the EU sub-portfolio comprises 3,848 companies with 8,745 production facilities across 61 countries and territories. Only 12.3% of plants carry non-zero coordinates directly from CT/GEM; the remainder rely on GDP-weighted country centroids — derived from the Kummu et al. (2025) gridded GDP dataset — as a geolocation fallback. Key descriptive statistics of the EU sub-portfolio are summarised in Table 5.

Table 5. *Descriptive statistics of the EU sub-portfolio used in the valuation. Source: Battiston & Puliga (2026).*

Category	Metric	Value
Portfolio size	EU companies (ISINs)	3,848
Portfolio size	EU production facilities	8,745
Portfolio size	Countries / territories covered	61
Geolocation	Plants with direct CT/GEM coordinates	12.3%
Sector mix (top 5, by plant count)	Information Technology	21.9%
Sector mix (top 5, by plant count)	Financials	15.6%
Sector mix (top 5, by plant count)	Health Care	11.6%
Sector mix (top 5, by plant count)	Consumer Discretionary	11.4%
Sector mix (top 5, by plant count)	Industrials	10.5%
Top countries (by plant count)	United Kingdom	1,047
Top countries (by plant count)	Sweden	1,047
Top countries (by plant count)	Germany	944
Top countries (by plant count)	France	836
Top countries (by plant count)	Spain	762

3.1.3 Methods

Each EDID news item is classified into an economic sector in terms of NACE codes combined with description keyword scoring. Economic impact scores are continuous values in [0.05, 1.0], assigned according to keyword severity, duration and quantification (e.g. "complete halt" scores 0.75–1.00 depending on sector; "limited" impact scores 0.07–0.10). Drought intensity is defined as the fraction of months per year in which SPEI falls below −2 — the severe-drought threshold, exceeded with probability 2.28% under a standard-normal reference distribution (Vicente-Serrano et al., 2010):

$f = \text{count}(\text{SPEI} < -2) / 12$

Cross-matching each EDID record's location, Köppen zone, NACE sector and severity score against the co-located SPEI time series — a linkage absent from the raw EDID, which contains neither SPEI, NACE nor climate-zone fields — produces the new sector- and zone-resolved dataset of (drought intensity, impact) pairs used for calibration.

The relationship between drought frequency f and sectoral impact is fitted via a power-law damage function, evaluated across 12 combinations of statistic and SPEI accumulation period (3, 6, 9, 12, 24 and 48 months) at both NUTS2 and NUTS3 geographic levels:

$I(f) = a(f + 0.01)^b$

The power law is preferred over logarithmic and linear alternatives because it exhibits finite saturation (for b < 1), is theoretically consistent with the climate-economics literature (Burke et al., 2015), and nests the linear case (b = 1) as a special case.

Fitted impact functions are then rescaled across the 15 European Köppen zones using an exponent-perturbation approach:

$\text{new} = b_{\text{base}} \cdot 1.01^{-beff} \cdot (\text{risk\_value} + 0.01)^{beff}$

with the exponent perturbation given by

$b_{\text{eff}} = b_{\text{base}} \cdot p$

where p takes one of seven discrete values, {0.70, 0.82, 0.92, 1.00, 1.07, 1.14, 1.21}, representing the adaptation level, mapped onto an adaptation_pct scale from −30% (maladaptation, amplified losses) to +30% (effective adaptation, dampened losses). The leading term is a normalisation factor that keeps rescaled values bounded in [0, 1] and anchors the function at risk_value = 1.0 for all p.

The rescaled damage functions are integrated into the CLIMACRED-PHYS model (Mandel et al., 2025), a structural credit-risk framework that computes financial risk metrics at the firm level, built up from information at the production-facility level. Climate impacts enter through capital destruction and business interruption, which propagate through a linear production technology into firm-level cash flows and, via a structural default boundary, into the probability of default and the market value of bonds and equity for each firm in the portfolio. In line with the ACCREU project, impacts are evaluated across four RCP scenarios (2.6, 4.5, 7.0, 8.5) at return periods of 5, 10, 50 and 200 years; RCP 2.6 is adopted as the baseline. Because the valuation chain was originally run only for RCP 4.5 and RCP 8.5, coverage is extended to RCP 2.6 and RCP 7.0 by linear interpolation of both hazard and post-valuation outputs — a simplification whose implications for the ordering of results across scenarios are discussed in Section 3.1.4.

3.1.4 Results & Discussion

Sectoral calibration

The power-law damage function fits best for Agriculture, at 12-month SPEI accumulation (R^2 = 0.996, b = 0.234, see Figure 36), indicating strong saturation: incremental damages diminish rapidly once drought frequency rises above moderate levels. Water supply (48-month accumulation, R^2 = 0.916, b = 0.133) fits nearly as well. Energy (24-month accumulation, R^2 = 0.684, b = 0.649, see Figure 37) and Riverine transportation (48-month, R^2 = 0.674) show a slower, more linear response, consistent with the delayed transmission of hydrological deficits to energy infrastructure and inland waterways. In terms of the highest absolute damage levels, the sector–zone combinations with the largest calibrated impact factors are concentrated in the Hot Mediterranean zone (Csa): Energy reaches an impact factor of 0.300, Riverine transportation 0.250, and Agriculture 0.220 — roughly four to seven times the corresponding factors in the Norwegian Coast or Iceland zones, confirming that both sector and climate zone matter for where damage functions saturate.

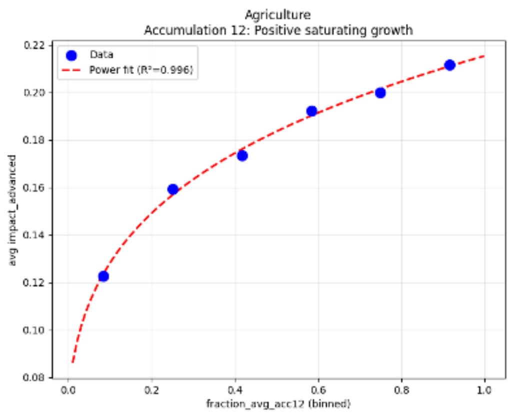

Figure 36. *Fitted damage function for Agriculture at 12-month SPEI accumulation (a = 0.215, b = 0.234, R^2 = 0.996). Source: Battiston & Puliga (2026).*

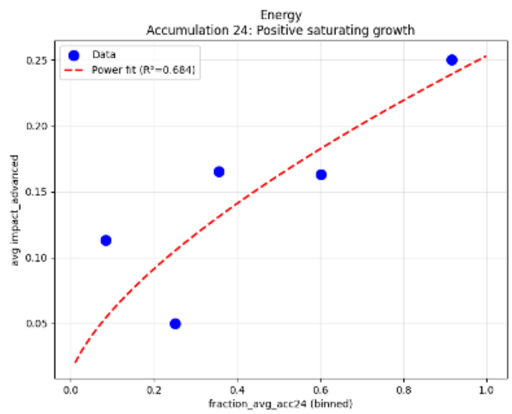

Figure 37. *Fitted damage function for Energy at 24-month SPEI accumulation (a = 0.251, b = 0.649, R^2 = 0.684). Source: Battiston & Puliga (2026).*

Financial impacts

Climate impacts first act on the physical, economic layer before propagating into financial losses: across the EU portfolio, plant-level capital destruction — the direct, economic-impact input to the valuation model. This capital-destruction and business-interruption layer is then carried through CLIMACRED-PHYS into losses on the bonds and equity actually held by financial institutions.

Figure 38 and Figure 39 show the average loss in % as a function of the return period (RP), and across RCP scenarios, for equity and bonds instruments, respectively.

Applying the calibrated damage functions through CLIMACRED-PHYS to the EU portfolio, under RCP 4.5 at a 200-year return period the mean bond loss is approximately 4%, against a mean equity loss of approximately 10%, reflecting the basic fact that equity is more risky than bonds as a financial instrument.

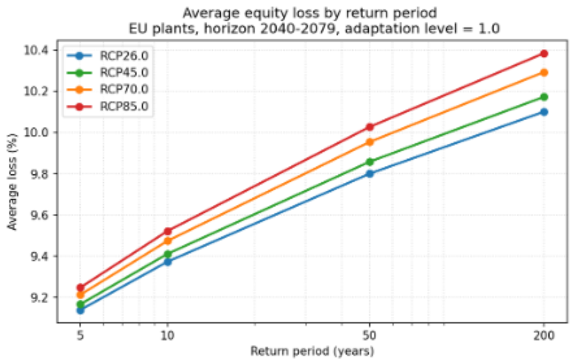

Figure 38. *The average loss in % is plotted as a function of the return period (RP), across RCP scenarios, for equity instruments.*

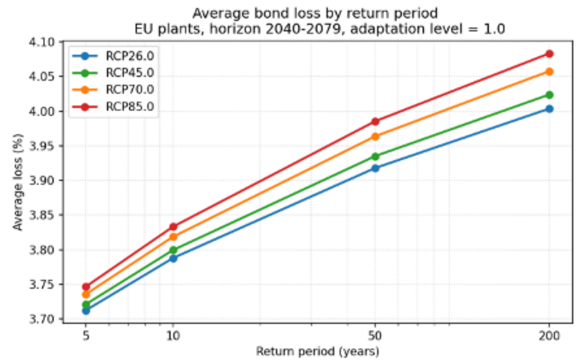

Figure 39. *The average loss in % is plotted as a function of the return period (RP), across RCP scenarios, for bond instruments.*

A counter-intuitive feature of the results is that losses do not increase strictly monotonically from RCP 2.6 through to RCP 8.5: RCP 2.6 produces losses only around 5% smaller than RCP 4.5, a much more modest gap than the difference in radiative forcing between the two scenarios would suggest. This is not a modelling artefact but a documented feature of the underlying climate data: only around 48.5% of grid cells satisfy the strict ordering of drought hazard across RCPs, because drought indices combine a temperature-driven potential-evapotranspiration term that scales monotonically with forcing with a precipitation term whose change is spatially heterogeneous and can even reverse sign between scenarios at the grid scale (Spinoni et al., 2018). In our data, several northern and central European regions project wetter conditions under stronger forcing during the mid-century transient period, before the full effect of higher emissions materialises, and CO_2-driven reductions in plant transpiration further compound this effect (Mankin et al., 2019). We treat this as an important caveat for how RCP-labelled loss estimates should be communicated to risk committees: the ordering across scenarios should not be assumed to be monotonic at the portfolio level, even though it holds on average across the full distribution.

Adaptation sensitivity

In line with the objectives of the ACCREU project, effort has been devoted to estimating the benefits of adaptation. This sensitivity analysis builds on the practice, coordinated within ACCREU, of assessing low, moderate and high levels of adaptation, and extends that three-level scheme to seven levels so as to explore the benefits of adaptation at finer granularity.

The sensitivity analysis on adaptation is carried out by perturbing the damage-function exponent across the seven-point grid — from p = 0.70 (−30%, maladaptation) through p = 1.00 (baseline) to p = 1.21 (+30%, the most effective adaptation level modelled) — shows that losses are amplified toward the maladaptation end of the grid and progressively dampened as p increases.

Figure 40 illustrates the results on output loss as a function of the adaptation level, across RCPs and RP. The identified “adaptation panel” (p = 1.14, +19.33%) produces lower mean output loss than baseline across all RCP × return-period combinations. The effect is more pronounced under higher-emission scenarios, where baseline hazard levels are higher and there is more “room” for adaptation to matter.

Figure 41 illustrates the results on financial losses for equity and bonds as a function of the adaptation level, across RCPs and RP, for bonds and equity, respectively. As expected, on average, the losses decrease with the level of adaptation and increase with the severity of the hazards (RP) and the climate scenario (RCP).

In terms of which sector–country combinations drive the largest financial losses, the pattern mirrors the sectoral calibration results above: Energy- and Agriculture-exposed firms located in Mediterranean and Hot Mediterranean climate zones (Spain, Italy, Greece, Portugal, and southern France) show the largest average equity losses, consistent with both the roughly 4× zone-level impact multiplier and the concentration of high- value production facilities in these regions.

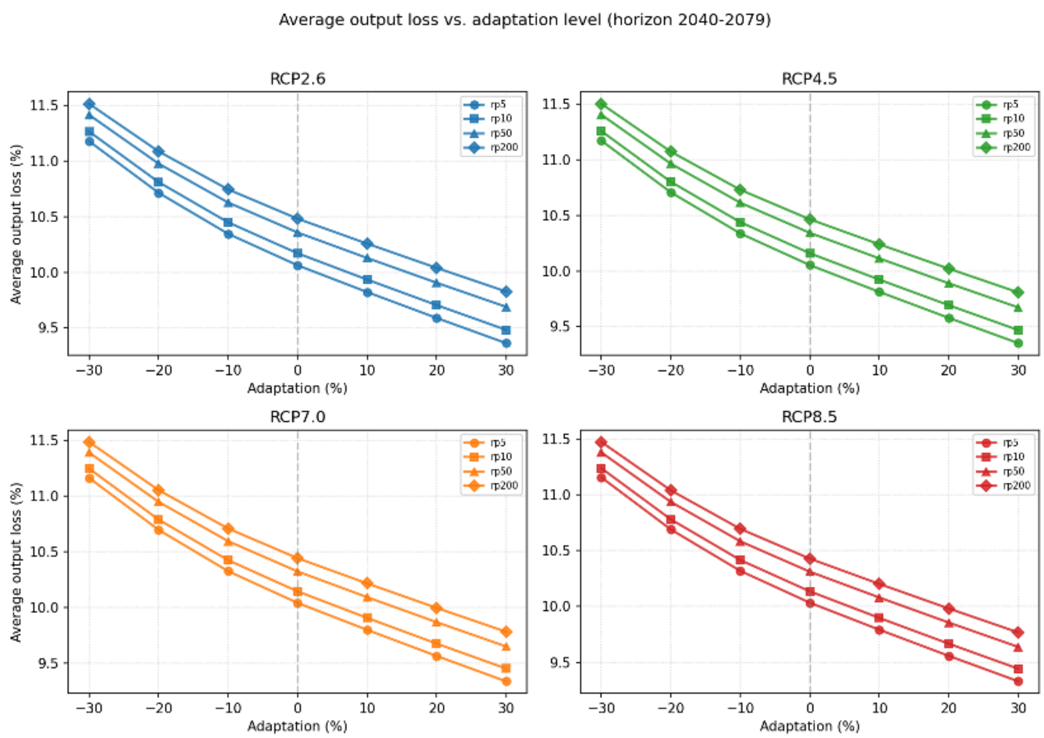

Figure 40. *The average loss in % is plotted as a function of the adaptation level (1 = baseline of no adaptation) across return periods (RP) and across RCP scenarios.*

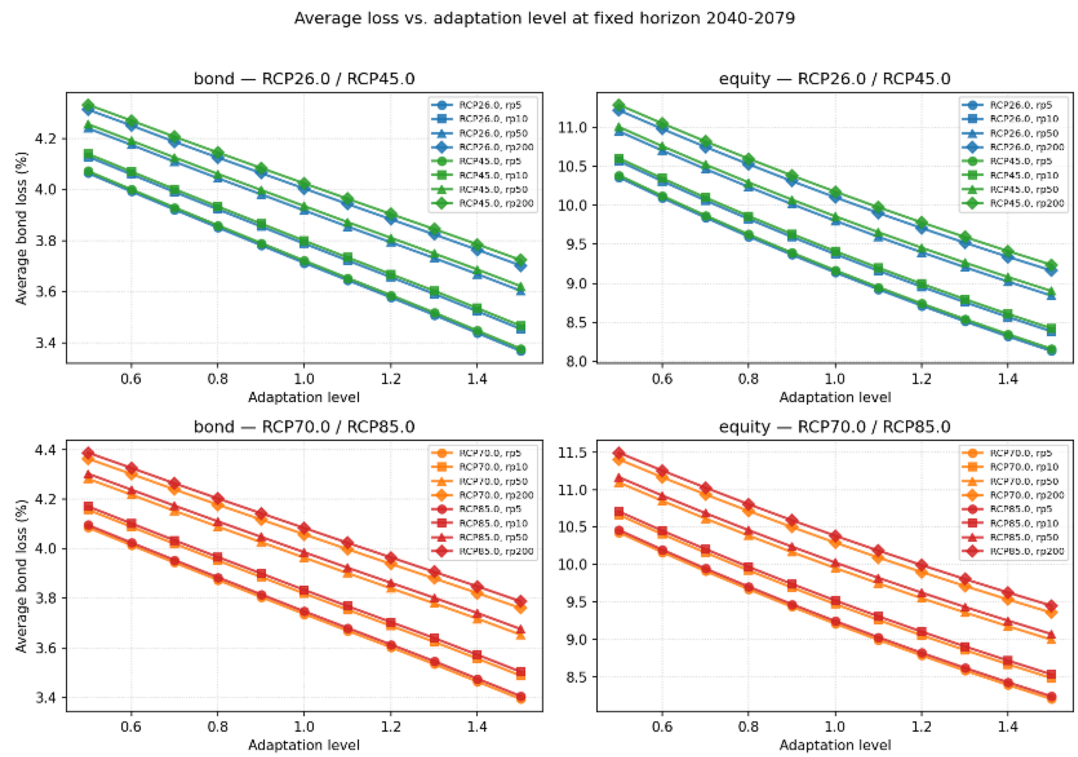

Figure 41. *The average loss in % on the value of equity and bonds is plotted as a function of the adaptation level (1 = baseline of no adaptation) across return periods (RP) and across RCP scenarios.*

Country-level comparison

In order to dive deeper into the origin of the heterogeneity of losses, we carry out a cross country comparison of output losses. Figure 42 shows the country rankings of output loss at RP = 10 year return period, across RCPs. Figure 43 shows the country rankings of output loss at RP = 200 year return period, across RCPs, with and without adaptation. Country-level impact rankings are consistent with independent water-risk assessments, which supports the external validity of the damage-function approach. Hungary is a useful case study precisely because its exposure is not obvious a priori: as a continental Central European country, it lacks the intuitive drought profile of Southern Europe. Yet WRI Aqueduct 4.0 (2023) ranks Hungary 16th globally (top 7%) and 1st in the EU-27 by irrigation-weighted drought exposure, and OECD (2026) independently describes Hungary as “among the most drought-exposed countries in Europe.” Our pipeline places Hungary among the highest-ranked EU countries by average equity loss at a 200-year return period, driven by a concentration of EV-battery manufacturing FDI — approximately EUR 1.5 billion, largely South Korean-owned — located in the Great Hungarian Plain, Hungary's most drought-exposed region. This corroborates nine independent peer-reviewed sources documenting EUR 1.6–2 billion in agricultural losses from the 2022 Hungarian drought alone and a recurrence of moderate drought roughly every two years (Biró & Kovács, 2023; Buzási et al., 2021).

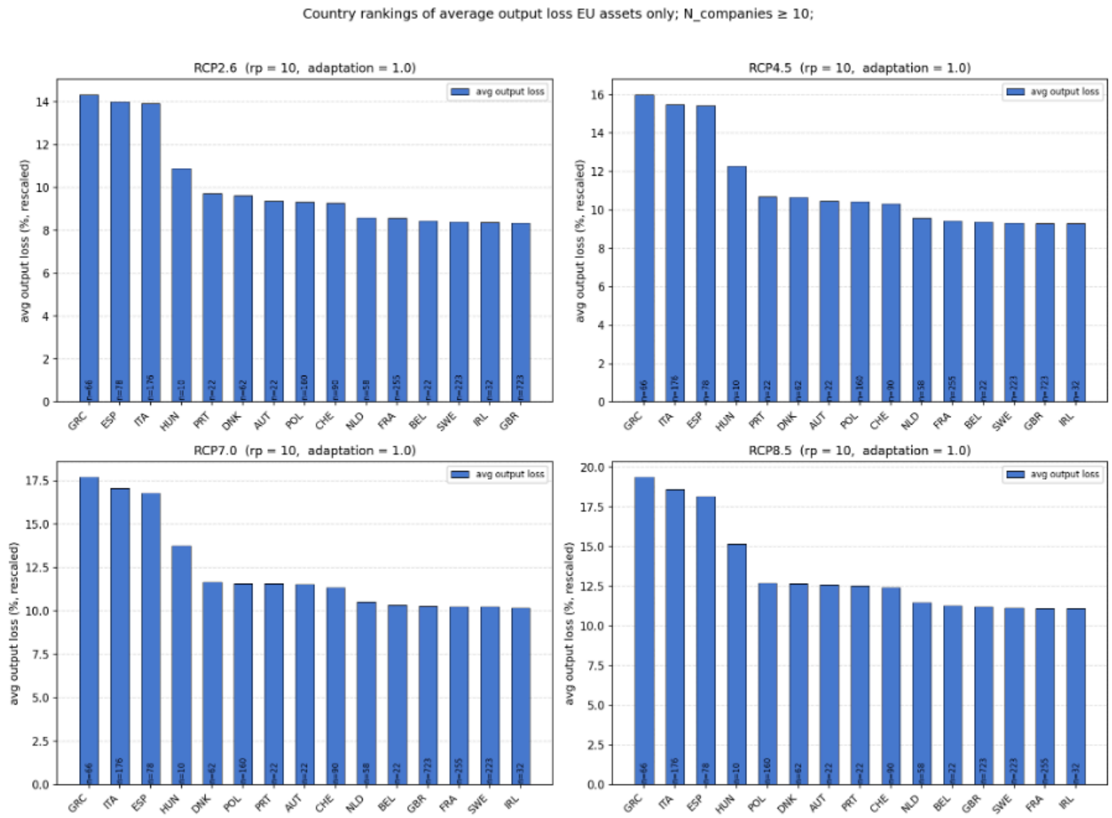

Figure 42. *Country rankings of average output loss at RP 10, across RCPs. Baseline adaptation (p = 1.00, 0%). Source: Battiston & Puliga (2026).*

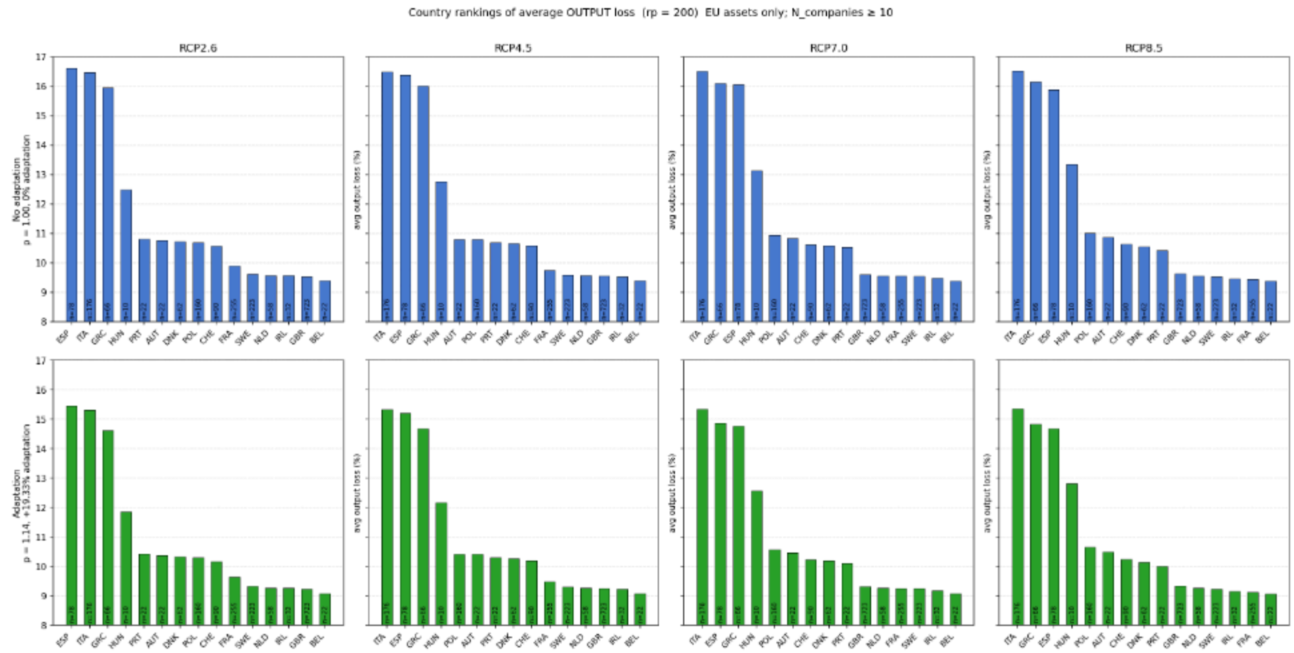

Figure 43. *Country rankings of output loss at a 200-year return period under the effective-adaptation panel (p = 1.14, +19.33%), compared against baseline. Source: Battiston & Puliga (2026).*

3.2 Assessment of Financial Risks Related to Flood

3.2.1 State of the Art and Issues Addressed

Floods are the costliest natural hazard facing the European Union, and anthropogenic warming is expected to raise their frequency and severity in the coming decades (Alfieri et al., 2015; Dottori et al., 2018). Assessing the financial consequences for firms — and for the banks, insurers and asset managers exposed to them — requires loss estimates granular enough to capture where risk concentrates, not merely its aggregate magnitude. This paper quantifies firm-level financial losses from riverine and coastal flooding across the EU corporate universe using a physical-asset valuation framework, characterising how losses conditional on a return period vary with return period, emission pathway (RCP), and adaptation level. This report focuses on the riverine (fluvial) dimension, historically the dominant driver of aggregate EU flood losses. This report is based on the working paper by Puliga and Battiston (2026), Financial risk for financial institutions from riverine floods in the EU, which develops the asset-level valuation framework and analysis summarised here.

Two recent events illustrate the stakes. The July 2021 floods in western Germany caused an estimated USD 40 billion (~EUR 35 billion) in economic losses (Munich Re, 2022), the costliest natural catastrophe in the country's history, of which only ~EUR 8.2 billion was insured (GDV, 2021). The May 2023 Emilia-Romagna floods produced a provisional damage estimate of EUR 8.8–8.9 billion (Regione Emilia-Romagna, 2023) — over 5% of the region's annual GDP — against insured losses of only ~EUR 495 million (PERILS, 2024). Such events run an order of magnitude above the EU-wide annual average of ~EUR 7.8 billion (0.06% of GDP), projected to reach EUR 24–48 billion (0.05–0.11% of GDP) by century's end absent further adaptation (Dottori et al., 2020, 2022). This gap between sub-0.1%-of-GDP annual averages and >5%-of-GDP single events shows that aggregate figures obscure the concentrated, tail-driven nature of riverine losses (Jongman et al., 2014).

This matters for resilience analysis because balance-sheet resilience is tested by tail events, not means: loss estimates conditional on a return period (RP) are more informative than unconditional averages. An RP of T years denotes a severity exceeded on average once every T years; a 100-year flood carries roughly a 22% chance of occurring at least once over the 10-year life of a typical corporate bond.

EU regulation has moved rapidly toward requiring physical climate risk assessment. EIOPA (2022) put aggregate EU insured exposure to river and coastal flood at EUR 28.9 trillion and EUR 9.1 trillion respectively, while noting that granular exposure data remain largely unavailable under Solvency II; the ECB's 2022 stress test found most banks still rely on simplified, top-down approaches (ECB Banking Supervision, 2022). The CSRD/ESRS E1 disclosure regime and the EU Taxonomy's climate-adaptation criteria now require asset- and location-specific vulnerability assessment, pushing flood risk assessment toward granular, return-period-conditional loss estimates at the level of individual assets and firms — the gap this paper addresses.

The paper asks two questions: whether cross-firm heterogeneity is large enough that a small sub-portfolio's conditional expected loss can substantially exceed the full-sample loss at a given RP; and how the conditional expected loss and its distribution (median, IQR) vary with RP, RCP and adaptation. Prior work on this dependence is almost exclusively aggregated at country or EU level (Alfieri et al., 2015; Dottori et al., 2018, 2020, 2022; Jongman et al., 2014). Two recent studies move to asset-level granularity across hazard types: Mandel et al. (2025) value losses on individual plants matched to owning firms, and Bressan et al. (2024) show that neglecting asset-level and tail-risk granularity leads investors to underestimate losses. This paper extends both by working throughout at the individual-asset/firm level for two flood mechanisms, and by introducing — for the first time in this literature — an explicit dependence of losses on adaptation level alongside RP and RCP.

3.2.2 Data

The riverine (fluvial) flood hazard analysis is built on the ISIMIP2b fluvial-flood product (DOI 10.48364/ISIMIP.303619), distributed through the WRI Aqueduct Floods v2 mirror (Frieler et al., 2017). The dataset comprises 279 rasters at 30 arc-second resolution reporting flood water depth in metres (specification in Table 6). The raster inventory spans the full Cartesian product of a historical baseline (WATCH/WFDEI reanalysis, representative year 1980), five CMIP5 GCMs (GFDL-ESM2M, HadGEM2-ES, IPSL-CM5A-LR, MIROC-ESM-CHEM, NorESM1-M), two RCP scenarios (4.5 and 8.5), three future horizons (2030, 2050, 2080), and nine return periods (2 to 1000 years). The five GCMs span the CMIP5 equilibrium-climate-sensitivity range from 2.4 K (GFDL-ESM2M) to 4.7 K (MIROC-ESM-CHEM) (IPCC AR5 WG1 Table 9.5; Andrews et al., 2012;

Forster et al., 2013), a spread that matters for financial risk assessment because flood damage is spatially concentrated: only a small fraction of assets lie in flood-prone areas, but those that do face disproportionate losses. Flood protection standards are applied per pixel via FLOPROS (Scussolini et al., 2016), so reported depths are residual hazard above defence levels; the underlying CaMa-Flood hydrodynamic model uses a local-inertial approximation (Bates et al., 2010) with SRTM sub-grid topography, preserving local topographic controls on inundation extent at final 30 arc-second resolution.

Table 6. *ISIMIP2b fluvial-flood raster specification (Frieler et al., 2017).*

Property	Value
Coordinate reference system	EPSG:4326 (WGS84 lat/lon)
Pixel size	1/120° (30 arc-seconds, ~0.93 km at the equator)
Grid dimensions	43,200 × 21,600 (global)
Data type	float32 (metres of flood water depth)
No-data value	−9999.0
Scenario coverage	1 historical baseline + 5 GCMs × 2 RCPs × 3 horizons × 9 return periods = 279 rasters

Flood hazard is translated into direct economic damage via the JRC PESETA IV depth-damage framework (Huizinga et al., 2017; Dottori et al., 2020). Each asset is first classified by dominant land-cover class using the CORINE Land Cover 2018 raster at 100 m resolution (EEA, 2019; 44 thematic classes), then mapped through the Huizinga six-category land-use system — residential, commercial, industrial, transport, agricultural, infrastructure (Huizinga, 2007; Huizinga et al., 2017). The flood depth at the asset location is evaluated against the depth-damage curve for its Huizinga sector, yielding a fractional loss in [0, 1] that is multiplied by the asset's replacement value. Each curve is concave and monotonic — damage rises steeply in the first 0–1 m of inundation, where foundations, electrical systems and ground-floor finishes are reached, and flattens at greater depths — reflecting the empirical finding that most structural and content losses occur within the first metre of water (Kreibich et al., 2010; Jongman et al., 2012). Curves are differentiated by four European macro-regions (North, West, South, East) to capture differences in construction standards and floor elevations, with maximum damage values calibrated from multinational construction-cost surveys (Huizinga et al., 2017).

The firm-level portfolio is drawn from the GEM/CT database (~20,000 listed firms globally with EU domicile). For the flood analysis, the plant grid and asset table are derived from the intersection of GEM/CT with the ISIMIP2b hazard rasters: the plant grid contains 9,630 EU plant records (name, ISIN, NACE sector, revenue, coordinates, usability flag), and the asset table provides 3,889 unique ISIN-level records (risk-free rate, return on assets, baseline probability of default, valuation and maturity years), matched via ISIN. Of the 8,906 usable plants after quality filtering, only those intersecting a flooded raster cell carry non-zero hazard intensity: in the reference scenario (below), 646 of 8,906 plants (7.3%) have a non-zero depth-damage fraction, affecting 519 of 3,859 matched firms (13.4%). Not all plant coordinates are publicly disclosed: of the 8,906 usable EU plants, 4,815

(55%) lack disclosed coordinates and are instead assigned an imputed location (Section 3.1.3), while the remaining 4,091 plants use their actual, disclosed coordinates.

The paper's reference scenario for both flood mechanisms is MIROC-ESM-CHEM, RCP4.5, 2050, return period 100 years. RCP4.5 is chosen as the most policy-relevant pathway — current-policy projections in IPCC AR6 track closer to SSP2-4.5 than the high-end SSP5-8.5 (Chen et al., 2021; Hausfather, 2020; Sarofim et al., 2024) — while missing carbon-cycle feedbacks make it a more defensible central estimate than RCP2.6 at mid-century (Smith & Gu, 2023). MIROC-ESM-CHEM is chosen as the reference GCM for its ~4.7 K equilibrium climate sensitivity, at the upper end of the CMIP5 ensemble, providing a conservative stress test: if losses are manageable under a high-sensitivity model, they should be smaller under lower-sensitivity ones (Watanabe et al., 2011; Watanabe & Takemura, 2020). Return period 100 years is chosen because it best captures tail risk relevant to long-lived instruments: the probability of a 100-year flood occurring within the 10-year life of a typical corporate bond is approximately 22%, materially above the credit-spread equivalent of typical investment-grade default risk. Per-ISIN and per-country figures in this report are, where the data permit, regenerated from a strictly European-only ISIN subset (Section 3.1.3); some figures retain the broader European or global grid where that subset is too sparse for stable statistics, a caveat noted at each such figure.

3.2.3 Methods

As a quality-assurance step, the published ISIMIP2b return-level rasters are independently reproduced by fitting GEV/Gumbel distributions to annual maxima (block size 365.2425 days) via maximum likelihood, using pyextremes v2.5.0 (Bocharov, 2026), with bootstrap confidence intervals (1,000 samples, $\alpha = 0.95$) used solely to verify internal consistency; they do not enter the downstream valuation, which reads flood depth directly from the published rasters at each asset's pixel. Climate-change deltas are computed per pixel, return period and GCM as the difference between future and historical return levels.

Because the coarse 30 arc-second rasters assign a single average depth per cell, each cell is downscaled to the 3 arc-second (~90 m) resolution of the MERIT DEM (Yamazaki et al., 2017) by partitioning it into a 10×10 sub-cell grid and redistributing the cell's total water volume across sub-cells according to their high-resolution elevations, preserving local topographic controls that the coarse grid would otherwise average away.

Damage estimates are integrated into the CLIMACRED-PHYS valuation framework (Mandel et al., 2025), which estimates firm-level financial losses through three channels: loss of fixed capital, loss of output via business-interruption days, and loss of labour productivity. For each asset i, damage is Damage = $V_i \times f\_damage(d_i)$, where V_i is replacement value, f_damage is the depth-damage curve for the asset's Huizinga sector S and CORINE terrain-type sub-class T, and d_i is the local (downscaled) flood depth. This paper extends the existing country-level implementation — which evaluates all assets in a country against a single continental curve — with an asset-level land-use dimension using CORINE Land Cover 2018, distinguishing residential, commercial, industrial, agricultural and infrastructure assets and providing per-country (214 countries) rather than per-continent maximum damage values. Business interruption is modelled as a constant daily rate of 240/365 ≈ 0.658 of annual revenue for each inoperable day, applied uniformly across all six Huizinga sectors; this is consistent with the FEMA HAZUS-MH flood model's default 240-day business-interruption period for facilities without power or access (FEMA, 2003) and with insurance-claim-based recovery-time estimates (Kreibich et al., 2010). Capital destruction and business interruption feed into scenario-dependent probability of default and the resulting bond and equity losses.

Because ISIMIP2b only provides rasters for RCP4.5 and RCP8.5, loss outputs for RCP2.6 and RCP7.0 are obtained by post-valuation linear interpolation (RCP2.6: extrapolation) at the model-output level, per GCM, year and return period: RCP7.0 is a convex combination (37.5% RCP4.5 + 62.5% RCP8.5) and RCP2.6 an affine extrapolation (147.5% RCP4.5 − 47.5% RCP8.5), with each interpolated series clipped to its plausible range.

Adaptation measures (flood defences, land-use planning, retrofits) are represented as a multiplicative perturbation $p \in [0,1]$ applied to hazard intensity, $f_{perturbed} = f \times (1 - p)$, applied equivalently at the hazard-raster or batch-valuation stage. Levels of $p = 0$ (baseline), 0.05, 0.10, 0.20, 0.25 and 0.50 are analysed as stylised moderate-to-ambitious adaptation scenarios; the perturbation scales intensity only, so the set of firms affected is unchanged.

For assets whose coordinates are not publicly disclosed (4,815 of the 8,906 usable EU plants, 55%), location is imputed as a GDP-weighted centroid within a 5 km buffer of the European river network (HydroSHEDS; Lehner et al., 2008), the buffer width chosen to match the typical 100-year inundation extent along medium-sized European rivers under the EU Floods Directive (2007/60/EC; European Parliament & Council, 2007). GDP is drawn from the Global Wealth Project v4 grid (Kummu et al., 2018), downscaled to 30 arc-seconds via HYDE 3.1 population density (HYDE, 2016). This shifts imputed locations toward both economically productive and flood-exposed areas, giving a conservative exposure estimate for non-disclosed facilities relative to a general population centroid.

Country-level results aggregate per-ISIN bond and equity losses weighted by each firm's revenue share at each plant location; the headline breadth metric, frac_impacted, is the share of firms in a country whose post-hazard survival drops below a 0.1% loss threshold, with 1% and 2% thresholds used to check whether incidence is shallow or deep. All per-ISIN and per-country figures in this report are regenerated from a strictly European-only ISIN subset — an ISIN is retained only if every one of its plants sits in one of 43 European ISO 3166-1 alpha-3 jurisdictions (Russia, Belarus, Ukraine, Moldova and Turkey are explicitly excluded) — which reduces the GEM/CT plant grid from 20,647 ISINs (54,584 plants) to 1,117 EU ISINs (1,655 EU plants); some figures retain the broader European or global grid where this subset is too sparse for stable statistics, as noted at each such figure.

A parallel, riverine-specific case study applies the same valuation pipeline to a Dutch dike-ring breach hazard dataset (LIWO kaart1, 25 m resolution; LIWO, 2024) rather than the ISIMIP2b grid, evaluating each of the Netherlands' 127 independently regulated dike rings (Rijkswaterstaat, 2012) at its own regulatory return period (250 to 10,000 years) and scaling flood depth across return periods via depth(rp) = depth_kaart1 × (rp/100,000)^0.3; results are reported separately in Section 3.2.4.

3.2.4 Results & Discussion

At the reference scenario (MIROC-ESM-CHEM, RCP4.5, 2050, RP=100, p=0), 519 of 3,859 matched European-plant ISINs (13.4%) carry a non-zero riverine loss, in both RCP4.5 and RCP8.5 — a substantially broader impact footprint than the 14–17-firm coastal tail, reflecting the wider spatial reach of fluvial inundation across the EU. Among impacted firms, the mean positive-loss equity loss (~2.0% under RCP4.5, ~2.2% under RCP8.5) runs roughly twice the bond channel (~1.0%), and maximum equity losses reach 51.7% (RCP4.5) and 50.3% (RCP8.5) — a heavier tail in equity than in bond.

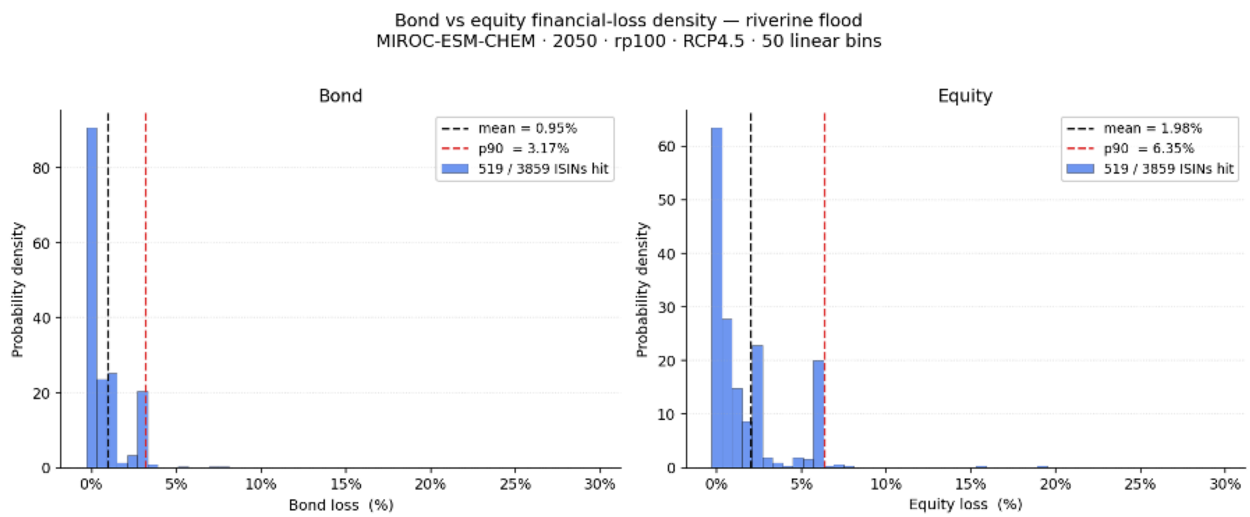

Figure 44. *Distribution of per-ISIN bond and equity financial losses, riverine flood, RCP4.5, reference scenario (2050, RP=100, p=0). Bond mean positive-loss 0.95%, equity 1.98%. Source: Puliga & Battiston (2026).*

The distribution of per-ISIN losses is strongly right-skewed: in the lowest density bin (loss < 0.6%), RCP4.5 places 280 of 3,859 ISINs (7.3%) and RCP8.5 places 269 (7.0%), consistent with the 13.4% any-loss headline; the mass above 1% loss sits in a long right tail, with the equity channel carrying roughly twice the ISIN count of the bond channel above that threshold. The p99/p50 ratio of the per-ISIN equity loss distribution stays in a narrow 7.21–8.76 band across all nine return periods and four RCPs, indicating that the shape of the loss distribution is stable across scenarios: what shifts with RP and RCP is the distribution's location, not its tail-to-median ratio — a useful regularity for extrapolating tail losses from a shift in the median.

Losses are geographically concentrated. Ranked by mean bond loss (RCP4.5, return periods 50/100/250 pooled, p=0), Denmark leads at 1.78% (max 3.79%, n=447 pooled points), followed by the Netherlands at 1.20% (max 1.45%, n=186); Austria's mean is far lower (0.17%) but its maximum (7.79%, rising to 8.48% under RCP8.5) is the largest in the dataset, driven by a single outlier firm among 408 otherwise near-zero pooled points — a single-firm concentration pattern echoed at the coastal level in the UK and Ireland. Four countries (Slovenia, Portugal, Latvia, Luxembourg) show zero mean and maximum loss across the pooled points.

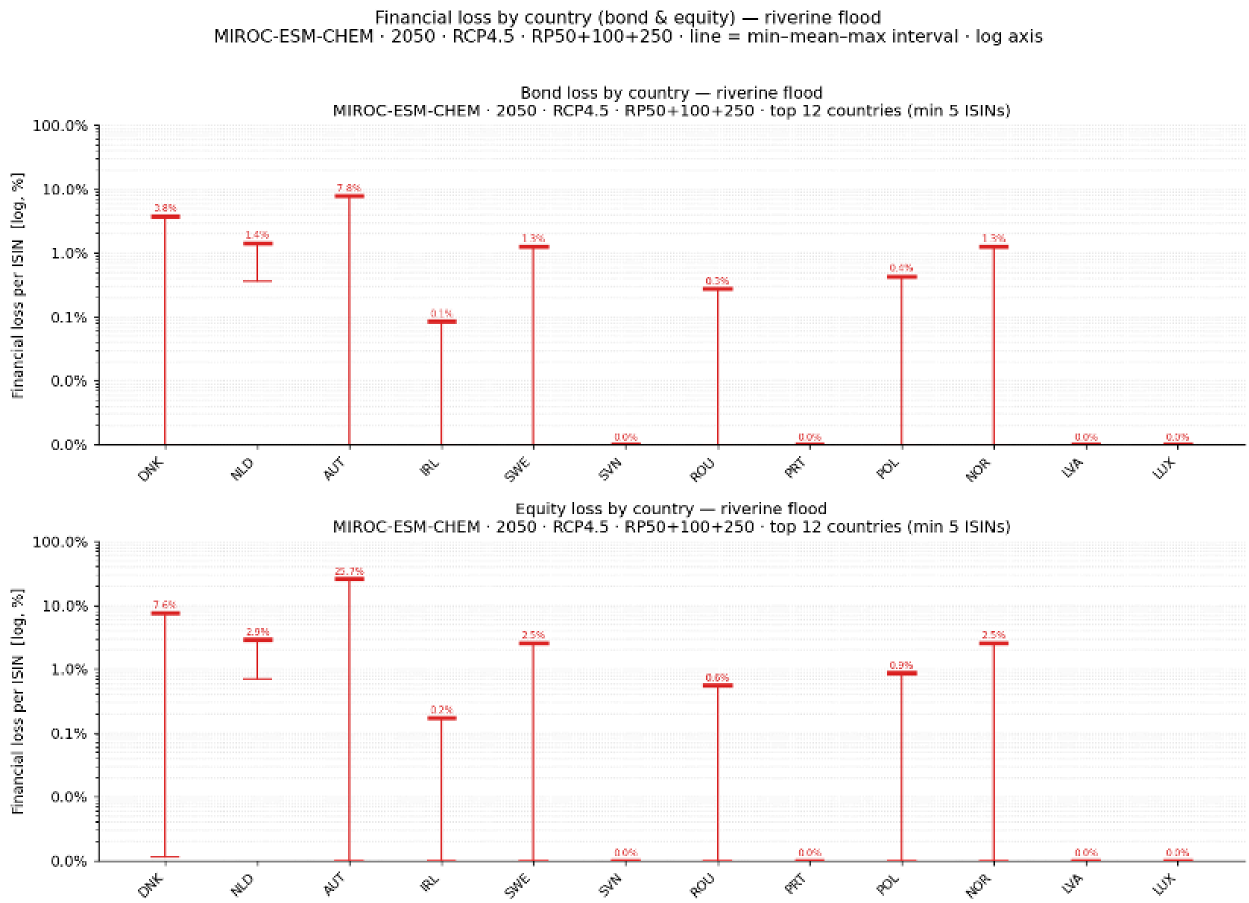

Figure 45. *Per-country bond and equity loss (mean, min–max range), riverine flood, RCP4.5, pooled RP 50/100/250, top-12 countries by median bond loss. Source: Puliga & Battiston (2026).*

Risk maps at the reference scenario confirm this clustering: Denmark and the Netherlands show 100% ISIN hit-rates (every plant-owning firm in-country carries some loss), with the two countries recording the highest mean equity loss (3.96% and 2.72% under RCP8.5), while larger, more diffusely exposed portfolios such as Germany's show broad but shallow exposure (13% of a 726-ISIN portfolio hit, at low average loss).

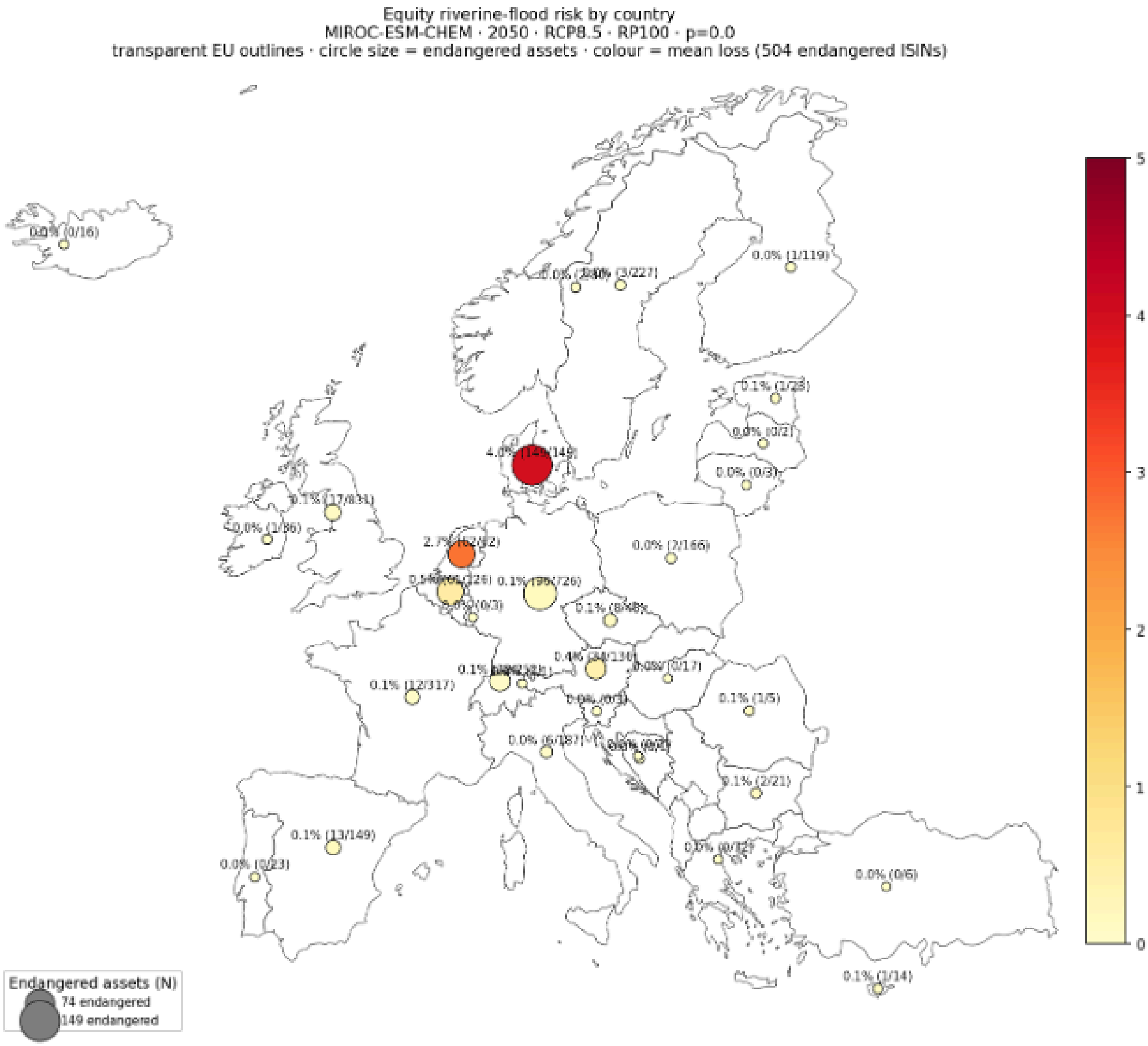

Figure 46. *Per-country mean equity loss and ISIN hit-rate, riverine flood, RCP8.5, reference year/RP (2050, RP=100, p=0). Circle size = number of endangered assets. Denmark 3.96%, Netherlands 2.72%, Belgium 0.55%. Source: Puliga & Battiston (2026).*

Loss grows with return period, non-linearly and consistently with the concave shape of the Huizinga damage curve, which rises steeply through 0–1 m of depth and saturates thereafter. Over the three pooled return periods (50, 100, 250 years), the RCP4.5 mean bond loss (p=0) is well fit by a log-linear relationship, $L = 0.108 + 0.0262 \times \log_{10}(RP)$, matching the three observed points (0.1084%, 0.1267%, 0.1504%) to within 0.0003 percentage points; the coastal analogue shows the curve steepening further beyond RP=100, so extrapolating this fit to RP=1000 would likely understate tail losses. Loss also grows with RCP severity: at RP=100, p=0, RCP8.5 sits systematically above RCP4.5 across the full adaptation sweep (e.g., mean bond loss 0.1421% vs 0.1267%), with an RCP8.5/RCP4.5 amplification factor of approximately 12% that holds consistently across bond and equity channels, return periods and adaptation levels.

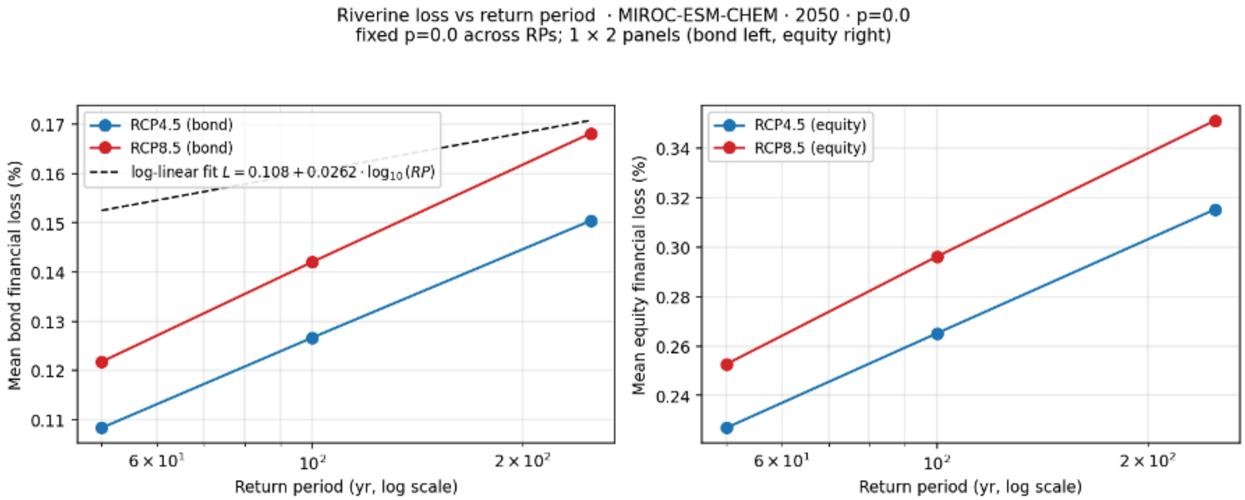

Figure 47. *Mean riverine bond and equity loss vs. return period (log-x axis), RCP4.5 and RCP8.5, 2050. The RCP4.5 bond panel also shows a log-linear reference line fit to the three sampled return periods (50, 100, 250); with only three points, this line is illustrative rather than a validated functional form — the underlying RP-dependence is the result this figure is included to show. Source: Puliga & Battiston (2026).*

Adaptation reduces losses in a near-monotone but not exactly linear way. At RCP4.5, RP=100, mean bond loss falls from 0.1267% at p=0 to 0.0646% at p=0.50 (RCP8.5: 0.1421% to 0.0725%); comparing observed values against the linear prediction implied by the depth-rescaling rule (f_perturbed = f × (1−p)) shows a deviation that grows monotonically with p, from +0.2% at p=0.05 to +2.1% at p=0.50 — the linear hazard-scaling rule slightly understates residual loss at high adaptation levels because the depth-to-loss transmission through the valuation model is itself non-linear.

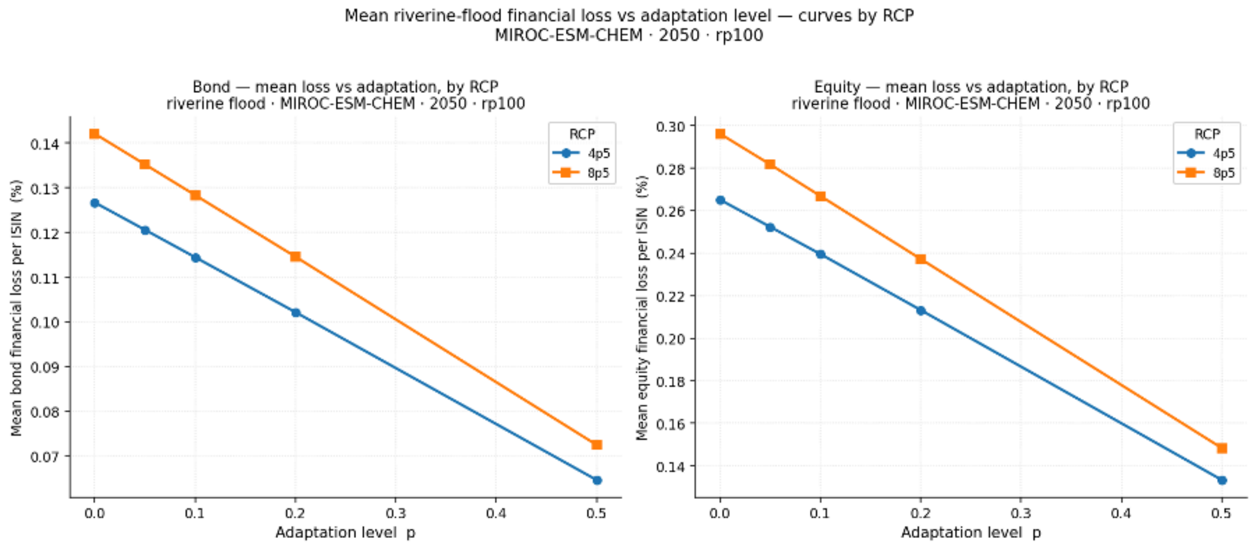

Figure 48. *Mean riverine bond and equity loss vs. adaptation level p, by RCP, at RP=100 (2050). RCP4.5 bond 0.127%→0.065%, equity 0.265%→0.133%; RCP8.5 bond 0.142%→0.073%, equity 0.296%→0.148%. Source: Puliga & Battiston (2026).*

This pattern held across all three sampled return periods and both RCPs. Because the adaptation-vs-loss relationship is only approximately linear, and because 99% of firms carry zero loss at any adaptation level with only the small impacted tail showing meaningful depth-sensitivity, this framework is best read as a sensitivity bracket rather than a precise functional relationship.

These results draw on two overlapping but distinct portfolio subsets: the strict European-only ISIN filter of Section 3.1.3 (1,117 ISINs, 1,655 plants), used for the per-country ranking above, and a broader "European-plant" filter (3,859 matched ISINs) used for the per-firm distribution and risk-map figures, retained where the stricter filter would be too sparse for stable statistics. Readers comparing figures across this section should note which subset underlies each number; the underlying paper flags this explicitly wherever the broader grid is used in place of the European-only subset.

The Dutch dike-ring case study — 121 plants owned by 81 Dutch-domiciled firms inside the LIWO flood envelope of the Netherlands' 127 independently regulated dike rings — is treated separately because breach of a ring dike is a structurally different hazard mechanism from a fluvial tail event. The most-protected rings, chiefly in the low-lying, densely populated Randstad (with safety standards historically up to 1:10,000 years; Rijkswaterstaat, 2012), experience the deepest design-event flooding precisely because their defences are only overtopped under the most extreme return periods; tail exposure is spatially concentrated in Zuid-Holland (dike ring 14).

3.2.5 Conclusion / Key Takeaways

Two conclusions follow from the riverine analysis. First, annual-average damage figures — however useful for macro-level policy — substantially understate the loss a concentrated portfolio can face: while the EU-wide average riverine loss sits below 0.1% of GDP, individual events (Germany 2021, Emilia-Romagna 2023) have caused losses exceeding 1% of national and 5% of regional GDP respectively, and at the firm level a small number of countries (Denmark, the Netherlands) and individual outlier firms (e.g., in Austria) carry losses many multiples of the portfolio-wide mean. Loss estimates conditional on a return period — rather than unconditional annual averages — are therefore the more decision-relevant metric for assessing balance-sheet resilience to tail events.

Second, the paper's systematic, asset-level treatment of loss as a function of return period, RCP and adaptation level shows that all three dimensions matter, but not equally or linearly. Loss grows non-linearly and consistently with return period (log-linear over the 50–250-year range sampled here, with evidence of further steepening beyond RP=100), and by an approximately constant ~12% RCP8.5-over-RCP4.5 amplification factor that is small relative to RP-driven variation. Adaptation reduces expected loss substantially — up to 50% at p=0.50 — but the reduction is only approximately linear in the perturbation level, understating residual loss at high adaptation by up to 2.1% at the aggregate level, and potentially more at the level of individual, heavily exposed firms. Taken together, these results argue for return-period- and firm-level-conditional risk assessment, rather than RCP- or adaptation-level headline figures alone, as the basis for financial flood-risk disclosure and portfolio stress-testing.

3.3 Assessment of Financial Risks Related to Dyke Breaches: The Netherlands Case Study

3.3.1 State of the Art and Issues Addressed

The Netherlands protects roughly half its national territory from flooding through a modular system of 127 independently regulated dike rings (dijkringen), each carrying a legally mandated safety standard — a normfrequentie — ranging from 1:250 years for the upper-Maas sandy-soil polders to 1:10,000 years for the densely populated Randstad coastal polders (Rijkswaterstaat, 2012). Since the 2017 Water Act, these standards have been differentiated by dike section (traject) according to expected consequences — casualties, economic damage, disruption of vital infrastructure — rather than held uniform within each ring, with all areas required to reach their target protection level by approximately 2050 (Deltares, 2016; Rijkswaterstaat, 2023). The technical basis for the standards is the Veiligheid Nederland in Kaart (VNK2) project, completed in 2014, which performed probabilistic quantitative risk analyses for all 127 major levee systems (Jongejan et al., 2012; WARTA, 2020).

A defining structural feature of the Dutch defence system is its modularity: a breach in one ring does not propagate to its neighbours because their defences remain intact, so a "national flood" is in practice a portfolio of independent single-ring breaches rather than one coherent event. This has direct consequences for financial risk — it renders the majority of a nationally domiciled portfolio immune to any single breach event while concentrating tail exposure at specific defended locations. Yet most European flood-risk stress tests treat the Netherlands as a single integrated entity and model it with fluvial and coastal flood hazards only (Alfieri et al., 2015, 2017; Dottori et al., 2018; Vousdoukas et al., 2018, 2020), systematically missing the conditional severity of dike-ring breaches — losses that, if a breach occurs, can reach nearly half a bond's equity at a single concentrated location.

This report addresses that gap by applying the CLIMACRED-PHYS structural credit-risk framework (Mandel et al., 2025) to the Dutch dike-ring system, using three official Rijkswaterstaat hazard datasets accessed through the Landelijk Informatiesysteem Water en Overstromingen (LIWO), and evaluates a 121-plant Dutch industrial portfolio owned by 93 unique ISINs (81 bonds) distributed across 12 dike rings. The resulting risk profile — modular immunity combined with concentrated tail exposure — is qualitatively distinct from both broad-based drought risk and probabilistically distributed fluvial flood risk analysed elsewhere (Puliga & Battiston, 2026a, 2026b), and motivates ring-level rather than purely portfolio-level stress testing for Dutch-domiciled financial institutions.

3.3.2 Data

Dutch flood-defence system and the VNK2 framework. The current delineation defines 127 numbered dike-ring areas (Rijkswaterstaat, 2012), each regulated under a specific *normfrequentie* — the legally mandated maximum exceedance probability of the design water level — ranging from 1:250 years (upper-Maas sandy-soil polders) to 1:10,000 years (Randstad coastal polders). VNK2 (completed 2014) performed probabilistic quantitative risk analyses for all 127 major levee systems, subdividing each ring into up to 13 ringdelen (ring segments) for which flood pattern and economic damage are approximately invariant to the precise breach location. Scenario probabilities are calculated for all combinations of failing and non-failing segments; with no relief and 13 segments the number of possible scenarios per ring reaches $2^{13} - 1 = 8{,}191$, underscoring the combinatorial complexity of Dutch flood risk.

LIWO hazard datasets. Three official Rijkswaterstaat hazard datasets are drawn from the Landelijk Informatiesysteem Water en Overstromingen (LIWO), a national flood information portal developed by Deltares and HKV (LIWO, 2024). The LIWO kaart1 raster (25 m resolution, national coverage) is the maximum water depth over all individual dike-ring breach scenarios — the per-cell maximum of the VNK (primary-defence), regional-defence, buitendijkse (unprotected), and worst-conceivable (Ernstigste Denkbare Overstroming, EDO) scenario families. It is therefore a spatial upper bound on single-ring breach depth, not a simultaneous national flood: the EDO scenarios represent compound events in which primary defences fail at many locations simultaneously under an approximately 1-in-100,000-year loading — a western-coast EDO would flood 14 dike rings, inundate roughly 6,000 km^2, affect 2.3 million inhabitants, and cause EUR 82 billion in damage (LIWO, 2024; Rijkswaterstaat, 2024). Two further layers come from the Klimaatatlas Zuid-Holland: a primary-defence breach scenario (2020) and a regional-defence breach scenario (2021), both at current-climate baseline (Provincie Zuid-Holland, 2020, 2021).

Dutch sub-portfolio. The portfolio is drawn from the GEM/CT (Global Energy Monitor / Climate TRACE) database, enriched via the Exa Labs geolocation pipeline, yielding 121 production facilities owned by 93 unique ISINs (81 bonds) across 12 dike rings. The portfolio is heavily concentrated in ring 14 (Zuid-Holland, 79 plants) and ring 44 (Kromme Rijn, 15 plants), with the remainder spread across inland rings 8, 36, 43, 45, 47, 52 and 53 (Table 7). Headquarters were deliberately excluded from the exposure analysis on the grounds that they typically house administrative rather than production functions.

Table 7. *Distribution of the Dutch sub-portfolio across dike rings.*

Dike ring	Plants	Notes
14 (Zuid-Holland)	79	Randstad coastal polder, design ~1:10,000 yr
44 (Kromme Rijn)	15	Inland, central Netherlands
8, 36, 43, 45, 47, 52, 53	27 (combined)	Inland rings
Total	121	Across 12 rings, 93 ISINs, 81 bonds

3.3.3 Methods

Hazard-to-damage pipeline. For each scenario, flood depth at each plant location is read from the corresponding LIWO inundation raster and translated into fractional asset damage via the PESETA IV depth-damage framework (Huizinga et al., 2017), with sector attribution via the CORINE Land Cover 2018 raster (EEA, 2019) mapped through the six-category Huizinga land-use system. Damage at asset i is Damage = V_i × f_damage(d_i), where V_i is replacement value and d_i is local flood depth; depth-damage curves are concave and monotonic, rising steeply in the first 0–1 m of inundation and flattening thereafter (Kreibich et al., 2010; Jongman et al., 2012).

Hydraulic scaling across return periods. For the LIWO kaart1 envelope, depth is scaled across return periods via depth(rp) = depth_kaart1 × (rp/100,000)^0.3, consistent with JRC reporting for Dutch riverine systems; the exponent below 1 reflects the concave relationship between return period and flood depth. For the per-ring design event, each ring's regulatory normfrequentie is used directly as the return period (e.g. rp = 10,000 for the Randstad coastal polders, rp = 250 for the upper-Maas sandy-soil polders).

Valuation framework. Damage estimates are integrated into the CLIMACRED-PHYS structural credit-risk framework (Mandel et al., 2025): capital destruction enters through an additive channel, and business interruption through a multiplicative channel set to a constant daily rate of 240/365 ≈ 0.658 years per unit of capital destruction, consistent with the FEMA HAZUS-MH flood model (FEMA, 2013). The valuation produces scenario-dependent probability of default and corresponding bond and equity losses.

Scenarios analysed. Ten scenarios are evaluated: LIWO kaart1 at seven return periods (100 to 100,000 years); the per-ring design event; the Klimaatatlas Zuid-Holland primary breach; and the Klimaatatlas Zuid-Holland regional breach. All scenarios are evaluated at current-climate baseline; RCP sensitivity is not a primary dimension because the Dutch defence system is designed to contain events well beyond RP 100 under current climate conditions.

3.3.4 Results and Discussion

The 127 Dutch dike rings are shown with the three hazard layers overlaid on the 121-plant portfolio: 96 plants lie entirely outside every flood envelope considered, while 25 plants flooded in at least one scenario are concentrated in ring 14 (Zuid-Holland).

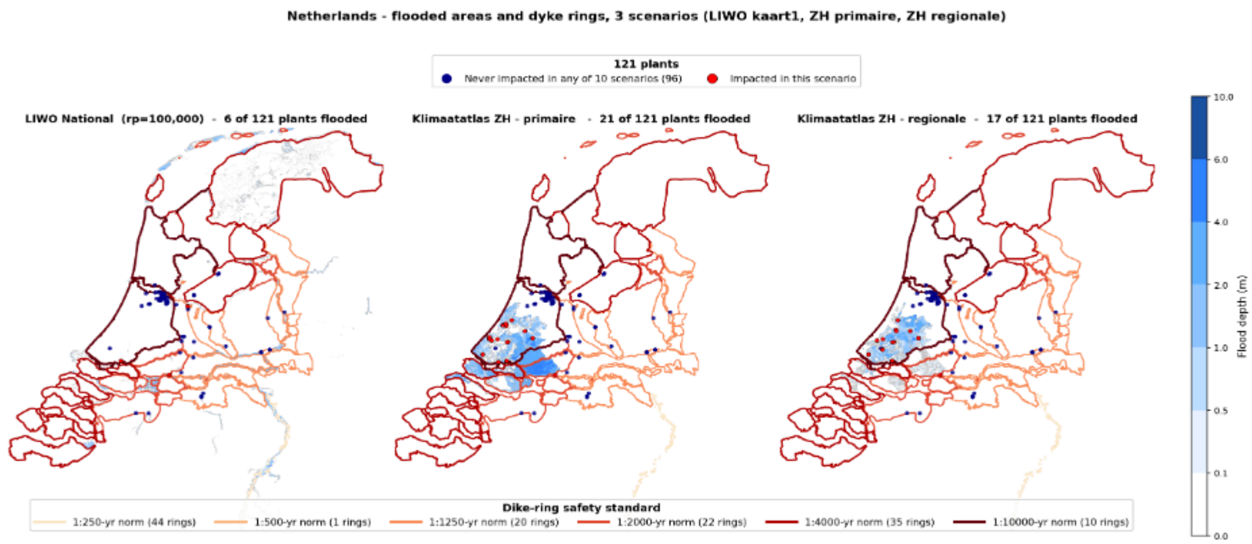

Figure 49. *Dike rings of the Netherlands with flood envelopes. Left: LIWO kaart1 national composite. Centre: Klimaatatlas Zuid-Holland primary breach. Right: Klimaatatlas Zuid-Holland regional breach. Grey dots: plants never flooded. Red dots: plants flooded in at least one scenario.*

National overview and the Utrecht case study. A national view of ROR (Risico's Overstromingen Nederland) APSFR (Areas of Potential Significant Flood Risk) zones, historical flood events, and a dike-breach scenario overlay for the province of Utrecht illustrates the mechanism behind the ring structure. The Utrecht inset classifies flood-affected cells into three inundation dynamics: droog (dry cells unaffected by the breach), langzaam-diep (slowly-deepening inundation, typically from cumulative riverine inflow into a low-lying polder), and snel-ondiep (rapidly-spreading shallow inundation, characteristic of a dune or embankment breach with limited volume but high flow velocity). This two-level view — national APSFR zoning plus provincial inundation dynamics — illustrates why the modular ring structure is essential to the financial analysis: a breach in one ring produces a localised inundation pattern with a well-defined spatial extent, while the failure of a different ring in a different province produces a qualitatively different footprint affecting a different subset of industrial assets. The conditional loss distribution is therefore best understood as a catalogue of localised scenarios — each ring's breach corresponds to a specific plant subset and a specific loss distribution — rather than a single integrated portfolio-level hazard.

Modular immunity. Across all ten scenarios, 96 of 121 plants (79.3%) register zero flood depth — they lie entirely outside every breach envelope considered. This is not because the country is uniformly well defended, but because the modular ring structure deflects water: a breach in ring

14 (Zuid-Holland) cannot reach a plant in ring 44 (Kromme Rijn) without a separate breach of the Kromme Rijn defences. Each plant lies within at most one ring's defended area, and any breach within that ring exposes only that ring's interior; plants in other rings — even adjacent ones — are unaffected unless their own ring's defences also fail.

Table 8. *Dutch dike-ring case study results across all ten scenarios.*

Scenario	Plants flooded	Max equity loss	Mean equity loss (81 bonds)	p90 equity loss
LIWO kaart1 (RP 100)	1	0.06%	<0.01%	<0.01%
LIWO kaart1 (RP 250)	1	0.15%	<0.01%	<0.01%
LIWO kaart1 (RP 500)	1	0.31%	<0.01%	<0.01%
LIWO kaart1 (RP 1,000)	1	0.61%	<0.01%	<0.01%
LIWO kaart1 (RP 10,000)	1	4.99%	<0.01%	<0.01%
LIWO kaart1 (RP 50,000)	1	9.71%	<0.01%	<0.01%
LIWO kaart1 (RP 100,000)	1	11.47%	<0.01%	<0.01%
Per-ring design event	1	0.61%	<0.01%	<0.01%
Zuid-Holland primary breach	25	47.00%	4.87%	24.83%
Zuid-Holland regional breach	25	46.54%	4.72%	23.91%

The kaart1 envelope floods only one plant — CORBION Gorinchem (ring 16) — at every return period from 100 to 100,000 years; maximum equity loss scales with return period per the hydraulic scaling law, from 0.06% at rp = 100 to 11.47% at the 100,000-year EDO loading. The per-ring design event similarly floods only CORBION (0.61% loss), because the remaining 120 plants' host rings have design standards that are not exceeded under the kaart1 envelope at their own regulatory return period.

The Klimaatatlas primary-breach scenario is materially different: a single primary-defence failure across a wider continuous area of ring 14 floods 25 plants concentrated in Rotterdam (5), The Hague (4), Leiden (3) and Zoetermeer (2). Maximum equity loss reaches 47.00% for EASE2PAY NV, a single-plant, single-location ISIN in Rotterdam; mean equity loss across all 81 bonds rises to 4.87%, with a p90 of 24.83%. The regional-breach scenario produces a comparable footprint — also 25 plants — with maximum equity loss of 46.54% (LYONDELLBASELL INDUSTRIES NV, also Rotterdam), mean 4.72%, p90 23.91%.

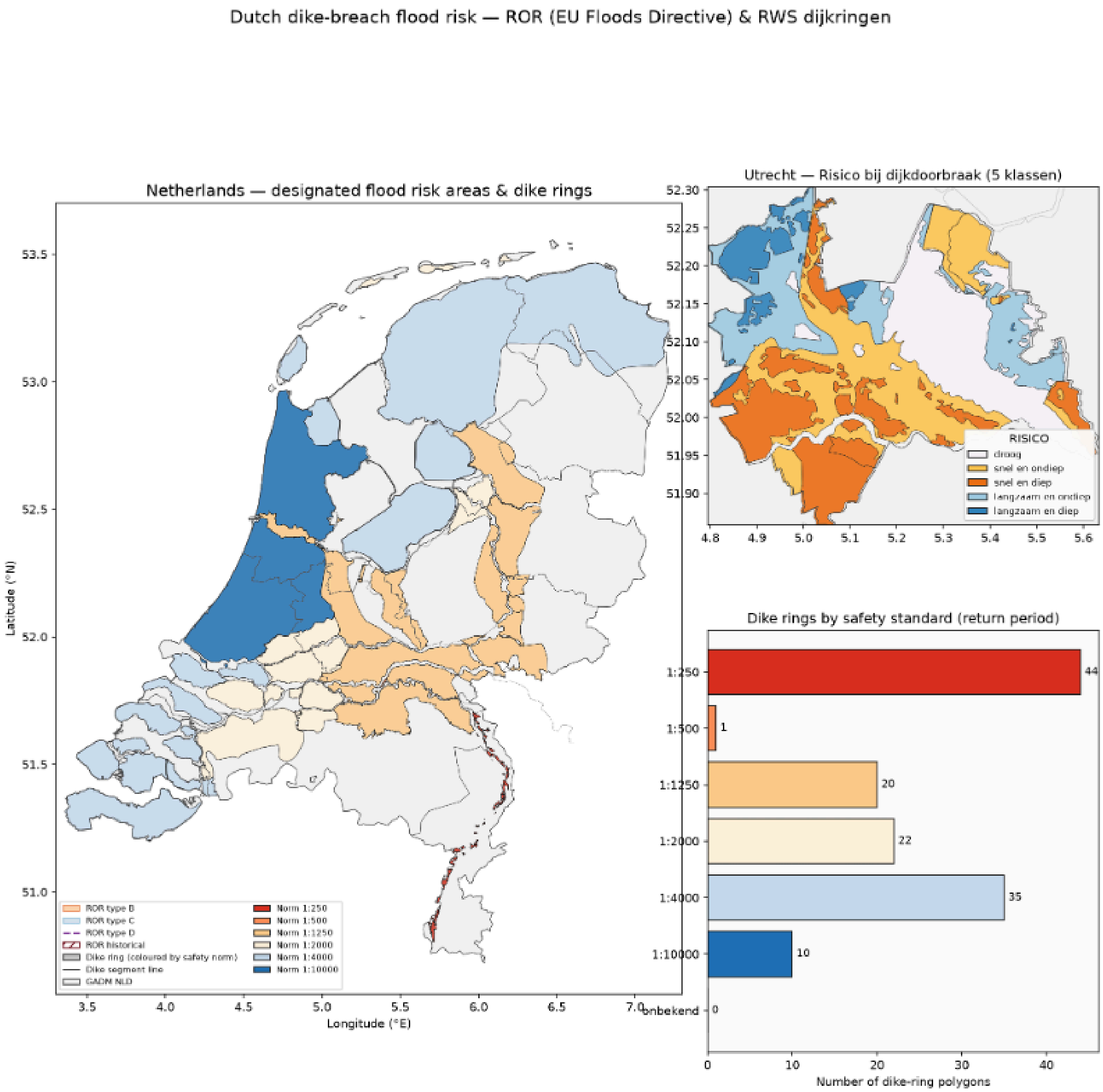

Figure 50. *National overview map of Dutch dike-ring flood risk: (left) national view with GADM provinces, ROR APSFR zones, historical flood events, and Utrecht dike-breach scenario overlay; (right) inset on the province of Utrecht with dry / langzaam-diep / snel-ondiep inundation classes.*

Table 9. *Top single-plant ISINs by equity loss under the Zuid-Holland primary breach scenario.*

ISIN	**Location**	**Ring**	**Equity loss**
EASE2PAY NV	Rotterdam	14 (Zuid-Holland)	47.00%
LYONDELLBASELL INDUSTRIES NV	Rotterdam	14 (Zuid-Holland)	46.54%
3 additional Zuid-Holland ISINs	Randstad cities	14	15–35%
All other 20 flooded plants	The Hague / Leiden / Zoetermeer	14	0.5–12%

The two top-loss ISINs are single-plant, single-location firms whose entire equity is concentrated at one Rotterdam industrial site. A 47% equity loss is comparable to a near-impairment event: productive capacity is destroyed, and recovery depends on reconstruction speed, business-interruption coverage, and the parent's willingness to recapitalise — both firms represent extreme cases of “geographic monoculture” in production-facility location.

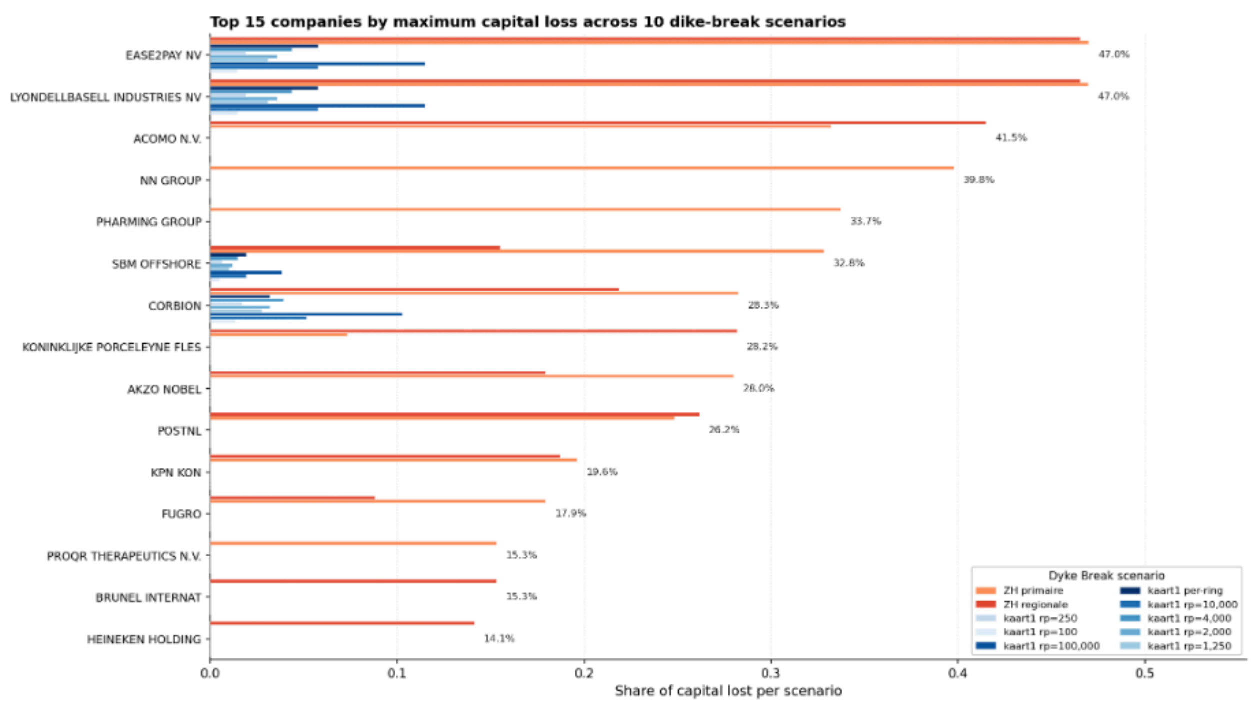

Figure 51. *Top 15 bonds ranked by maximum capital loss across all 10 scenarios, with stacked bars showing the contribution of each scenario to the total loss.*

Ranking the 15 bonds with the highest maximum capital loss across all ten scenarios reveals three structural features: tail concentration at the two single-location ISINs above; scenario cross-subsidisation, where some bonds reach the top 15 only by aggregating losses across several moderate scenarios rather than one dominant scenario; and ring-14 dominance, with the combined Zuid-Holland contribution exceeding the combined LIWO kaart1 contribution by roughly a factor of 20.

RP 100 implications. At the 100-year return period — the design standard for much of the Dutch flood defence system — the vast majority of the portfolio remains unaffected; for ring 14 (designed to approximately 1:10,000 years) the RP 100 event produces no breach under normal conditions. This is the core distinction for financial risk assessment: unconditional breach probability is very low at RP 100 for high-standard rings, while conditional severity, if a breach occurs, is very high — a stress test run only at RP 100 captures the severity dimension but not the probability dimension.

Table 10. *Cross-scenario comparison: conditional severity vs. unconditional probability.*

Regime	Representative scenario	Mean equity loss	Max equity loss
Conditional immunity — plant outside any breached ring	kaart1 (most plants)	<0.01%	0%
Conditional mild — plant in ring with breach but at low depth	kaart1, CORBION	<0.01%	11.47%
Conditional severe — plant in ring 14 under Zuid-Holland breach	Klimaatatlas primary	4.87%	47.00%

The contrast between the conditional-immunity and conditional-severe regimes — a roughly 4,700× spread in mean equity loss — quantifies the asymmetric risk absorption of the modular defence system. Portfolio-wide expected loss under any single scenario is dominated by the breach location rather than by the breach probability; this is the structural feature that distinguishes dike-ring risk from probabilistically distributed fluvial or coastal flood risk.

Three implications follow for portfolio stress testing. First, portfolio-level metrics computed under conventional fluvial- or coastal-flood hazard layers systematically miss dike-ring conditional severity: mean equity loss under LIWO kaart1 is below 0.01% in every return-period scenario, but rises to 4.87% (p90 24.83%) under the Zuid-Holland primary breach — the difference between a stress test that finds "no material exposure" and one that finds "20% of bonds could lose more than a quarter of their value under a single breach in ring 14." Second, the 79.3% modular immunity is not robust to compound events: the kaart1 envelope assumes ring independence and does not capture two adjacent rings breaching simultaneously, a scenario that could expand the affected footprint well beyond the 25 plants identified here. Third, the concentration of tail exposure at specific defended locations argues for ring-level rather than purely portfolio-level analysis; a full expected-annual-loss calculation would require summing over all 127 rings weighted by their regulatory breach probabilities, a computation that is tractable but not performed in this analysis because per-ring breach probabilities are not consistently published.

Table 11. *Comparative risk profile across hazard types (Puliga & Battiston, 2026a, 2026b).*

Hazard type	Mean equity loss	Tail concentration	Dominant driver
Drought (RP 200, RCP 4.5)	~11.7%	Moderate	Broad spatial extent of meteorological drought
Fluvial flood (RP 100, RCP 4.5)	~0.1–0.5%	Heavy (p99/p50 ≈ 7–8)	Concentration along major river corridors
Dike-ring breach (ZH primary)	4.87%	Extreme (max 47%)	Modular defence, ring 14 concentration

The dike-ring profile is best described as near-zero expected loss with high conditional severity — distinct from drought (high mean, broad distribution) and fluvial flood (low mean, heavy tail). The three profiles call for different hedging strategies: broad diversification for drought, tail-risk management for concentrated river-corridor exposures, and conditional-severity analysis at the ring level — complemented by ring-level insurance products where available — for dike-ring risk.

The analysis is less sensitive to RCP choice than the broader European flood analysis because the Dutch defence system is designed to contain events up to very high return periods; the primary climate-change implication is a slow increase in breach probability over decades rather than a shift in conditional severity. Key limitations: plant coordinates are geocoded via corporate-registry cross-referencing and are accurate at ring level but only approximate at the sub-ring-segment level; compound breaches across adjacent rings are not modelled; the hydraulic scaling law is a stylised representation rather than per-ring depth-return-period curves; and headquarters flooding, though excluded from the exposure analysis, could still disrupt corporate decision-making and supply-chain coordination in ways the framework does not capture.

3.1.5 Conclusion / Key Takeaways

The Dutch dike-ring system demonstrates that modular flood-defence infrastructure can effectively contain the breadth of financial exposure — 79.3% of plants remain unaffected across all scenarios considered — while concentrating severity at specific locations where defence failure produces catastrophic losses. The maximum equity loss of 47% for a single-location bond under the Zuid-Holland primary breach scenario underscores the materiality of conditional tail risk. Financial institutions with Dutch exposure should complement portfolio-level metrics (expected loss, VaR) with conditional-severity analysis at the ring level, particularly for rings protecting high-value industrial clusters — most notably ring 14 (Zuid-Holland) and other Randstad coastal polders, where design standards are highest but breach exposure is most concentrated.

Future work should extend the analysis in three directions: modelling compound adjacent-ring breach patterns and their conditional loss distribution; computing per-ring expected annual losses by combining LIWO breach scenarios with regulatory breach probabilities; and extending the ring-level approach to other European countries with modular flood-defence infrastructure, notably Germany (Deichverbände) and the United Kingdom (Environment Agency dike-and-embankment network).

References

Alfieri, L., Burek, P., Feyen, L., & Forzieri, G. (2015). Global warming increases the frequency of river floods in Europe. Hydrology and Earth System Sciences, 19(5), 2247–2260.

Andrews, T., Gregory, J. M., Webb, M. J., & Taylor, K. E. (2012). Forcing, feedbacks and climate sensitivity in CMIP5 coupled atmosphere-ocean climate models. Geophysical Research Letters, 39(9), L09712.

Ara Begum, R., Lempert, R., Elham, A., Benjaminsen, T. A., Bernauer, T., Cramer, W., Cui, X., Mach, K., Nagy, G., & Stenseth, N. C. (2022). Chapter 1: Point of Departure and Key Concepts. In Climate Change 2022 – Impacts, Adaptation and Vulnerability: Working Group II Contribution to the Sixth Assessment Report of the Intergovernmental Panel on Climate Change (pp. 151–214). Cambridge University Press. Doi: 10.1017/9781009325844.015.1817

Bates, P. D., Horritt, M. S., & Fewtrell, T. J. (2010). A simple inertial formulation of the shallow water equations for efficient two-dimensional flood inundation modelling. Journal of Hydrology, 387(1–2), 33–45.

Bates, P.D., Horritt, M.S., & Fewtrell, T.J. (2010). A simple inertial formulation of the shallow water equations for efficient two-dimensional flood inundation modelling. Journal of Hydrology, 387, 33–45.

Bocharov, P. S. (2026). pyextremes: Extreme value analysis in Python (Version 2.5.0) [Software]. https://github.com/georgebv/pyextremes

Bressan, G., Đuranović, A., Monasterolo, I., & Battiston, S. (2024). Asset-level assessment of climate physical risk matters for adaptation finance. Nature Communications, 15, Article 5371.

Chen, C., Zhao, P., Schneider, S. H., et al. (2021). Using AR5 scenarios to project future climate change: a meta-analysis. Climatic Change, 165(3–4), 41.

Climate TRACE (2025). Climate TRACE Emissions Inventory, version 4.3.1. Zenodo, doi:10.5281/zenodo.15691479.

CPB (2004). Balans van de volksgezondheid en de zorg. Centraal Planbureau voor de Economische Dynamiek, The Hague.

Deltares (2016). Waterwet en gevolgen voor de regionale wateroverstroomingskans. Deltares report 1209236-000.

Dottori, F., Mentaschi, L., Bianchi, A., Alfieri, L., & Feyen, L. (2020). River flood losses in Europe under the JRC PESETA IV framework (JRC Technical Report, EUR 30555 EN). Publications Office of the European Union.

Dottori, F., Szewczyk, W., Ciscar, J.-C., et al. (2018). Increased human and economic losses from river flooding with anthropogenic warming. Nature Climate Change, 8(9), 781–786.

Dottori, F., Szewczyk, W., Ciscar, J.-C., Zhao, F., Alfieri, L., Hirabayashi, Y., Bianchi, A., Mongelli, I., Frieler, K., Betts, R. A., & Feyen, L. (2022). Increased flood risk in Europe under climate change (JRC130737). Publications Office of the European Union.

European Banking Authority, European Insurance and Occupational Pensions Authority, & European Securities and Markets Authority (2024). One-off "Fit-for-55" climate scenario analysis [Joint report with the ECB and ESRB].

European Central Bank Banking Supervision (2022). 2022 climate risk stress test. European Central Bank.

European Commission (EC) (2021). Commission Delegated Regulation (EU) 2021/2139 of 4 June 2021 supplementing Regulation (EU) 2020/852 (Taxonomy Climate Delegated Act). Official Journal of the European Union.

European Commission (EC) (2022). Directive (EU) 2022/2464 of 14 December 2022 as regards corporate sustainability reporting (CSRD). Official Journal of the European Union.

European Commission (EC) (2023). Commission Delegated Regulation (EU) 2023/2772 supplementing Directive 2013/34/EU as regards sustainability reporting standards (ESRS). Official Journal of the European Union.

European Environment Agency (EEA) (2019). CORINE Land Cover 2018 (raster 100 m), Europe, 6-yearly. Copernicus Land Monitoring Service, doi:10.2909/960998c1-1870-4e82-8051-6485205ebbac.

European Environment Agency (EEA) (2019). CORINE Land Cover 2018 raster dataset. EEA. https://doi.org/10.2909/71c95a07-e296-44fc-bfeb-347e7bb831d4

European Insurance and Occupational Pensions Authority. (2022). European insurers' exposure to physical climate change risk: Potential implications for non-life business (EIOPA-22/278).

European Parliament & Council (2007). Directive 2007/60/EC of the European Parliament and of the Council of 23 October 2007 on the assessment and management of flood risks. Official Journal of the European Union, L 288, 27–34.

Exa Labs (2024). Exa: Search API for AI agents. https://exa.ai

FEMA (2013). HAZUS-MH 2.1 flood model: Business interruption default duration update. Department of Homeland Security / Federal Emergency Management Agency Technical Memo.

FEMA (Federal Emergency Management Agency). (2003). HAZUS-MH Multi-Hazard Loss Estimation Methodology — Flood Model. Department of Homeland Security.

Forster, P. M., Andrews, T., Good, P., et al. (2013). Evaluating adjusted forcing and forcing feedback metrics for historical and future climate in CMIP5 models. Journal of Geophysical Research: Atmospheres, 118(3), 1139–1150.

Frieler, K., Lange, S., Piontek, F., et al. (2017). Assessing the impacts of 1.5°C global warming — simulation protocol of the Inter-Sectoral Impact Model Intercomparison Project (ISIMIP2b). Geoscientific Model Development, 10(12), 4321–4345.

GDV (Gesamtverband der Deutschen Versicherungswirtschaft). (2021). 2021 teuerstes Naturgefahrenjahr für die Versicherer [Press release].

Global Energy Monitor (2026). Global Integrated Power Tracker, March 2026 release. https://globalenergymonitor.org/projects/global-integrated-power-tracker

Hausfather, Z. (2020, March 5). CMIP6: The next generation of climate models explained. Carbon Brief.

Huizinga, J. (2007). Flood damage functions for EU member states. HKV Consultants report, prepared for the JRC (JRC105688).

Huizinga, J., de Moel, H., & Szewczyk, W. (2017). Global flood depth-damage functions — Methodology and the database with guidance (JRC Technical Report EUR 28522 EN). Publications Office of the European Union.

Huizinga, J., de Moel, H., & Szewczyk, W. (2017). Global flood depth-damage functions: Methodology and the database with guidelines. JRC Technical Report, EUR 28552 EN, doi:10.2760/16510.

HYDE (History Database of the Global Environment). (2016). HYDE 3.1: Global population density dataset. Netherlands Environmental Assessment Agency (PBL).

Jongejan, R.B., et al. (2012). The VNK2 project: A probabilistic analysis of flood risk in the Netherlands. Deltares Report.

Jongman, B., Hochrainer-Stigler, S., Feyen, L., Aerts, J. C. J. H., Mechler, R., Botzen, W. J. W., Bouwer, L. M., Pflug, G., Rojas, R., & Ward, P. J. (2014). Increasing stress on disaster-risk finance due to large floods. Nature Climate Change, 4(4), 264–268.

Jongman, B., Kreibich, H., Apel, H., Barredo, J.I., Bates, P.D., Feyen, L., et al. (2012). Comparative flood damage model assessment: towards a European approach. Natural Hazards and Earth System Sciences, 12, 3733–3752.

Jongman, B., Kreibich, H., Apel, H., et al. (2012). Comparative flood damage model assessment: towards a European model. Environmental Science & Policy, 23, 100–111.

Jonkman, S. N., Voortman, H. G., Kanning, W., & van der Meer, M. T. (2018). Flood risk in the Netherlands: analysis of the dike-ring approach. Risk Analysis, 38(5), 1003–1020.

Jonkman, S.N., Kok, M., Vanhardeveld, W., & Duits, M. (2018). Flood risk assessment in the Netherlands: A review of methods and data. Water, 10(11), 1565.

Kreibich, H., et al. (2010). Is flow velocity relevant for flood damage assessment? Natural Hazards and Earth System Sciences, 10, 1161–1173.

Kreibich, H., Piroth, K., Seifert, I., et al. (2010). Costing floods: a survey of methods and their application. Natural Hazards and Earth System Sciences, 10(11), 2187–2207.

Kummu, M., Taka, M., & Guillaume, J. H. A. (2018). Gridded global datasets for Gross Domestic Product and Human Development Index over 1990–2015. Scientific Data, 5, 180004.

Lehner, B., Verdin, K., & Jarvis, A. (2008). New global hydrography derived from spaceborne elevation data. Eos, Transactions American Geophysical Union, 89(10), 93–94.

LIWO (2024). Landelijk Informatiesysteem Water en Overstromingen — kaart 1: Maximale Waterdiepte Nederland. Rijkswaterstaat. https://basisinformatie-overstromingen.nl

LIWO (Landelijk Informatiesysteem Water en Overstromingen). (2024). LIWO documentation and dataset access. https://www.liwo.nl/

Mandel, A., Battiston, S., & Monasterolo, I. (2025). Mapping global financial risks under climate change. Nature Climate Change, 15, 329–334.

Mandel, A., Tiggeloven, T., & Frame, D. J. (2025). Climate financial risk on corporate assets. Nature Climate Change, 15(4), 387–394. https://doi.org/10.1038/s41558-025-02244-x

Munich Re (2022, January 10). Hurricanes, cold waves, tornadoes: Weather disasters in USA dominate natural disaster losses in 2021 [Press release].

PERILS AG (2024, May 22). EUR 495m — PERILS releases final loss estimate for the Emilia-Romagna floods of May 2023 [Press release].

Provincie Zuid-Holland (2020). Klimaatatlas — overstromingsbeeld primaire keringen 25m. Data.overheid.nl, dataset 34858.

Provincie Zuid-Holland (2021). Klimaatatlas — overstromingsbeeld regionale keringen 25m. Data.overheid.nl, dataset 34846.

Puliga, M. & Battiston, S. (2026a). Drought risk assessment in Europe: From news-based impact functions to financial valuation. Working Paper, Ca' Foscari University of Venice.

Puliga, M. & Battiston, S. (2026b). Flood risk assessment in Europe: A land-cover-aware depth-damage approach. Working Paper, Ca' Foscari University of Venice.

Puliga, M., & Battiston, S. (2026). Financial risk for financial institutions from riverine floods in the EU. Working Paper.

Regione Emilia-Romagna, Agenzia per la sicurezza territoriale e la protezione civile (2023). Alluvione: oltre 8,8 miliardi di euro, la stima provvisoria dei danni [Press release].

Rijkswaterstaat (2012). Dijkringen 2012 — dike-ring polygons shapefile. EPSG:28992.

Rijkswaterstaat (2023). Waterveiligheid in Nederland: Stand van zaken 2023. Ministerie van Infrastructuur en Waterstaat.

Rijkswaterstaat. (2012). Dijkringgebieden Nederland — 127 dike-ring polygons [Dataset].

Sarofim, M. E., Smith, C. J., & Waugh, D. W. (2024). Climate trajectories under current policies: SSP vs RCP comparison. Earth's Future, 12(3), e2023EF004243.

Scussolini, P., Aerts, J. C. J. H., Jongman, B., et al. (2016). FLOPROS: an evolving global database of flood protection standards. Natural Hazards and Earth System Sciences, 16(5), 1049–1061.

Smith, C. J., & Gu, H. (2023). Effective radiative forcing and observed warming: the role of missing feedbacks. Geophysical Research Letters, 50(8), e2023GL103345.

Van Alphen, J., et al. (2014). Flood Risk Assessment in the Netherlands: A Country Update. WL | Delft Hydraulics technical report.

Van Dantzig, D. (1956). Economic decision problems for flood prevention. Econometrica, 24, 276–287.

Vousdoukas, M.I., et al. (2018). Climatic and socioeconomic controls of future coastal flood risk in Europe. Nature Climate Change, 8(9), 776–780.

Vousdoukas, M.I., et al. (2020). Sandy coastlines under threat of erosion. Nature Climate Change, 10(3), 260–263.

WARTA (2020). Waterveiligheidsrapportage 2020. Ministerie van Infrastructuur en Waterstaat.

Watanabe, S., & Takemura, T. (2020). Evaluation of historical climate simulations of MIROC family models. Journal of Climate, 33(15), 6503–6524.

Watanabe, S., Hajima, T., Sudo, K., et al. (2011). MIROC-ESM-CHEM: a global atmospheric chemistry-climate model. Geoscientific Model Development, 4(4), 823–850.

Yamazaki, D., Ikeshima, D., Tawatari, R., et al. (2017). A high-accuracy map of global terrain elevations. Geophysical Research Letters, 44(11), 5844–5853.